

AN ELECTROMAGNETIC (EM-60) SURVEY
OF THE McCOY GEOTHERMAL PROSPECT, NEVADA

Michael Wilt, Ramsey Haught, and Norman E. Goldstein

Earth Sciences Division
Lawrence Berkeley Laboratory
University of California
Berkeley, California 94720

December 1980

DISCLAIMER

This book was prepared as an account of work sponsored by an agency of the United States Government. Neither the United States Government nor any agency thereof, nor any of their employees, makes any warranty, express or implied, or assumes any legal liability or responsibility for the accuracy, completeness, or usefulness of any information, apparatus, product, or process disclosed, or represents that its use would not infringe privately owned rights. Reference herein to any specific commercial product, process, or service by trade name, trademark, manufacturer, or otherwise, does not necessarily constitute or imply its endorsement, recommendation, or favoring by the United States Government or any agency thereof. The views and opinions of authors expressed herein do not necessarily state or reflect those of the United States Government or any agency thereof.

This work was supported by the Assistant Secretary for Resource Applications, Office of Industrial and Utility Applications and Operations, Geothermal Energy Division of the U. S. Department of Energy under Contract W-7405-ENG-48.

DISCLAIMER

This report was prepared as an account of work sponsored by an agency of the United States Government. Neither the United States Government nor any agency Thereof, nor any of their employees, makes any warranty, express or implied, or assumes any legal liability or responsibility for the accuracy, completeness, or usefulness of any information, apparatus, product, or process disclosed, or represents that its use would not infringe privately owned rights. Reference herein to any specific commercial product, process, or service by trade name, trademark, manufacturer, or otherwise does not necessarily constitute or imply its endorsement, recommendation, or favoring by the United States Government or any agency thereof. The views and opinions of authors expressed herein do not necessarily state or reflect those of the United States Government or any agency thereof.

DISCLAIMER

Portions of this document may be illegible in electronic image products. Images are produced from the best available original document.

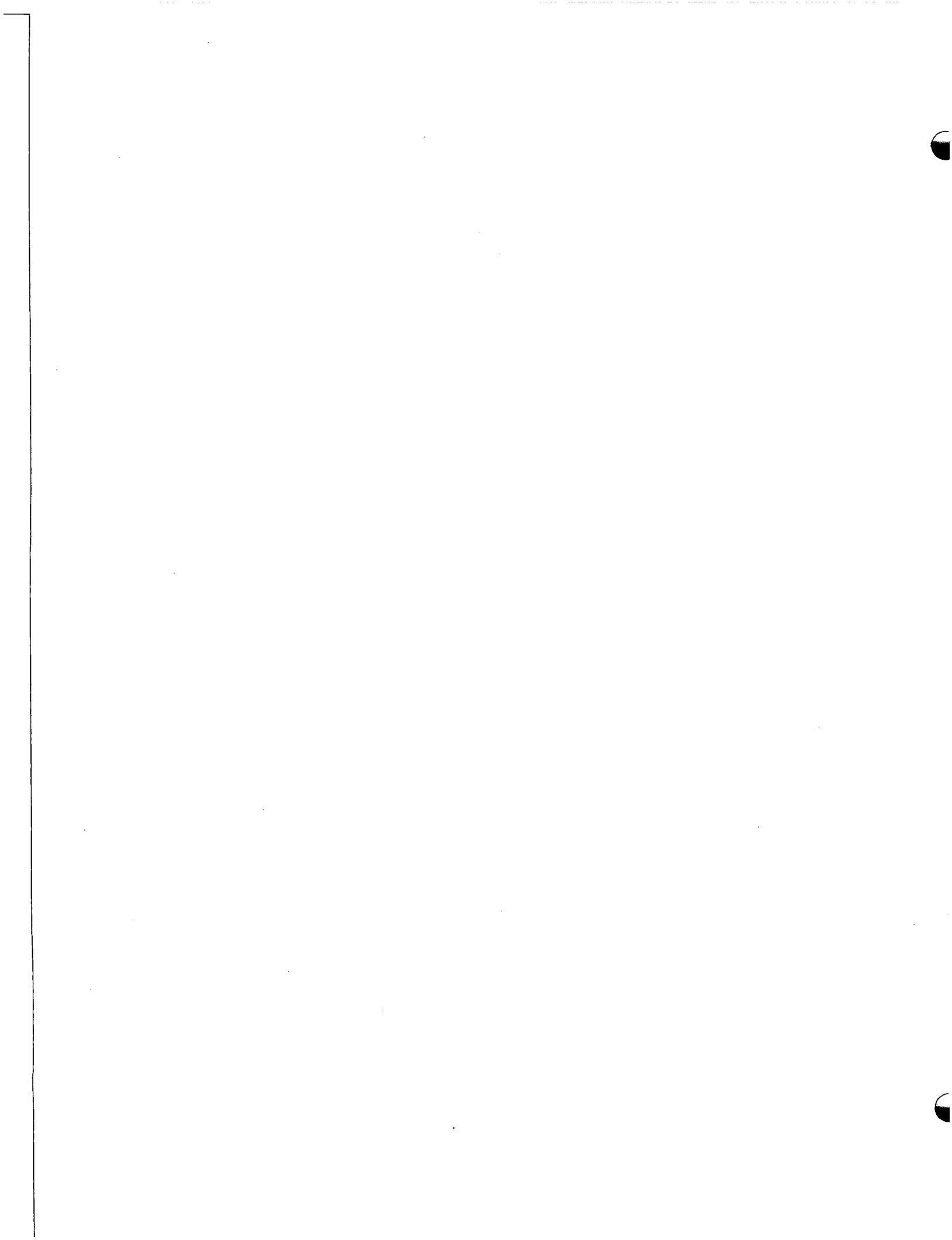


Table of Contents

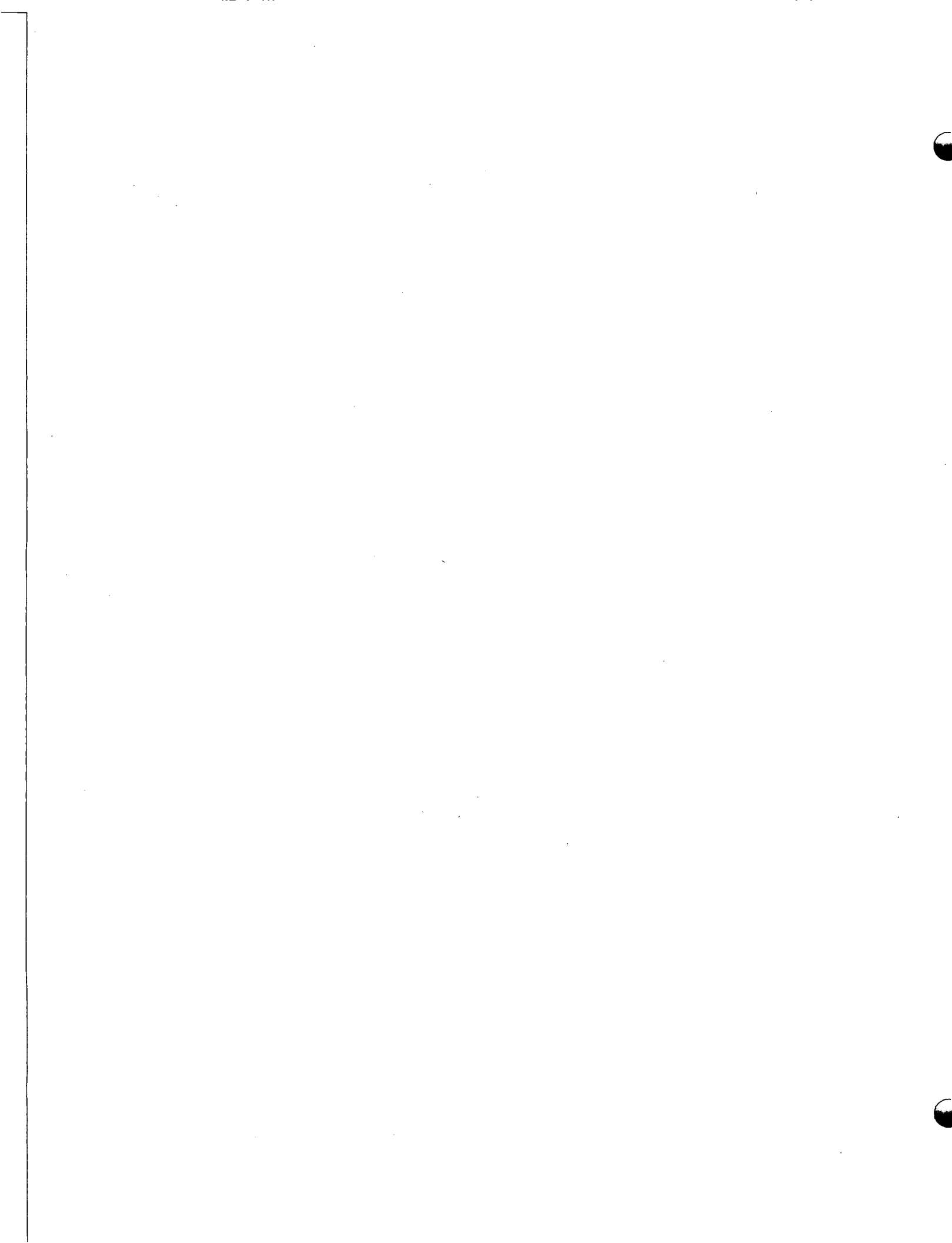
Abstract	1
Introduction	3
Geology	3
Geophysics	5
Electromagnetic Survey	7
Interpreted Resistivity Profiles	18
Acknowledgment	25
References	25
Appendix A: EM-60 Electromagnetic System	26
Appendix B: Final Working Data Set	39
Appendix C: Layered-Model Inversions of Soundings	56

ABSTRACT

A frequency-domain electromagnetic survey was conducted at 19 stations over a 200 km² area encompassing the McCoy geothermal prospect, Churchill County, central Nevada. The McCoy area is characterized by high heat flow, mercury mineralization, and recent volcanics. Three horizontal-loop transmitters were used with receivers from 0.5 to more than 4.0 km from the loops. Receiver stations were arranged along a pair of crossing north-south and east-west lines. Data were interpreted first with a simple apparent resistivity formula and then with a least-squares lumped-model inversion program. The rough terrain and complex geology introduce an element of uncertainty to the interpretations.

The north-south line suggests a thinning of the volcanic surface rocks northward toward the McCoy mercury mine, where a resistivity discontinuity occurs. The high-temperature gradients on the south end of the line can be correlated with a conductive zone (<10 ohm-m) at a depth of 200-500 m and occurring within the lower part of the Tertiary volcanics and the underlying Mesozoic limestones. We also see evidence for a deeper conductor, below 2 km.

The east-west line of stations indicates high resistivity associated with exposed Mesozoic rocks, a thickening ridge of lower-resistivity sediments and volcanics at the western end of the line, and a very thin alluvial cover in Antelope Valley at the eastern end of the line.



INTRODUCTION

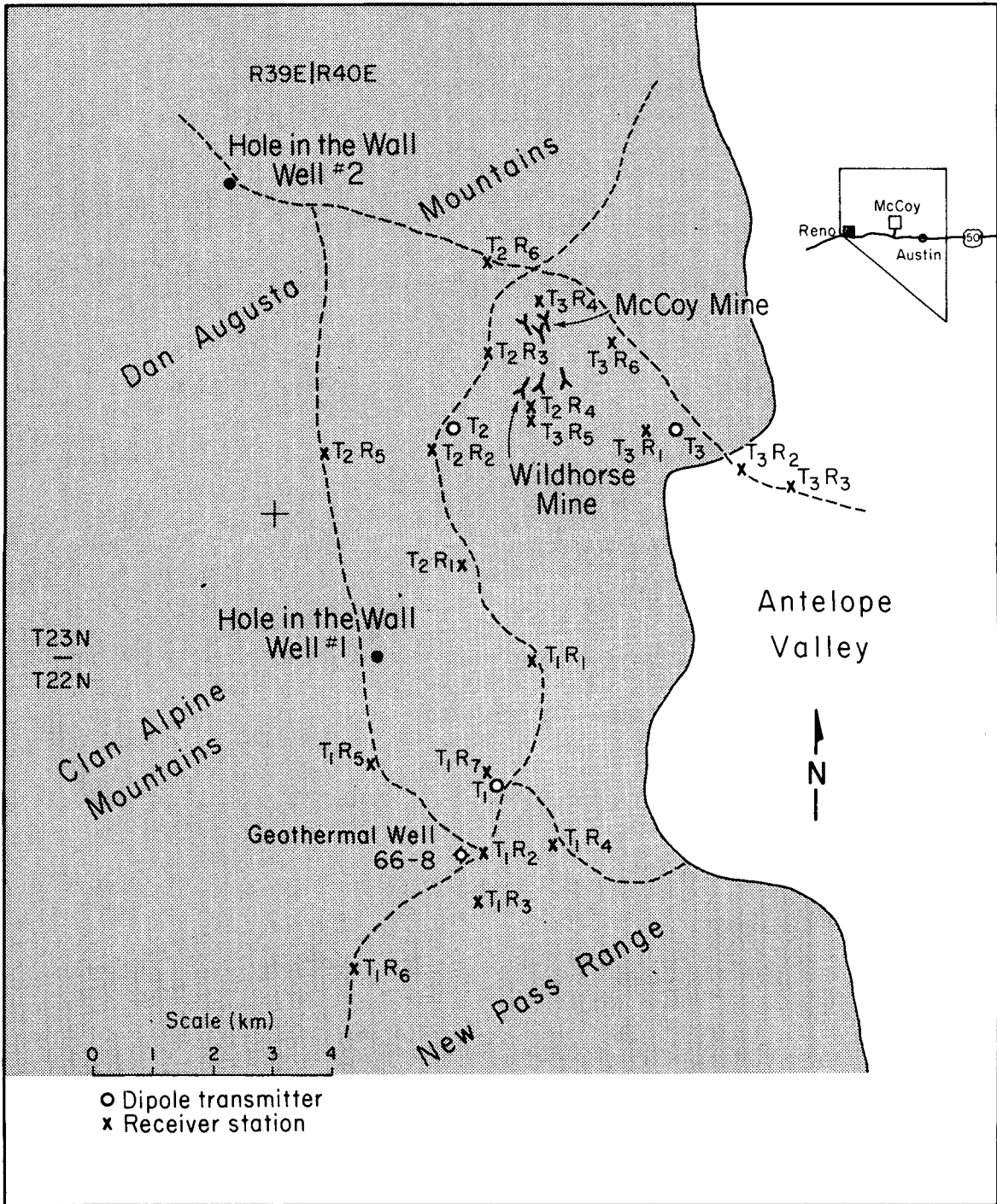
As part of the Department of Energy's program to stimulate the development of geothermal resources by private industry, Lawrence Berkeley Laboratory (LBL) has performed a series of electromagnetic surveys with the EM-60 frequency-domain system over promising targets in Nevada. This paper describes the results of our survey over the McCoy geothermal prospect in Churchill County, central Nevada (Figure 1).

The McCoy prospect is located 72 km northwest of Austin, between Dixie and Antelope Valleys on the west and east, respectively, and at the junction of the Dan Augusta Mountains, the Clan Alpine Mountains, and the New Pass Range. Elevations within the mountainous prospect area vary between 1200 and 1900 m, and local terrain variations are severe.

The McCoy geothermal area was chosen for study for three reasons. First, preliminary work by Amax, Inc. showed a thermal anomaly of large dimensions, indicating substantial geothermal potential. Second, because very little other geophysical work had been done there previously, the EM results could be evaluated independently. Third, the area provided an opportunity to test the EM-60 system in mountainous terrain with laterally discontinuous geology.

GEOLOGY

The McCoy region has been mapped on a reconnaissance scale by Stewart and McKee (1977) and Wilden and Speed (1974), mainly in connection with potential mining resources. No detailed geologic maps are available for the prospect area. Major rock units in the area include a thick assemblage of Tertiary volcanic flows and tuffs; Triassic and Jurassic sandstones,



XBL 8010-2861

Figure 1. Survey location map of the McCoy prospect.

shale, limestone, and conglomerate; and several groups of Pennsylvanian and Permian eugeosynclinal sediments. All rocks have been extensively faulted by Basin and Range type faulting, which followed the main episode of Tertiary volcanism and continues into the present. The dominant trend of the faulting is north-northeast, parallel to the range fronts. Significant east-west faults have also been mapped, however, and several are related to ore deposits.

Hydrothermal alteration is extensive in the central part of the prospect. A fossil travertine deposit 2 km² in area and 10m thick occurs adjacent to and west of the McCoy mine, and may be related to the mercury mineralization there. The Wildhorse mine, located 5 km south of the McCoy mine, is also a mercury deposit, but neither site is being actively mined. There are no active hot springs in the prospect, but there is a warm well near the McCoy mine.

GEOPHYSICS

Figure 2 is a temperature gradient map of the McCoy prospect (Olson et al., 1979). Thermal gradients were computed from temperature variations in 45 holes ranging from 12 to 100 m in depth. The map indicates anomalously high gradients over an area of at least 100 km². Gradients are especially high near the McCoy mine and about 3 miles southeast of the Hole in the Wall water well no. 1. Heat flow values were calculated from these thermal gradients and thermal conductivity measured from collected well cuttings. The resultant heat flow data indicate values as high as 10 times the regional average, which is 2 to 2.5 heat flow units (HFU). Chemical analysis of a warm-water well near the McCoy mine suggests a minimum reservoir temperature of 186°C.

TEMPERATURE GRADIENT

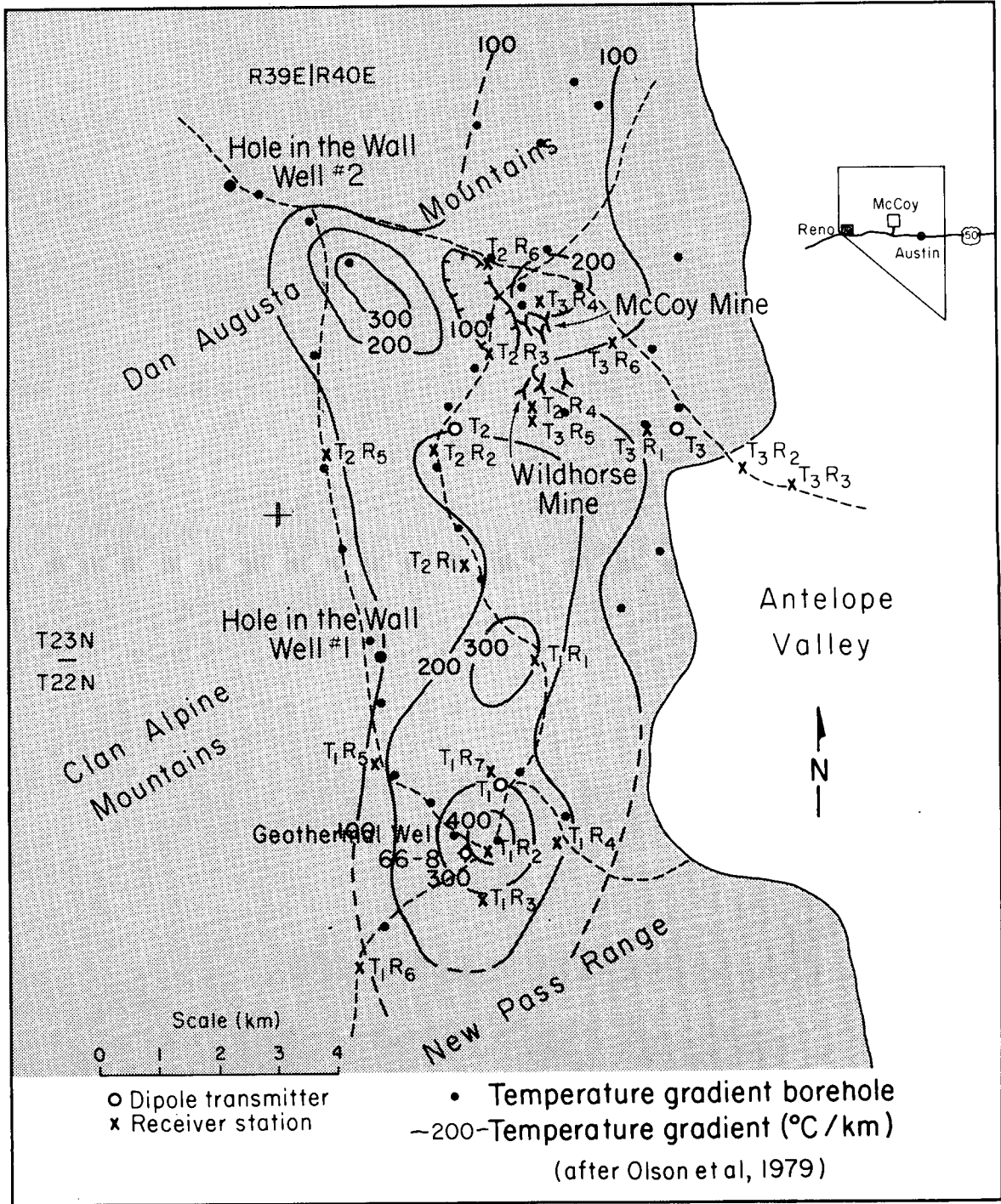


Figure 2. Temperature gradient map of the McCoy region.

Magnetic, gravity, self-potential (SP), and magnetotelluric (MT) measurements have all been made at McCoy, but so far only the SP data and some MT data have been interpreted (Olson et al., 1979). The general contour pattern of the SP data (Figure 3) is different from that of the thermal data; the SP indicates pronounced northeasterly and northwesterly orientations of equipotential contours, suggesting that regional faulting in these two directions may be an important control. In local details, however, the SP and thermal anomalies show interesting similarities and correlations, the clearest of which is in the area of the McCoy mine. This SP anomaly may be related to ore mineralization or hydrothermal alteration, but because of its elongation parallel to nearby cross faults, and because it appears to be dipolar, the SP anomaly may also be related to deep-water circulation along faults (Olson et al., 1979; Corwin and Hoover, 1978). The temperature anomaly near geothermal well 66-8 appears to be on the flank of a broad SP anomaly, as yet not completely defined by survey.

ELECTROMAGNETIC SURVEY

The transmitter and receiver stations occupied for the EM-60 survey are shown in Figure 1. The survey consisted of 19 frequency-domain electromagnetic soundings from three horizontal transmitter loops at transmitter-receiver separations ranging from 450 m to more than 4 km. The stations are grouped in three clusters, one within the area of the southern heat flow anomaly, a second northward near the Wildhorse mine, and a third at the eastern margin of the Dan Augusta Mountains. The survey was designed such that north-south and east-west trending sections could be made from interpreted soundings, but the coverage is still sparse in view of the large prospect

SELF POTENTIAL

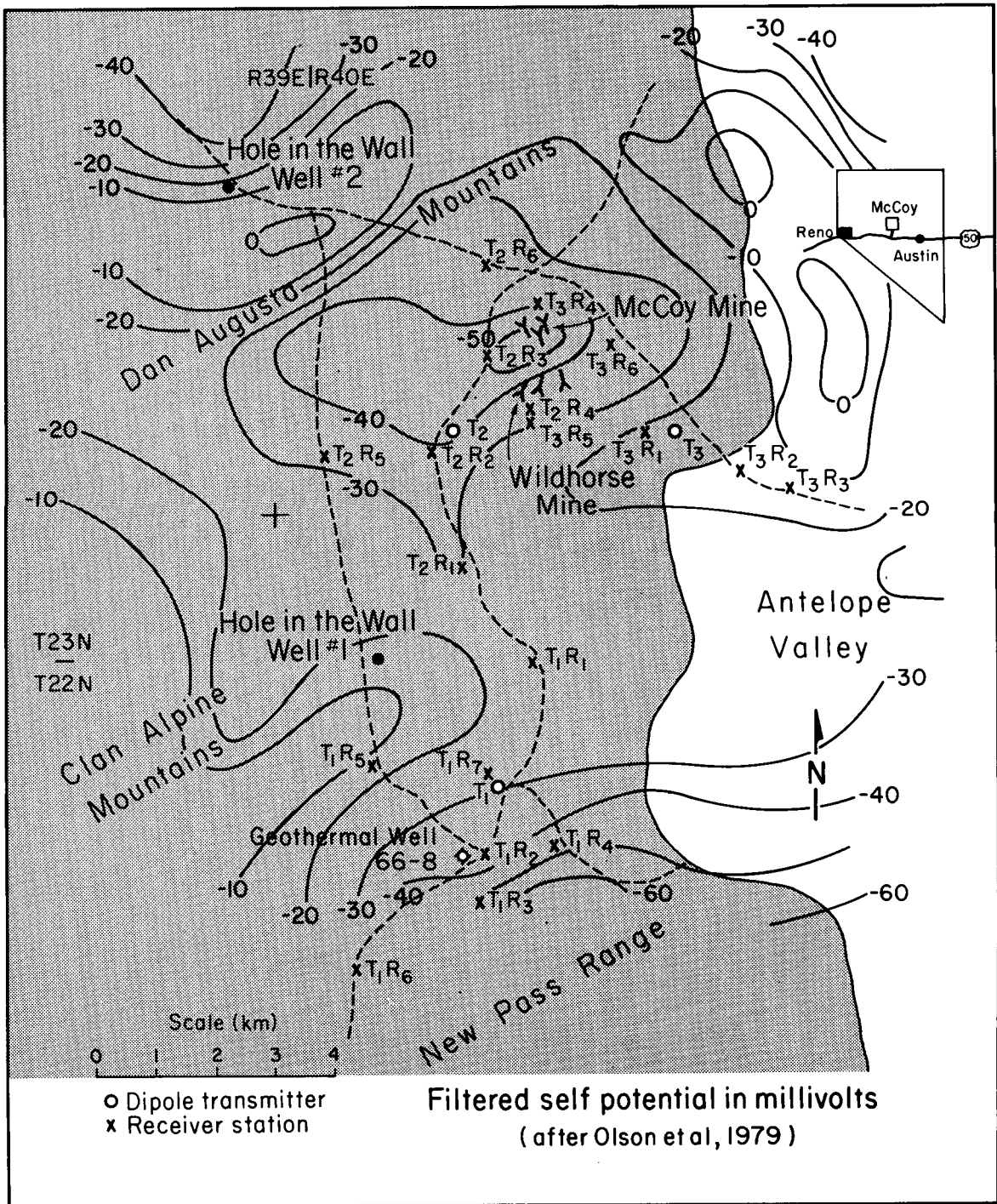


Figure 3. Self-potential map of the McCoy region.

area. Soundings were made in 11 field days during October and November, 1979, often during periods of blizzard, hail, and subfreezing temperatures.

The EM-60 soundings were made by impressing square-wave currents at frequencies within the band 0.001 to 1000 hz into a horizontal wire loop and measuring the vertical and radial magnetic fields at receiver sites. A more detailed description of the system and procedure is given in Appendix A. For this survey we took data at frequencies from 0.05 to 1000 hz, with data recorded for at least two to three frequency decades for each station.

Data quality for McCoy stations was fair to good at all sites. Recording times varied from less than an hour for the near stations to more than 4 hours for the more distant sites. Two stations could normally be obtained per 12 hour field day.

Data Analysis and Interpretation

EM sounding data at McCoy were reduced to a set of spectral plots corresponding to the observed radial and vertical magnetic fields and the ellipticity and ellipse inclination (or tilt angle) of the combined fields. The amplitude spectra are normalized by the primary magnetic field by calculating the free-space primary field due to the dipole transmitter and dividing the observed fields by this number. The reduced spectral data are given in Appendix B along with the estimated measurement errors.

After reduction, the soundings were first interpreted using an apparent resistivity formula, and later data were fitted to layered model curves by least-squares inversion. The apparent resistivity calculations were used in qualitative evaluation and for "first guess" models of the inversion routine. The inversion program can fit all or any part of observed spectral data to layered model curves and will give parameter resolution based on

observed standard error of data. Plots of the results of layered-model inversions are given in Appendix C. Although successful inversions were made for all stations, not all of the observed data were used in obtaining the fits. Some data were found to be noisy and distorted, and these were deleted prior to inversion. Absolute phase data were not obtained at several stations because of the difficulty of establishing a phase-reference wire over the rough terrain. At certain stations, the phase-reference wire was removed when it was found to contaminate signals with noise -- a serious problem when signal levels were low.

The Effect of Topography

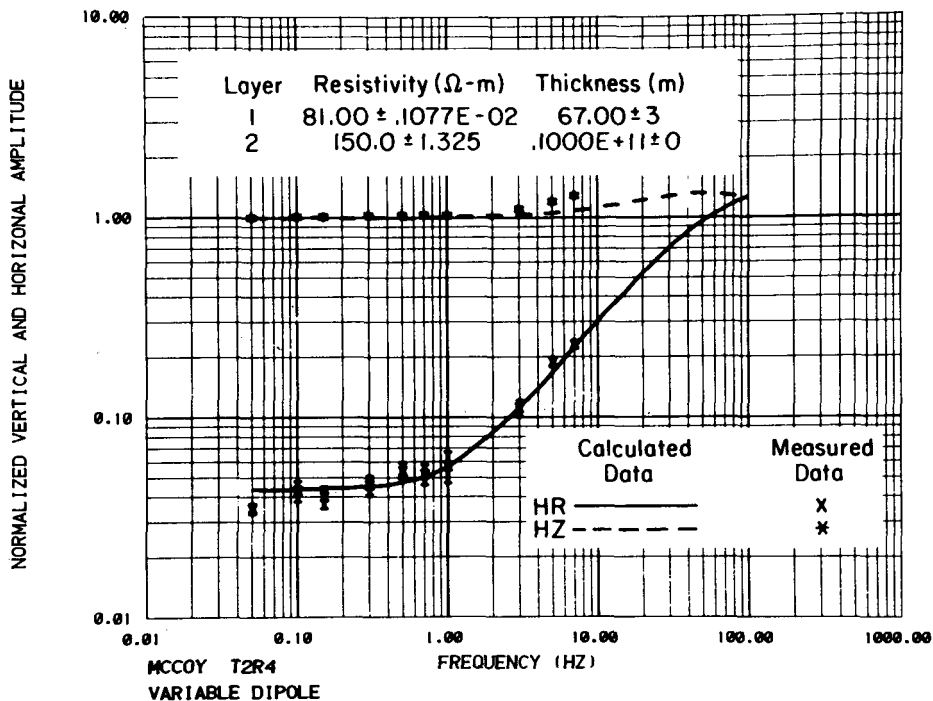
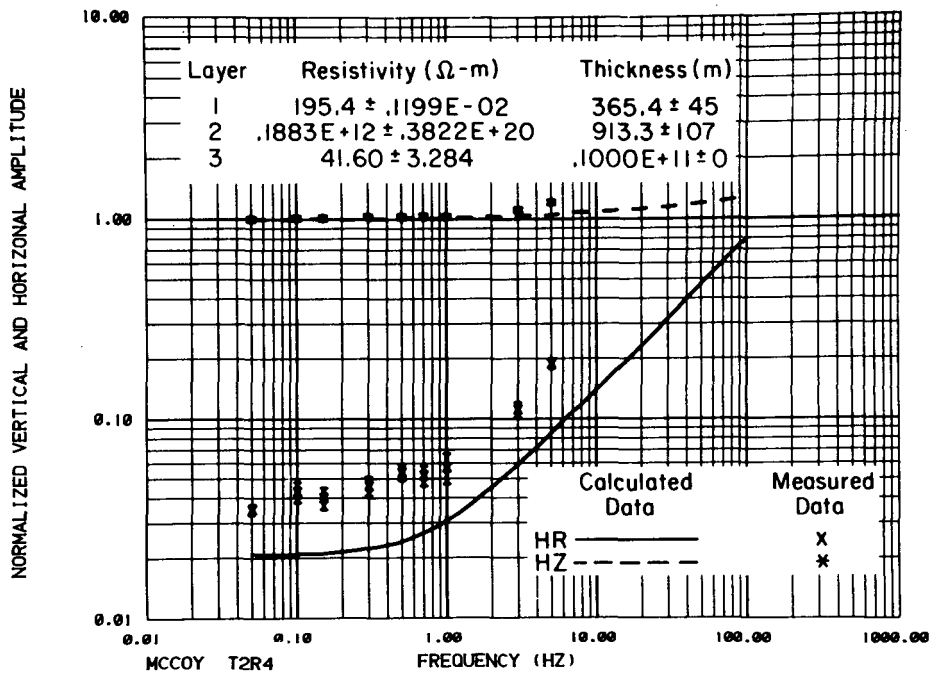
Because of the hilly terrain at McCoy, differences in elevation between transmitter and receiver stations were significant. These differences can be accounted for in interpretation, but the effect of the intervening terrain cannot. For the McCoy region, where the near-surface resistivity is fairly high, the effect of terrain may not be a significant factor. In any case, terrain effects are ignored because we are unable to account for them in models. Another effect of terrain is that two of the transmitter loops had to be laid out on inclined surfaces. This effect also influenced data interpretation, particularly for stations in line with the tilted dipole--i.e., stations at which there is a signal from the horizontal component of the magnetic dipole. The predominant combined effect of elevation differences and inclined dipole moment is to alter the inclination of the observed primary field at the receiver site. Although differences in elevation once accurately measured can be routinely taken into account for layered-model inversion, the effect of a tilted dipole requires calculations combining vertical and horizontal magnetic dipole solutions at the

appropriate strengths and inclination. The procedure is slightly more complicated and considerably more expensive in terms of computer time than the vertical dipole solutions. A computer program to perform forward model calculations of a tilted dipole over a layered media has recently been written (Haught et al., 1980), and we have tested the program with data taken at McCoy.

An example of the effect of the tilted dipole is given in Figure 4, which shows two interpretations for a set of EM sounding data at McCoy from a tilted dipole. In the top two graphs, the data set is fit to a vertical-dipole solution, ignoring the 1 degree of dipolar tilt. Of the various two- or three- layer models that we considered, the one that gives the best fit is a three-layer section that indicates the presence of a conductor at about 1 km in depth. The bottom two graphs in Figure 4 show a layered-model fit for a two layer section with a tilted dipole source. Here the fit is superior, and with no indication of a deeply buried conductor. Ignoring the effect of dipole tilt can therefore give misleading results, particularly in regions of high resistivity, such as McCoy, where small secondary magnetic fields may easily become distorted by dipolar tilt.

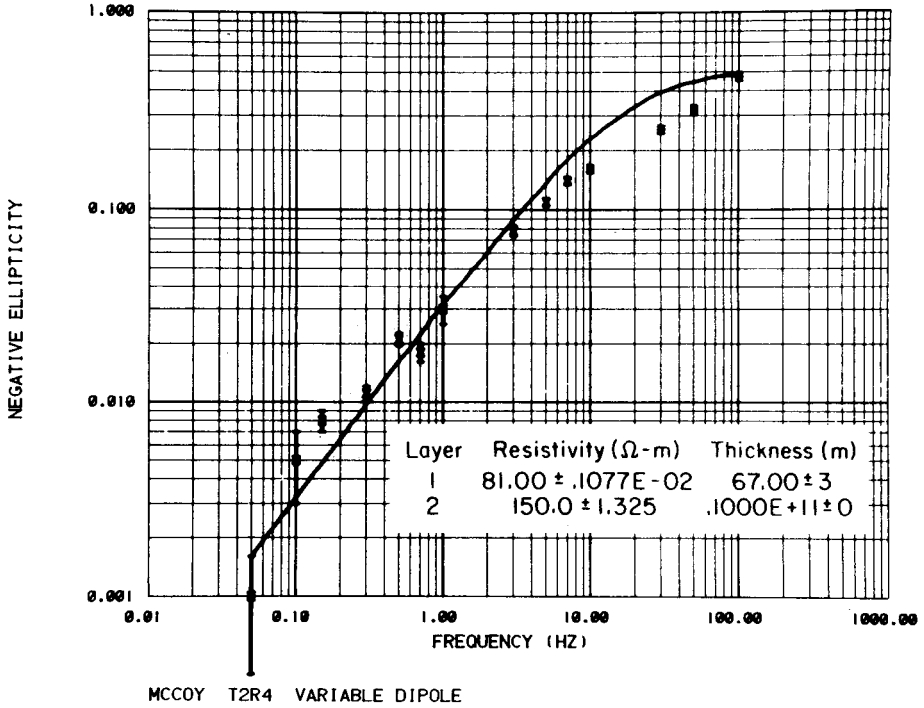
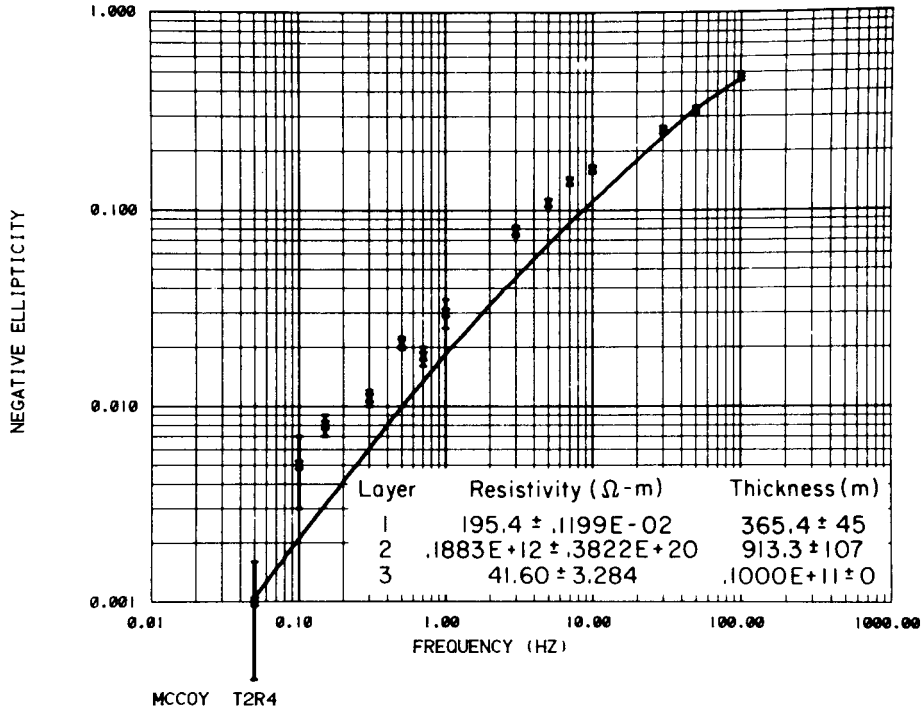
Apparent Resistivity Plots

We constructed apparent resistivity spectral plots to obtain an initial model for use in the inversion code and for qualitative interpretation of well-behaved sounding data (Stark et al., 1980). The plots are made from sounding data by comparing amplitude-phase and polarization ellipse values to corresponding values on a homogeneous half-space curve. The resistivities calculated from the half-space curve are then plotted against frequency to obtain an apparent resistivity spectral plot. Such plots are useful



XBL 812-2617

Figure 4. Comparison of inversions from a vertical dipole source (top graphs) and a variable dipole source (bottom graphs).



XBL 812-2617A

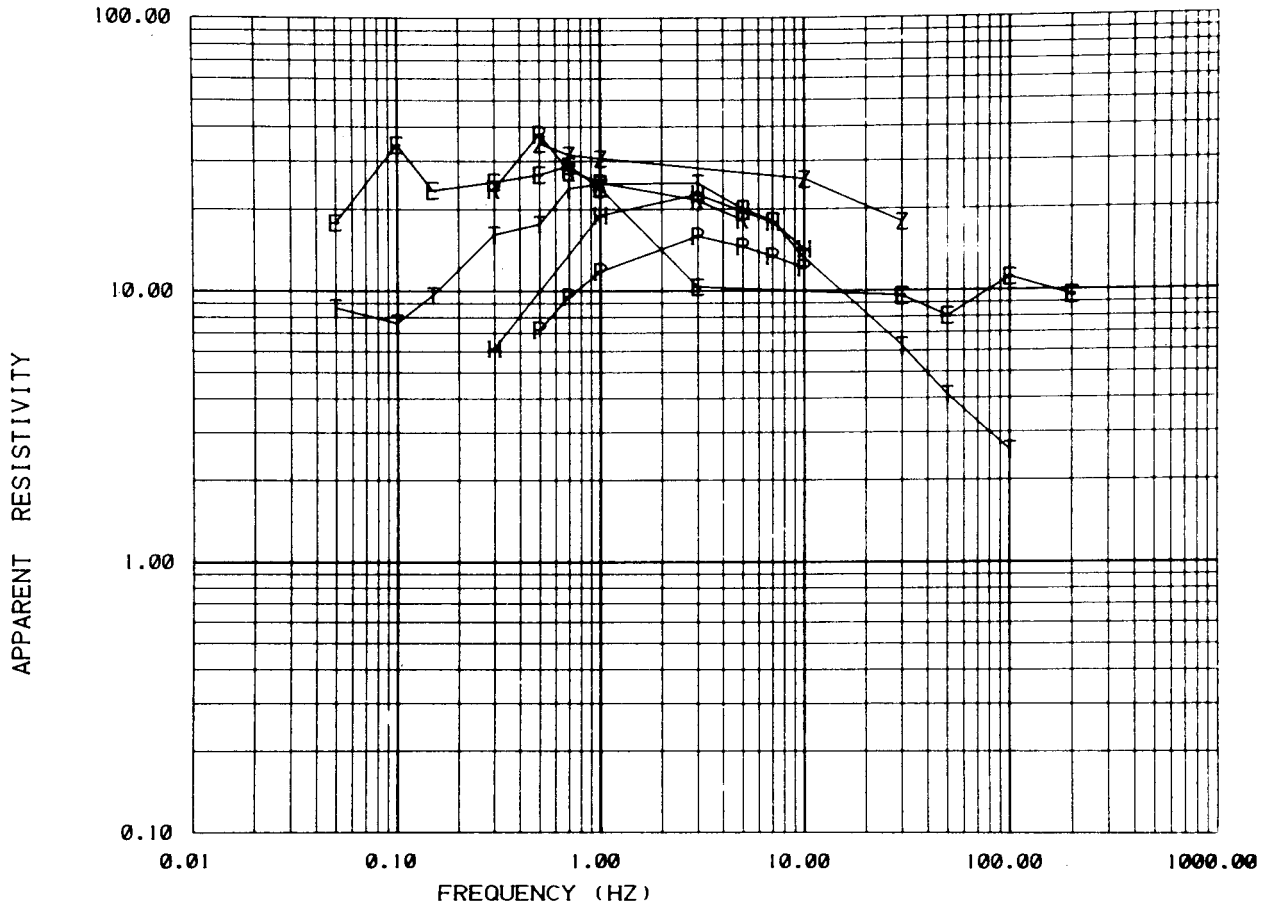
Figure 4. Continued.

for determining the probable number of layers, for judging data quality, and for characterizing the sounding. The apparent resistivity curves can be used effectively only if there is no elevation difference between source and receiver and no tilting of the transmitter dipole. Only 4 of the 19 soundings at McCoy, all from transmitter 1, satisfy these criteria; apparent resistivity curves for these stations are given in Figures 5 to 7.

Figure 5 is an apparent resistivity spectral plot for station T_1R_1 . The figure shows apparent resistivity values plotted for all six types of data; HZ is vertical amplitude, PHZ is vertical phase, HR is radial amplitude, PHR is radial phase, ELL is ellipticity, and TILT is the tilt angle of the polarization ellipse. There is considerable agreement in the shape of the curves, but substantial scatter exists among values calculated for each parameter. The curve shapes suggest a three-layer section consisting of a conductive surface layer, a resistive intermediate layer, and a conductive deeper layer. The apparent resistivity plot for sounding T_1R_7 (Figure 6), which was located closer to the transmitter, indicates a more resistive surface layer overlying the conductor, and does not suggest the presence of the deep conductor. The two sections are compatible, however, if we consider that the closer station is more sensitive to the shallow subsurface and the more distant is sensitive to the deeper parts of the section. Apparent resistivity plots (Figures 5 to 7) then indicate a four-layer section for the region near transmitter 1. This basic section was successfully tried on layered model inversions for this area.

Figure 7, an apparent resistivity plot for a large-separation sounding (T_1R_6), shows a marked decrease in apparent resistivity at low frequencies, indicating the presence of a good conductor at depth. Although station T_1R_1 (Figure 5) indicates a similar decrease at lower frequencies, only

EM APPARENT RESISTIVITY PLOT



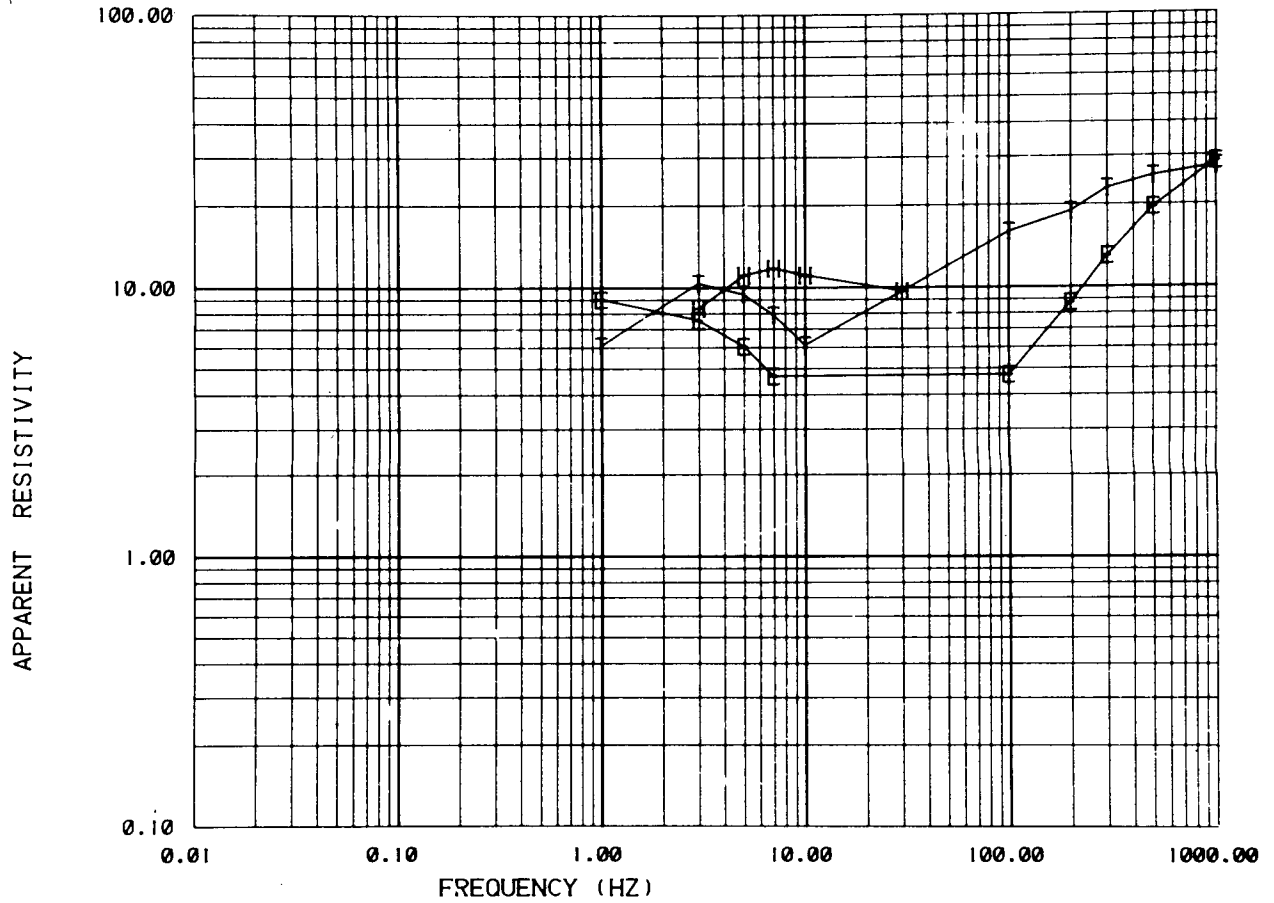
MCCOY STATION T1R1

HZ	Z
PHZ	P
HR	R
PHR	H
ELL	E
TILT	T

XBL 8010-12190

Figure 5. Apparent resistivity spectral plot for EM station T₁R₁.

EM APPARENT RESISTIVITY PLOT



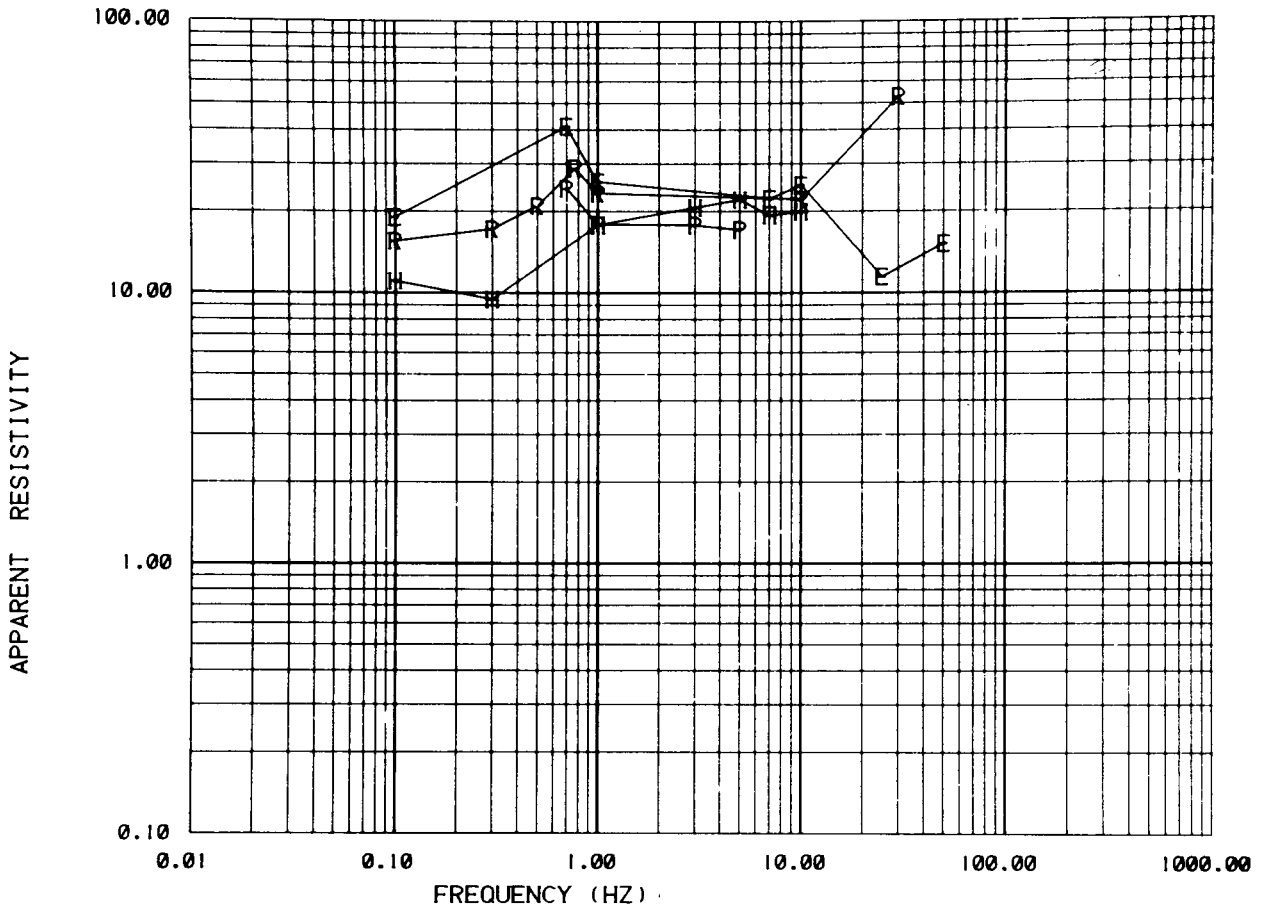
MCCOY STATION T1R7

HZ	Z
PHZ	P
HR	R
PHR	H
ELL	E
TILT	T

XBL 8010-12188

Figure 6. Apparent resistivity spectral plot for EM station T₁R₇.

EM APPARENT RESISTIVITY PLOT



MCCOY STATION T1R6

HZ	Z
PHZ	P
HR	R
PHR	H
ELL	E
TILT	T

XBL 8010-12189

Figure 7. Apparent resistivity spectral plot for EM station T1R6.

station T_1R_6 has sufficient higher-frequency data to show that the decrease was not due to geomagnetic noise contamination or some other effect. It is significant to note that had the apparent resistivity algorithm been known at the time of the survey, it is likely that additional large-separation soundings would have been made, since the results of T_1R_6 would have been known in the field.

INTERPRETED RESISTIVITY PROFILES

Layer-model inversions for all 19 stations at McCoy are given in Appendix B. Fair to good fits and reasonable one-dimensional interpretations were obtained for all sites. Because of the sparse distribution of stations, discussion is limited to results obtained along two profiles, a 13 km nine-station north-south profile that bisects the prospect in its elongate dimension (Figure 8), and a 9 km eight-station east-west profile that crosses the northern end of the prospect (Figure 10). The profiles are made by plotting layer parameters obtained from one-dimensional inversions for stations located along or close to the profile. The interpreted sections were plotted at a point halfway between source and receiver.

Figure 8 includes five soundings made from transmitter 1 and four from transmitter 2, with a gap of 4 km between the sounding groups. The gap was necessary because the difficult terrain prohibited establishing a third transmitter between the other two. The soundings from transmitter 1 differ markedly in character from soundings made from the northern loop (Figure 8). In the southern end, the sections generally indicate a resistive surface layer ranging from 100 ohm-m or more in mountainous stations to about 20 ohm-m for the lower-lying stations. The thickness of this unit is 100-300 m, and it probably represents a sequence of dry or undersaturated

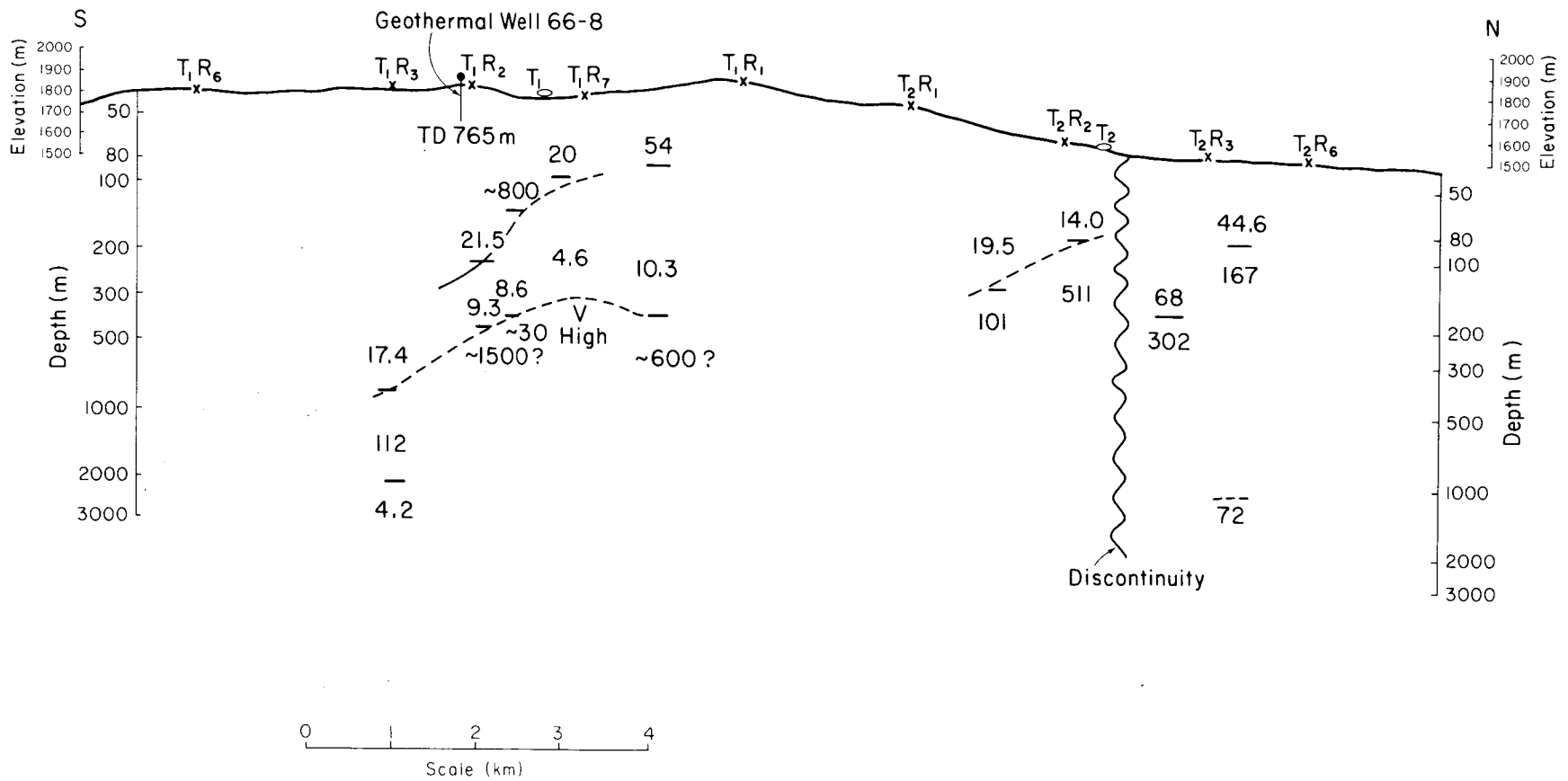




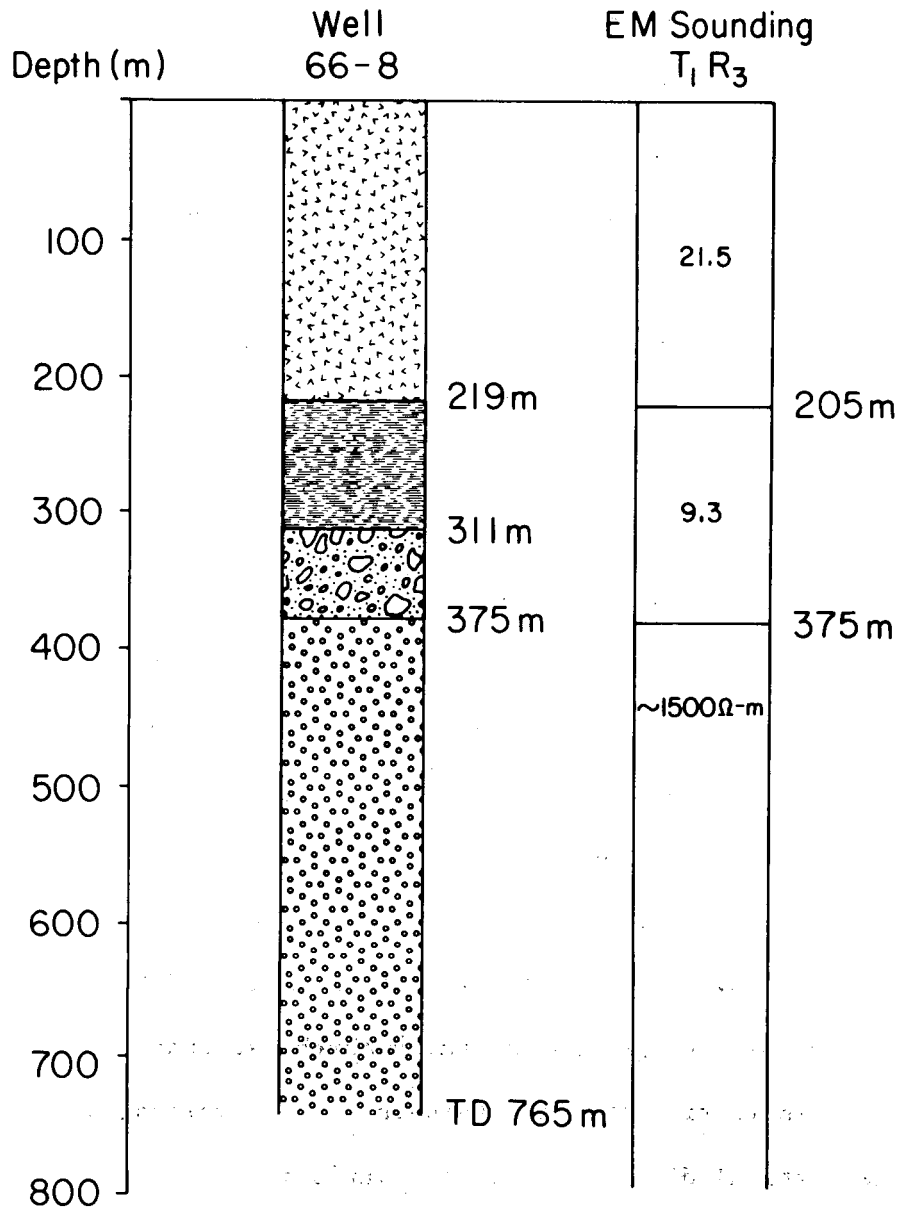


Figure 8. North-south profile of interpreted EM soundings over the McCoy prospect; stations used are plotted at the top of the figure. Layered-model parameters, resistivity (ohm-m), and depth (m) are plotted at a point halfway between source and receiver.

XBL 8010-2859

Tertiary flows and tuffs. Shallow wells in the region show a deep (>100 m) water table (Olson et al., 1979). Near 200 m in depth, a conductive layer is detected from all EM soundings near transmitter 1. This layer ranges from 200 to 300 m in thickness and 5 to 10 ohm-m in resistivity and suggests either a sequence of clay-rich tuffs or perhaps a warm-water aquifer. The resistivity of 5-10 ohm-m is consistent with geothermal aquifers, and the thermal gradients could be conservatively extrapolated to more than 100°C. Beneath the conductive layer at a depth of 300-400 m, the EM soundings indicate the presence of a much more resistive formation. The calculated resistivity of this unit ranges from 100 to 1000 ohm-m, but the true value is probably closer to the lower end of this range, since the lower values are consistent with the more depth-sensitive, larger-separation soundings. Because the EM induction method is generally much less sensitive to resistive bodies than to conductors, the depth to and resistivity of this unit are poorly resolved. Fortunately, a 765 m well has been drilled in the area near EM station T₁R₃ (Figure 1), and the driller's log has been published (National Geothermal Well Report, 1980). Figure 9 indicates a generalized lithologic section from this well adjacent to an interpreted EM induction sounding. The figure indicates that the conductive layer corresponds closely to the rocks between the lower boundary of the Tertiary volcanics and the upper boundary of the Mesozoic quartz conglomerate. Boiling water was reported to be flowing in the well at depths corresponding to this conductor (Art Lange, Amax geologist, 1980, personal communication). The figure also shows that the lower, more resistive unit corresponds to the quartz conglomerate. The depth correlation, although not exact, is quite good, and the high resistivity of this part of the Mesozoic section is consistent with older, less permeable formations.

-  Tv Tertiary Volcanics
-  Tj Mesozoic Limestone
-  Tc Triassic Sandstone Conglomerate
-  Tc Triassic Quartz Conglomerate



XBL 8010-2858

Figure 9. Generalized lithologic log from geothermal test well 66-8 compared with a layered-model inversion from EM station T₁R₃.

The inversion of sounding T_1R_6 indicates the presence of a 4 ohm-m layer at a depth exceeding 2000 m. Although no other soundings at McCoy indicate such a conductive body at depth, none of the others have sufficient transmitter-receiver separation to detect such a feature. As this conductor is detected at only one station, its delineation should be treated with some skepticism until confirmed with another set of measurements. It is possible that the field curves that detected this deep conductor are affected by the presence of a topographic ridge between the source and receiver (i.e., channeling of currents) or some other lateral effect. Because the presence of this body suggests a good geothermal target, further investigation is warranted.

Figure 8 indicates that the northern section of the profile is considerably different from the southern. The volcanic sequence is perhaps only 100 m or less thick at the north, where the section is dominated by high-resistivity Mesozoic rocks. A glance at the elevation profile in Figure 8 suggests that the thinning of the volcanics is related to the drop in elevation between southern and northern stations, since the decrease in elevation between these two stations is approximately equal to the decrease in thickness of the volcanic section. The elevation of the Mesozoic probably does not appreciably change from south to north, at least as far north as transmitter 2, indicating that the thinning of the volcanics is not related to any large vertical displacement. The variation in thickness may instead indicate that volcanic vents were located closer to the southern stations. North of transmitter 2, the resistivity at the surface layer is appreciably higher, suggesting the crossing of a lateral discontinuity near transmitter 2. The reconnaissance geologic map shows a major northwest-trending fault

in this region (Wilden and Speed, 1974), and this may represent a lateral lithologic change or a ground-water barrier.

The east-west profile is drawn from stations crossing the eastern margin of the Dan Augusta Mountains into Antelope Valley (Figure 10); stations used are located to the south of the above-mentioned northwest-trending fault. The predominant feature of this profile is the high resistivity associated with the higher-elevation eastern escarpment of the Dan Augusta Mountains. Resistivities of 500-1000 ohm-m are associated with out-cropping Mesozoic rocks in the mountains; soundings also indicate slightly lower resistivities (80-100 ohm-m) at a depth of 300-400 m. West of the eastern margin ridge, a low-resistivity surface layer overlies the Mesozoic section. This layer is from 100-200 m thick, thickens westward, and probably consists of Tertiary volcanics and alluvium. Soundings in Antelope Valley just east of the Dan Augusta Mountains indicate a fairly resistive section. Surface resistivities range from 20 to 200 ohm-m in the faults, and layered models indicate that resistivities do not appreciably change at depth. These data suggest a very shallow alluvial cover to this valley and an underlying resistivity consistent with Mesozoic basement rocks.

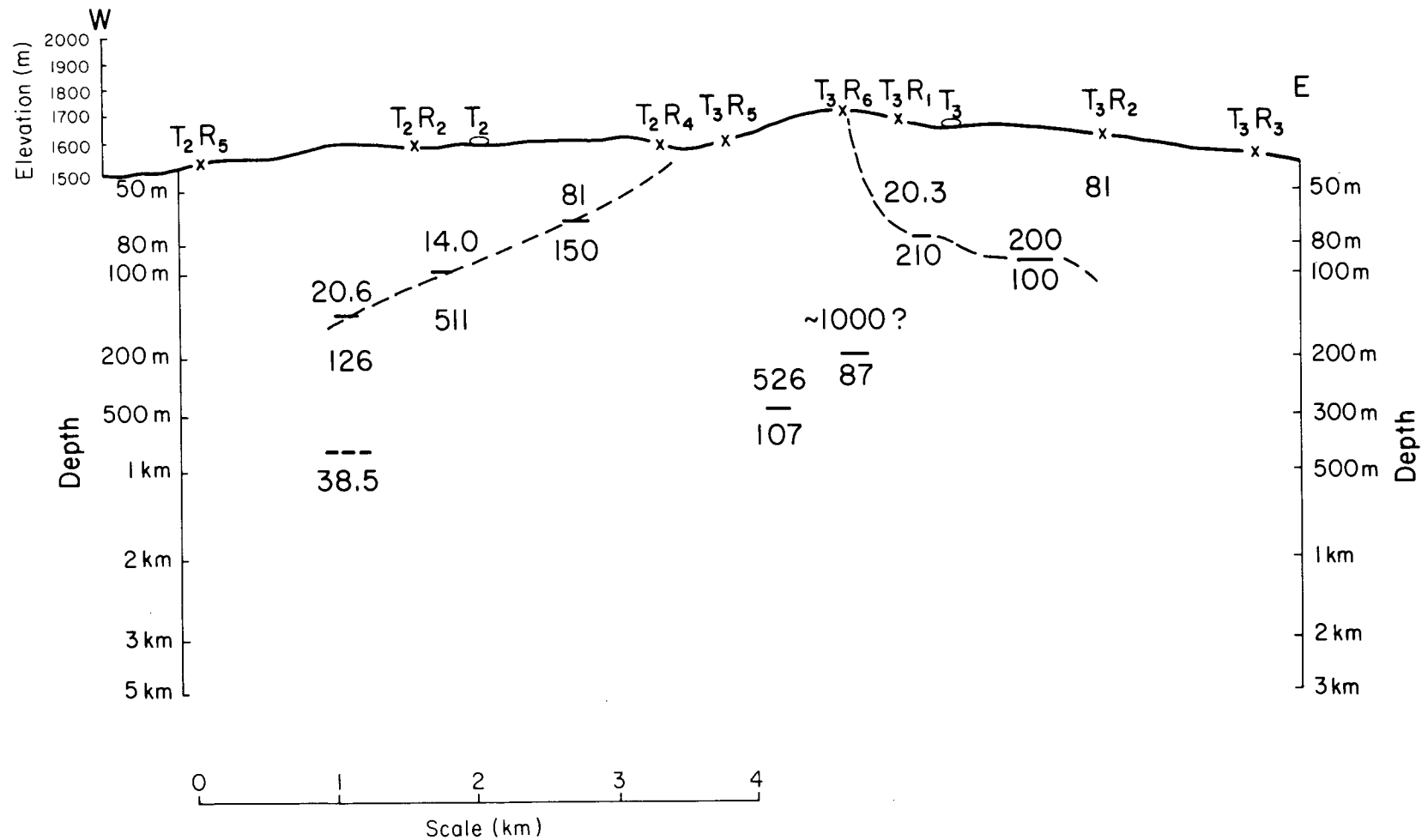


Figure 10. East-west profile of interrupted EM soundings over the McCoy prospect; stations used are plotted at the top of the figure. Layered-model parameters, resistivity (ohm-m), and depth (m) are plotted at a point halfway between source and receiver.

XBL 8010-2860

ACKNOWLEDGEMENT

This work was supported by the Assistant Secretary for Resource Applications, Office of Industrial and Utility Applications and Operations, Geothermal Energy Division of the U.S. Department of Energy under Contract W-7405-ENG-48.

REFERENCES

- Corwin, R.F., and D.B. Hoover, 1979. The self-potential method in geothermal exploration: *Geophysics*, v. 44, no. 2, p. 226-245.
- Haught, J.R., M.J. Wilt, and N.E. Goldstein, 1980. Deep induction sounding for geothermal exploration from an arbitrarily oriented magnetic dipole: *Abstr. Soc. Explor. Geophysics Annual Meeting*, Houston, Texas.
- National Geothermal Well Report, 1980. Drilling progress in Nevada: *National Geothermal Well Report*, p. 10 (well no. 66-E).
- Olson, H.J., F. Dellechiaie, H.D. Pilkington, and A. Lange, 1979. The McCoy geothermal prospect status report of a possible new discovery in Churchill and Lander Counties, Nevada, *in* Expanding the Geothermal Resources Council: *Transactions, Geothermal Resources Council Annual Meeting*, v. 3, p. 515-519.
- Stark, M., M. Wilt, and R. Haught, 1980. A simple method for determining apparent resistivity from electromagnetic sounding data: *Abstr. Soc. Explor. Geophysics Annual Meeting*, Houston, Texas.
- Stewart, J.H., and E.H. McKee, 1977. Geology and mineral deposits of Lander County, Nevada: *Nevada Bureau of Mines and Geology, Bull.* 93.
- Wilden, R., and R.C. Speed, 1974. Geology and mineral deposits of Lander County, Nevada. *Nevada Bureau of Mines and Geology, Bull.* 83.

APPENDIX A

EM-60 ELECTROMAGNETIC SYSTEM

In 1976 LBL, in conjunction with the University of California, Berkeley, made preliminary measurements with a prototype large-moment horizontal-loop EM prospecting system (Jain, 1978) in a geothermal area in Nevada. Encouraging results from this work led to the development of the EM-60 horizontal-loop system (Morrison et al., 1978), which has now been operated for over 500 hours at various geothermal sites in Nevada and Oregon.

The EM-60 electromagnetic system was originally designed to fill a gap in existing technology for geothermal exploration between the shallow-penetration dc resistivity method and the deep-exploration MT technique. The system was planned for cost-effective shallow to intermediate-depth exploration for conductive geothermal targets. It was designed to eliminate or diminish field problems in geothermal areas that have hampered both dc resistivity and MT. Some advantages of the EM method are: (1) the maximum depth of exploration with EM is approximately equal to the distance between the transmitter and receiver, which is almost five times the source-receiver separation for dc resistivity; (2) the EM method is faster and less expensive than either dc resistivity or MT; and (3) distant lateral inhomogeneities, which often affect MT data, have relatively minor significance for EM because the strength of the fields strongly decreases with increasing distance from the transmitter.

SYSTEM DESCRIPTION

The system, as shown schematically in Figure A-1, consists of two sections: a transmitter section consisting of the power, source, control electronics, timing, and a transistorized switch capable of handling large

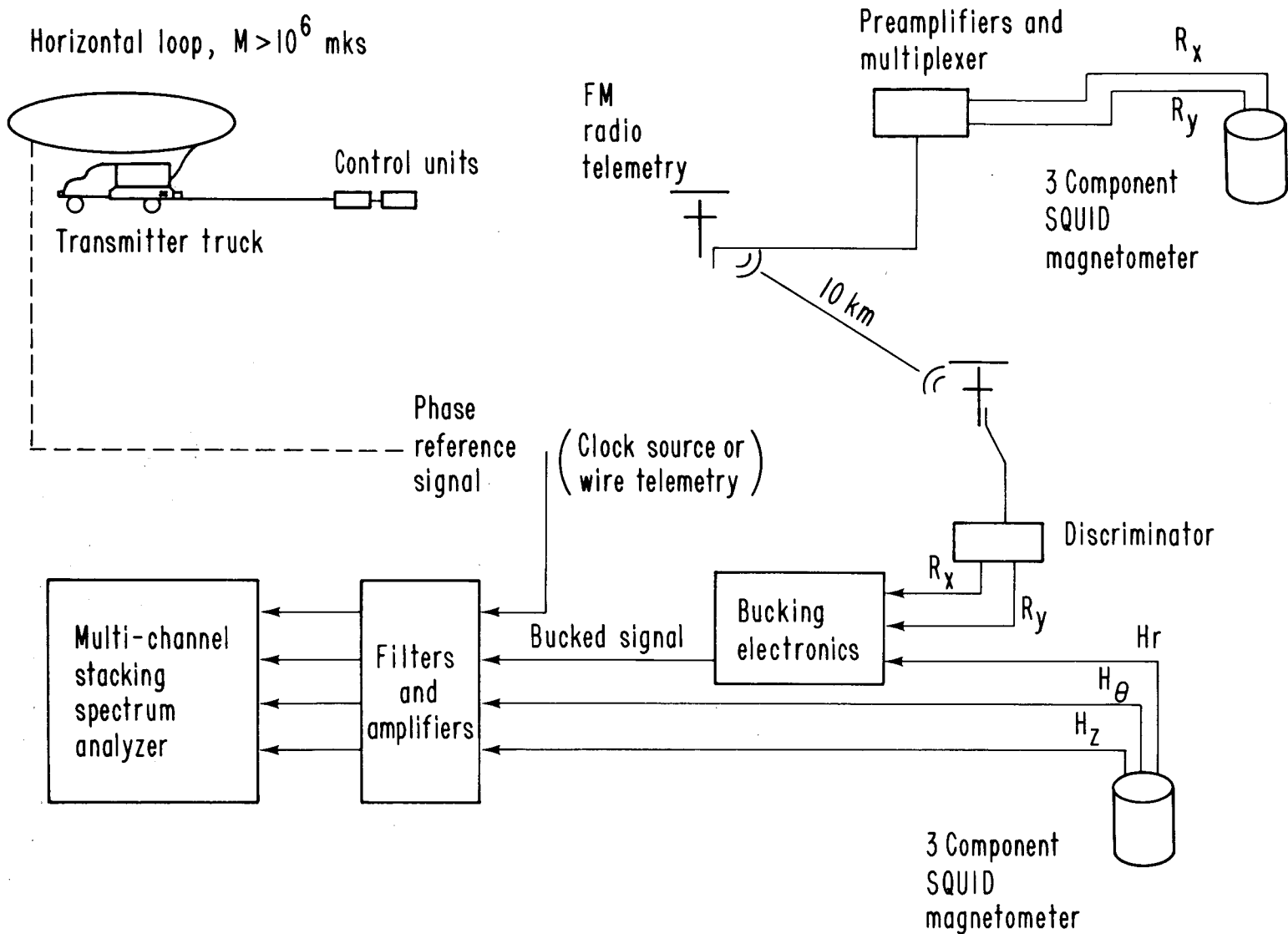


Figure A-1. Schematic diagram of the EM-60 system.

current; and a receiver section consisting of magnetic or a combination of magnetic and electric-field detectors, signal-conditioning amplifiers, anti-alias filters, and a multichannel programmable receiver (spectrum analyzer).

Transmitter System

The EM-60 transmitter is powered by a Hercules gasoline engine linked to a 60 kW, 400 Hz, 3 ϕ aircraft alternator. The two components are mounted in the bed of a 1 ton, four-wheel-drive truck. The output is full-wave rectified and capable of providing ± 150 V at up to 400 A to the horizontal coil. The square-wave current pulses are created by means of a transistorized switch, which consists of two parallel arrays of from 6 to 60 transistors in interchangeable modules within the "crate" (the lower, outward-pivoting box in Figure A-2).

The dipole moment, which is a measure of the strength of the signal, is determined by the resistance and inductance of the loop. At frequencies below 50 Hz, inductive reactance is negligible and the dipole moment is governed by the load resistance. Four turns of no. 6 wire in a square or circular loop 50 m in radius will yield a dipole moment of about 3×10^6 mks. This provides adequate signal for soundings where transmitter-receiver separations are less than about 5 km, which corresponds to a maximum depth of exploration of about 5 km. At frequencies above about 100 Hz, the inductance causes the moment to decrease and the current waveform to become quasi-sinusoidal. High frequency information is thus more difficult to obtain at large transmitter-receiver separations.



Figure A-2. The EM-60 transmitter.

CBB 789-12736

Receiver Section

For the 50 m transmitter loop normally used in geothermal prospecting, the fields can be detected as much as 5 km away from the transmitter by means of a three-component SQUID magnetometer oriented to measure the vertical, radial, and tangential components with respect to the loop. Signals are amplified, anti-alias filtered, and inputted to a six-channel, programmable, multifrequency phase-sensitive receiver (Figure A-1). Through the receiver key-pad, the operator sets the following parameters controlling signal processing: (1) fundamental period of the waveform to be processed; (2) maximum number of harmonics to be analyzed, up to 15; (3) number of cycles in increments of 2^N to be stacked prior to Fourier decomposition; and (4) number of input channels of data to be processed. Processing results in a raw amplitude estimate for each component and a phase estimate relative to the phase of the current in the loop. Phase referencing is maintained with a hard-wire link between a shunt on the loop and the receiver, and this reference voltage is applied directly to channel 1 of the receiver for phase comparison. Raw amplitude estimates must be later corrected for dipole moment and distance between loop and magnetometer.

In practice, the hard-wire link was found to be a source of noise, particularly above 50 Hz. This has required the elimination of the absolute phase reference at high frequencies in favor of relative phase measurements between vertical and radial components. With relative phase measurements, interpretation is based on the ellipse polarization parameters (e.g., the ellipticity and tilt angle of the field ellipse traced out by the combined observed magnetic fields). Using relative phase measurements, data can often be obtained to much higher frequencies than absolute phase data. The dangers of using relative phase alone are that the observation errors

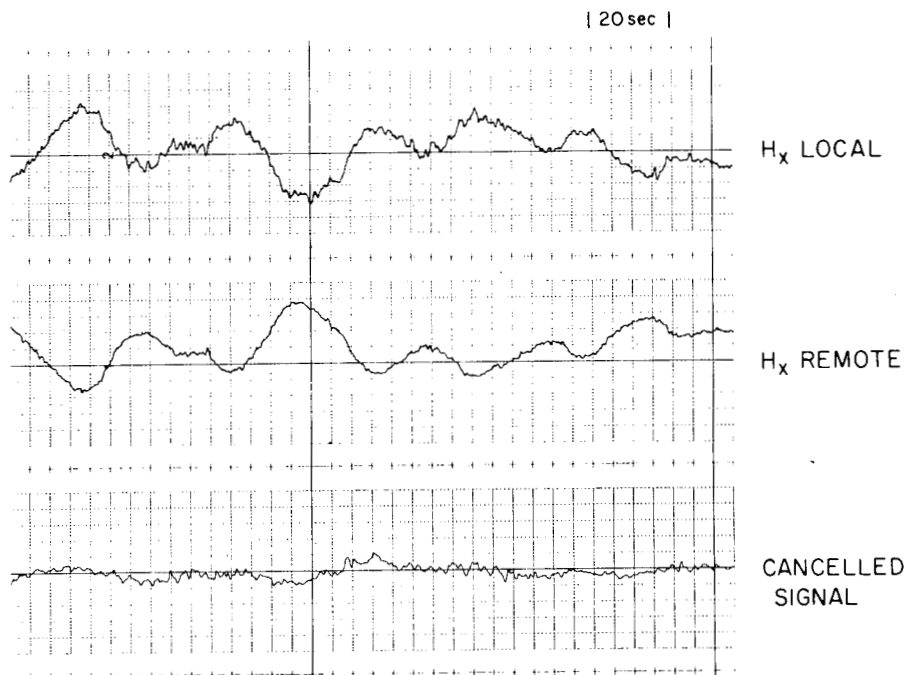
are larger than errors for the individual fields and that the interpreted spectra seem to be less sensitive to deeply buried horizons.

At low frequencies (<0.1 Hz), natural geomagnetic signal amplitude increases roughly as $1/f$ and the secondary (induced) magnetic field decreases as $1/f$. The net result is an effective signal-to-noise ratio that decreases as $1/f^2$, making noise cancellation imperative for recovery of low-frequency information. To cancel geomagnetic noise, a second (reference) magnetometer is placed far enough from the transmitter loop (usually at least 10 km) so that the observed remote fields will consist only of the geomagnetic fluctuations. Once installed, the reference magnetometer can often remain fixed over the course of a survey. The remote signals are transmitted to the mobile receiver station from the transmitter via FM radio telemetry. Before the loop is energized, the remote signals are inverted, adjusted in amplitude, and then added to the base station geomagnetic signal to produce essentially a null signal. A good example of this simple noise-cancellation scheme is shown in Figure A-3. The resulting signal-to-noise improvement of roughly 20 dB has allowed us to obtain reliable data to 0.05 Hz, a gain of three or four important data points on the sounding curve. These points are invaluable for resolving deeper horizons.

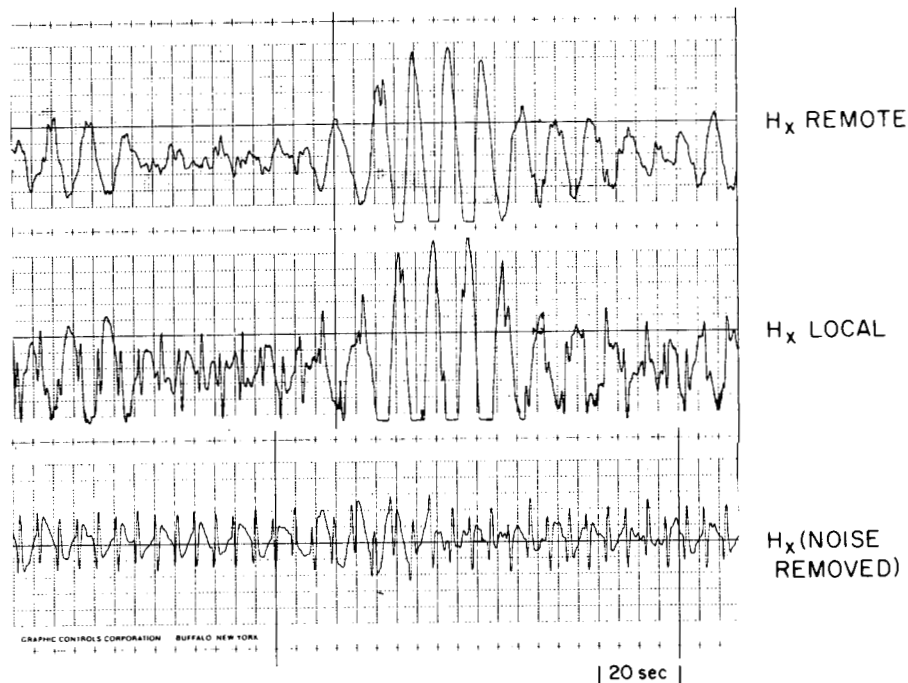
DATA INTERPRETATION

Apparent Resistivity Function

Apparent resistivity curves can be calculated from EM spectra by matching observed field data to generalized, homogeneous half-space curves. The generalized curves are a plot of field value versus induction number (B), which is a function of the frequency, transmitter-receiver separation, and resistivity of the half-space. A resistivity spectrum can therefore



A. NATURAL MAGNETIC
FIELD CANCELLATION



B. SAMPLE FIELD RECORD
TRANSMITTER FREQUENCY = 0.1 Hz

XBL 811-2584

Figure A-3. Example of data improvement using the telluric noise cancellation scheme. (A) Natural geomagnetic signal and initial cancelling at the receiver site with transmitter off. (B) Same system with transmitter on.

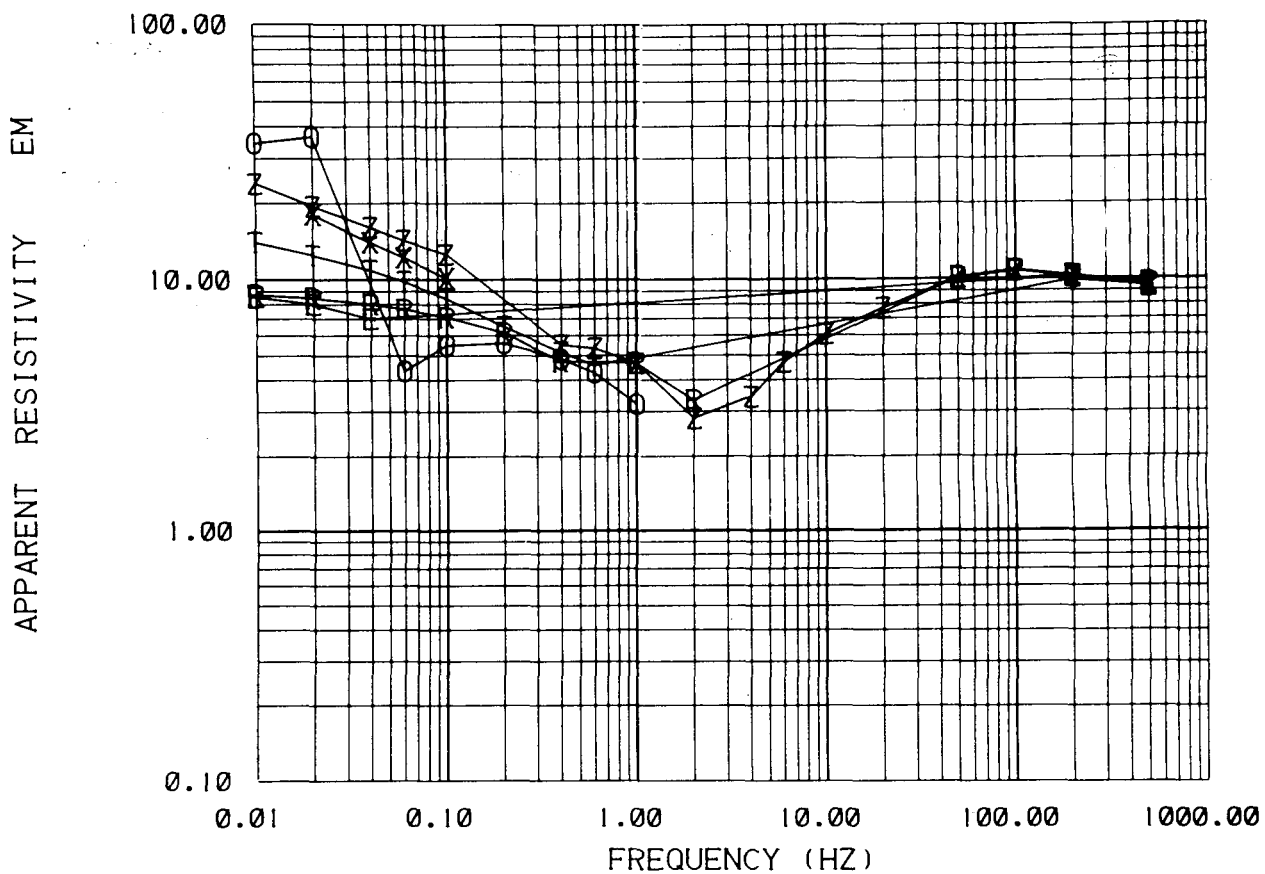
be obtained by matching observed data to the generalized curve and calculating the conductivity from the induction number. For a multilayered section, an apparent resistivity curve is obtained from this calculation.

An example of an apparent resistivity curve calculated from a three-layer model is given in Figure A-4; calculated for each type of measured data reflect the layered-model section shown at the bottom, although there is scatter between the curves. The curves are generally used for qualitative interpretation. They give asymptotic values for earth resistivities and indicate the resistivity type section, thus allowing more accurate "first guesses" for the layered-model inversion algorithm. The curves are also useful for evaluating data quality in the field and for isolating noisy data for deletion prior to inversion.

Layered-Model Inversion

Basic quantitative interpretation is accomplished by direct least-squares inversion of observed data to fit one-dimensional models. The program used fits amplitude-phase and/or ellipse polarization parameters jointly or separately using the Marquardt algorithm to fit arbitrarily layered models (Inman, 1975). This program allows the use of ellipse polarization parameters to fit high-frequency points separately where absolute phase data is much noisier while simultaneously using absolute phase data at the lower frequencies where the phase reference may allow for better parameter solution. Observed data are weighted by the standard deviation of field measurements. These are accurate representations of true error if noise sources are random. When sources are nonrandom, which is the usual case, the error estimates are probably somewhat low, thus leading to low estimates of parameter errors.

EM APPARENT RESISTIVITY PLOT



THREE LAYER R=5.0 KM

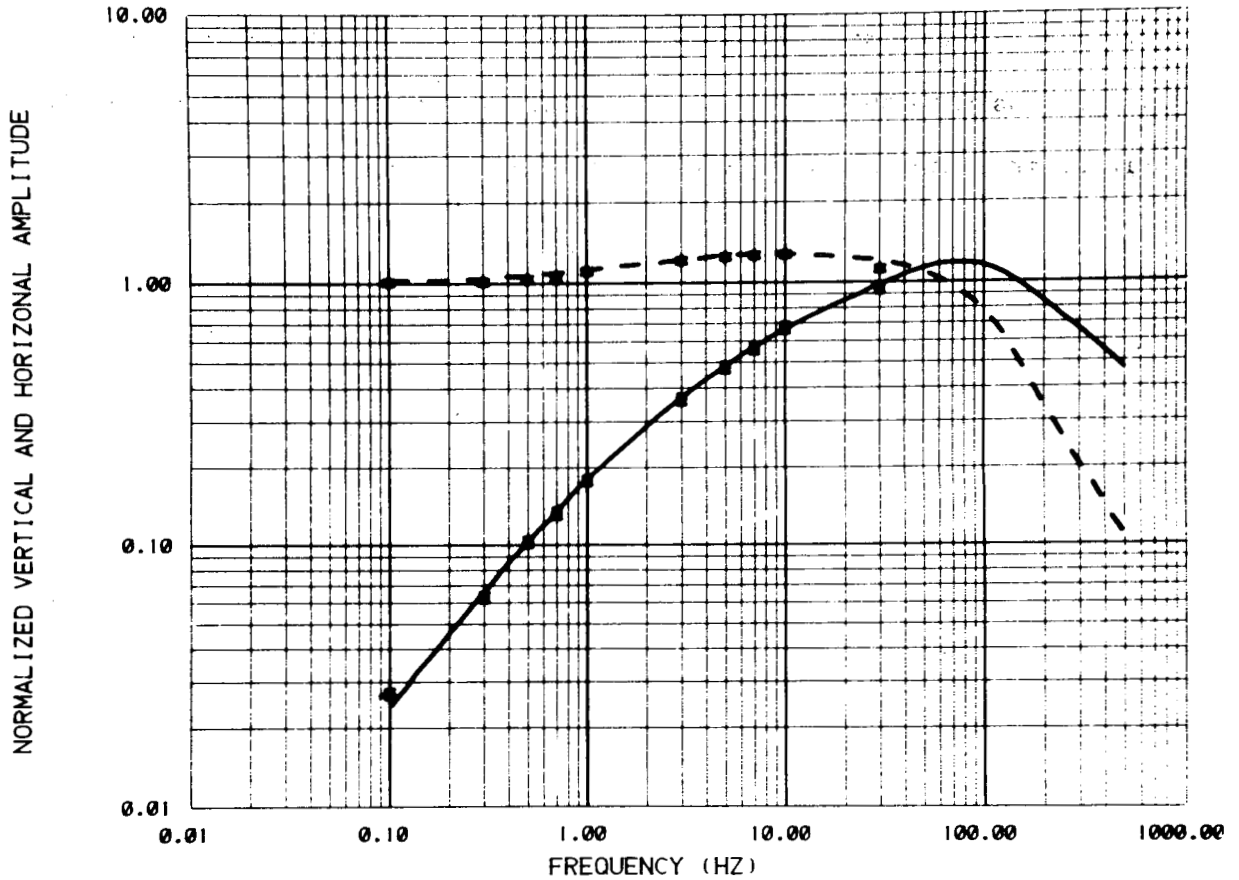
HZ	Z	LAYER	RESISTIVITY	THICKNESS
PHZ	O	1	10.00	200.00
HR	R	2	2.00	500.00
PHR	X	3	100.00	*****
ELL	E			
TILT	T			

XBL 8011-7519

Figure A-4. EM apparent resistivity spectra calculated from layered-model theoretical data.

An example of a layered-model inversion for an EM-60 sounding is given in Figures A-5 and A-6. The spectra shown, amplitude and ellipticity, are three of the six spectra normally calculated for a field sounding. The data were fit jointly to the two-layer model shown at the bottom of each figure. Note that amplitude data were interpreted to 30 Hz and that ellipticity was used to 500 Hz. Two-dimensional modeling, although currently possible, is cumbersome and prohibitively expensive (Lee, 1978).

COMPARISON OF CALCULATED AND MEASURED DATA



SODA LAKE .72 KM NW T1

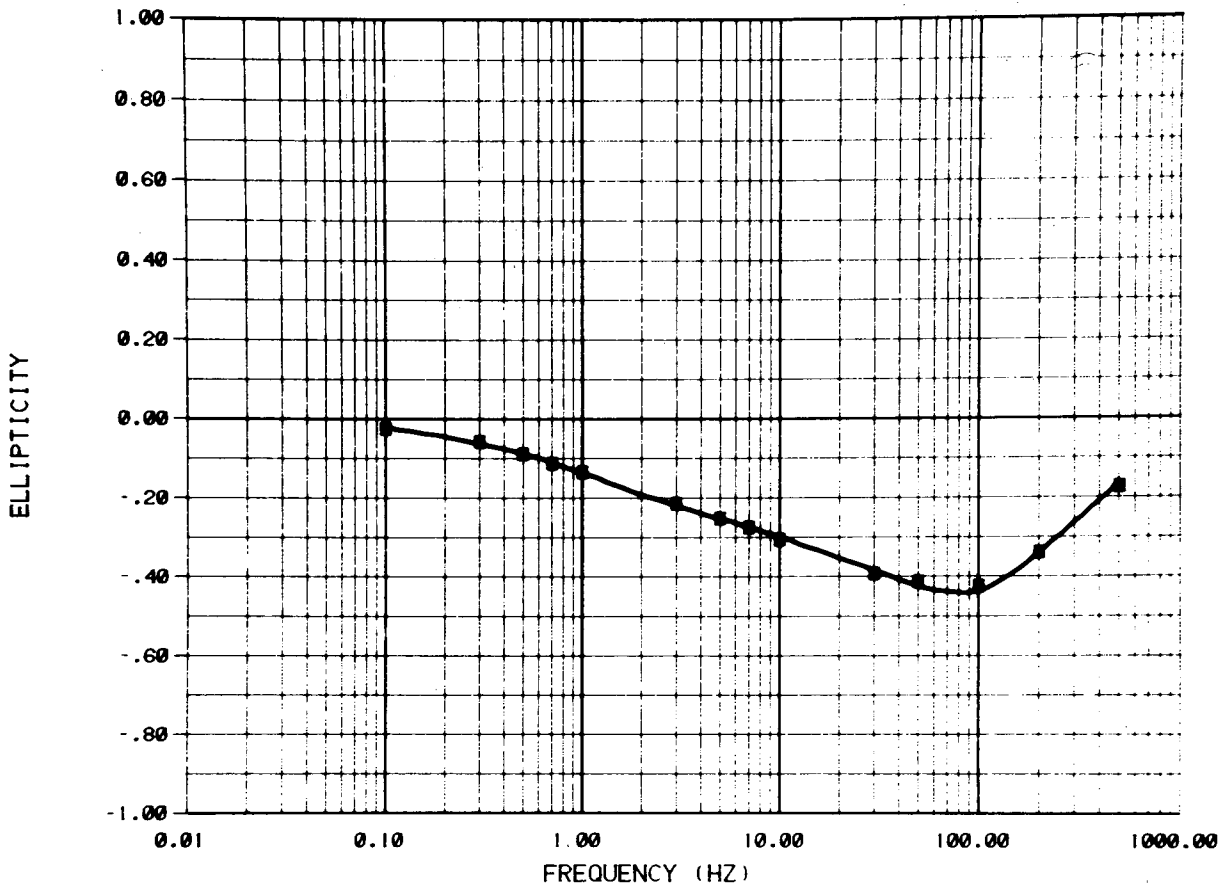
CALCULATED DATA		MEASURED DATA		LAYER	RESISTIVITY(OHM-M)	THICKNESS(M)
HR	—————	HR	X	1	12.11 ± .00	305.4 ± 2.
HZ	— — — —	HZ	*	2	1.77 ± .02	.1000E+11 ± 0.

DATA VARIANCE ESTIMATE 15.23

XBL 806-10148

Figure A-5. Example of EM-60 amplitude spectra fit to a two-layer model.

COMPARISON OF CALCULATED AND MEASURED DATA



SODA LAKE .72 KM NW T1

CALCULATED DATA	MEASURED DATA	LAYER	RESISTIVITY(OHM-M)	THICKNESS(M)
ELLIPTICITY ———	ELLIPTICITY X	1	12.11 ± .00	305.4 ± 2.
		2	1.77 ± .02	.1000E+11 ± 0.

DATA VARIANCE ESTIMATE 15.23

XBL 806-10150

Figure A-6. Example of EM-60 ellipticity spectra fit to a two-layer model.

REFERENCES

- Inman, J.R., 1975, Resistivity inversion with ridge regression: *Geophysics*, v. 40, no. 5, p. 798-817.
- Jain, B., 1978, A low frequency electromagnetic prospecting system: Ph.D. dissertation, Department of Engineering Geosciences, University of California, Berkeley, Lawrence Berkeley Laboratory, LBL-7042.
- Lee, K.H., 1978, Electromagnetic scattering by a two-dimensional inhomogeneity due to an oscillating magnetic dipole: Ph.D. dissertation, Department of Engineering Geosciences, University of California, Berkeley, Lawrence Berkeley Laboratory, LBL-8275.
- Morrison, H.F., N.E. Goldstein, N. Hoversten, G. Oppliger, and C. Riveros, 1978 Description, field test and data analysis of a controlled-source EM system (EM-60), Lawrence Berkeley Laboratory, LBL-7088.

APPENDIX B

FINAL WORKING DATA SET

station: mccoys tlr1 seperation=2200 meters
 number of turns=4 loop radius=50 meters
 hr mag const=7.936 hz mag const=7.092

frequency	hz amp	amp err	hz phase	phase err
0.050	1.037	0.014	180.489	0.484
0.100	1.000	0.017	181.133	0.211
0.150	1.008	0.002	180.529	0.550
0.300	1.027	0.002	180.000	0.000
0.500	1.047	0.002	181.120	0.120
0.700	1.077	0.002	180.800	0.000
1.000	1.115	0.001	179.540	0.220
3.000	1.293	0.033	166.310	0.223
5.000	1.286	0.002	149.000	0.245
7.000	1.326	0.068	132.900	0.245
10.000	1.206	0.025	113.000	0.000
30.000	0.368	0.002	73.600	0.192

frequency	hr amp	amp err	hr phase	phase err
0.050	0.049	0.004	233.933	21.655
0.100	0.038	0.004	229.133	4.349
0.150	0.068	0.009	240.829	5.042
0.300	0.112	0.003	246.333	1.706
0.500	0.171	0.008	242.600	1.030
0.700	0.208	0.007	246.200	0.927
1.000	0.310	0.006	245.140	0.571
3.000	0.768	0.004	226.870	0.437
5.000	1.067	0.009	208.736	0.518
7.000	1.303	0.062	194.132	0.869
10.000	1.587	0.033	172.200	0.200
30.000	1.500	0.007	126.200	0.837

frequency	ellipticity	ellip err	tilt angle	tilt err
0.050	-0.026	0.012	89.592	0.409
0.100	-0.027	0.003	88.515	0.252
0.150	-0.057	0.009	88.135	0.319
0.300	-0.099	0.004	87.498	0.118
0.500	-0.143	0.008	85.472	0.166
0.700	-0.174	0.006	85.279	0.143
1.000	-0.249	0.005	83.024	0.207
3.000	-0.465	0.010	68.874	0.759
5.000	-0.555	0.009	55.208	0.323
7.000	-0.584	0.011	45.825	3.200
10.000	-0.530	0.002	30.746	0.076
30.000	-0.190	0.002	8.783	0.153
30.000	-0.196	0.009	5.737	1.273
50.000	-0.141	0.002	5.685	0.112
100.000	-0.118	0.002	3.198	0.106
200.000	-0.076	0.004	0.285	0.088

station: mccoys tir2 separation=1150 meters
 number of turns=4 loop radius=50 meters
 hr mag const=7.936 hz mag const=7.092

frequency	hz amp	amp err	hz phase	phase err
0.100	1.030	0.000	179.000	0.000
0.300	1.036	0.001	180.000	0.000
0.500	1.045	0.001	180.000	0.000
0.700	1.052	0.001	180.133	0.211
1.000	1.052	0.000	181.400	0.164
3.000	1.133	0.001	181.387	0.201
5.000	1.233	0.001	178.160	0.024
7.000	1.322	0.002	173.167	0.211
10.000	1.398	0.000	164.400	0.245
30.000	1.234	0.001	102.200	0.000
50.000	0.524	0.000	32.050	0.250

frequency	hr amp	amp err	hr phase	phase err
0.100	0.060	0.001	348.800	0.516
0.300	0.067	0.002	324.667	1.726
0.500	0.080	0.003	314.889	3.867
0.700	0.098	0.004	300.300	1.910
1.000	0.129	0.001	295.200	0.374
3.000	0.320	0.001	268.770	0.000
5.000	0.496	0.001	244.000	0.245
7.000	0.645	0.003	230.833	0.422
10.000	0.813	0.001	214.000	0.000
30.000	1.075	0.001	142.200	0.000
50.000	0.575	0.001	69.750	0.029

frequency	ellipticity	ellip err	tilt angle	tilt err
0.100	-0.011	0.001	93.257	0.036
0.300	-0.037	0.002	93.000	0.104
0.500	-0.053	0.005	93.051	0.210
0.700	-0.080	0.004	92.670	0.147
1.000	-0.112	0.001	92.859	0.041
3.000	-0.277	0.001	86.771	0.058
5.000	-0.356	0.001	79.288	0.073
7.000	-0.381	0.003	72.791	0.250
10.000	-0.379	0.002	65.662	0.069
30.000	-0.359	0.000	50.135	0.034
50.000	-0.340	0.002	41.612	0.045
50.000	-0.343	0.002	42.034	0.114
100.000	-0.181	0.002	31.310	0.109
200.000	-0.142	0.006	34.900	0.849
500.000	-0.080	0.022	33.422	0.676

station: mccoys tir3 seperation=2000 meters
 number of turns=4 loop radius=50 meters
 hr mag const=7.936 hz mag const=7.092

frequency	hz amp	amp err	hz phase	phase err
0.050	1.095	0.006	181.643	0.166
0.100	0.999	0.001	180.800	0.000
0.150	1.007	0.020	181.257	0.143
0.300	1.001	0.002	180.450	0.148
0.500	1.018	0.001	180.750	0.157
0.700	1.043	0.004	180.800	0.000
1.000	1.042	0.000	178.864	0.021
3.000	1.118	0.001	170.360	0.046
5.000	1.143	0.002	159.000	0.245
7.000	1.129	0.001	148.300	0.200
10.000	1.028	0.000	132.000	4.472
30.000	0.414	0.009	52.533	0.211
50.000	0.095	0.002	-16.200	0.707

frequency	hr amp	amp err	hr phase	phase err
0.050	0.054	0.006	310.314	18.965
0.100	0.046	0.002	329.371	2.159
0.150	0.044	0.003	303.829	7.151
0.300	0.063	0.002	291.333	3.997
0.500	0.088	0.003	280.500	3.052
0.700	0.112	0.003	270.200	0.927
1.000	0.162	0.001	268.200	0.583
3.000	0.412	0.003	242.170	0.245
5.000	0.621	0.007	225.800	0.200
7.000	0.771	0.007	213.700	1.020
10.000	0.891	0.009	195.000	0.000
30.000	0.849	0.022	119.283	0.271
50.000	0.429	0.004	58.725	0.601

frequency	ellipticity	ellip err	tilt angle	tilt err
0.050	-0.026	0.008	91.023	0.829
0.100	-0.024	0.002	92.254	0.103
0.150	-0.035	0.003	91.334	0.289
0.300	-0.058	0.002	91.304	0.254
0.500	-0.085	0.003	90.831	0.244
0.700	-0.107	0.003	89.929	0.100
1.000	-0.155	0.001	89.893	0.096
3.000	-0.345	0.003	82.540	0.041
5.000	-0.471	0.005	74.375	0.267
7.000	-0.552	0.009	66.668	0.769
10.000	-0.603	0.051	54.608	1.362
30.000	-0.429	0.004	13.414	0.238
50.000	-0.212	0.002	3.448	0.322
50.000	-0.195	0.004	7.565	0.071
100.000	0.006	0.029	-11.300	0.407

station: mccoys tir4 separation=1450 meters
 number of turns=4 loop radius=50 meters
 hr mag const=7.936 hz mag const=7.092

frequency	hz amp	amp err	hz phase	phase err
0.100	1.005	0.001	179.893	0.093
0.300	1.013	0.000	179.571	0.202
0.500	1.022	0.001	179.500	0.189
0.700	1.030	0.001	178.800	0.000
1.000	1.032	0.000	178.000	0.000
3.000	1.056	0.001	170.603	0.307
5.000	1.060	0.003	162.848	0.479
7.000	1.043	0.005	155.833	0.667
10.000	0.947	0.001	141.000	0.000
30.000	0.616	0.003	79.920	0.235

frequency	hr amp	amp err	hr phase	phase err
0.100	0.065	0.004	350.904	1.767
0.300	0.067	0.001	336.286	1.169
0.500	0.071	0.002	320.625	2.299
0.700	0.074	0.002	310.657	1.610
1.000	0.090	0.000	297.833	0.307
3.000	0.191	0.001	258.253	0.347
5.000	0.282	0.002	239.720	0.483
7.000	0.361	0.003	225.500	0.730
10.000	0.406	0.001	201.083	0.083
30.000	0.401	0.006	118.160	0.549

frequency	ellipticity	ellip err	tilt angle	tilt err
0.100	-0.010	0.002	93.647	0.247
0.300	-0.026	0.001	93.460	0.084
0.500	-0.044	0.003	93.086	0.105
0.700	-0.053	0.002	92.739	0.073
1.000	-0.075	0.001	92.493	0.020
3.000	-0.181	0.001	89.560	0.062
5.000	-0.258	0.001	86.292	0.048
7.000	-0.320	0.002	82.339	0.174
10.000	-0.353	0.001	76.177	0.052
30.000	-0.310	0.007	59.700	0.400
30.000	-0.306	0.003	53.681	0.402
50.000	-0.200	0.005	44.905	0.086
100.000	-0.111	0.006	33.314	0.342

station: mccoys tir5 seperation=2200 meters
 number of turns=4 loop radius=50 meters
 hr mag const=7.936 hz mag const=7.092

frequency	hz amp	amp err	hz phase	phase err
0.050	1.002	0.006	180.450	0.375
0.100	0.948	0.023	180.129	0.130
0.150	1.008	0.001	180.975	0.118
0.300	0.961	0.022	179.386	0.156
0.500	0.953	0.024	179.100	0.237
0.700	0.983	0.031	177.540	0.121
1.000	1.089	0.001	176.000	0.000
3.000	1.137	0.002	158.370	0.245
5.000	1.083	0.003	140.700	0.100
7.000	1.028	0.065	125.783	0.317
10.000	0.669	0.001	107.420	0.180
30.000	0.181	0.008	78.967	0.881

frequency	hr amp	amp err	hr phase	phase err
0.050	0.058	0.007	200.471	4.667
0.100	0.058	0.005	216.371	2.531
0.150	0.083	0.005	223.900	2.506
0.300	0.106	0.005	230.629	2.101
0.500	0.151	0.007	236.467	1.004
0.700	0.194	0.010	238.600	1.319
1.000	0.295	0.001	242.440	0.413
3.000	0.710	0.004	228.250	0.326
5.000	0.983	0.007	213.460	0.368
7.000	1.220	0.088	200.883	0.392
10.000	1.066	0.002	185.900	0.100
30.000	0.872	0.039	156.033	0.307

frequency	ellipticity	ellip err	tilt angle	tilt err
0.050	-0.018	0.004	86.930	0.432
0.100	-0.035	0.002	87.135	0.275
0.150	-0.055	0.003	86.536	0.310
0.300	-0.085	0.003	86.032	0.285
0.500	-0.132	0.004	85.018	0.250
0.700	-0.170	0.007	84.437	0.110
1.000	-0.245	0.001	83.435	0.104
3.000	-0.549	0.004	72.420	0.343
5.000	-0.725	0.004	54.033	0.540
7.000	-0.731	0.007	28.316	0.601
10.000	-0.599	0.002	11.210	0.182
30.000	-0.202	0.002	2.774	0.128
50.000	-0.120	0.000	2.167	0.115
100.000	-0.066	0.004	1.012	0.164
150.000	-0.078	0.015	0.439	0.920
200.000	-0.046	0.011	1.676	0.441

station: mccoys tir6 separation=4050 meters
 number of turns=4 loop radius=50 meters
 hr mag const=7.936 hz mag const=7.092

frequency	hz amp	amp err	hz phase	phase err
0.100	1.171	0.011	185.950	0.461
0.300	1.064	0.010	177.500	0.189
0.500	1.145	0.009	181.300	0.398
0.700	1.274	0.008	177.941	0.640
1.000	1.306	0.011	166.143	0.800
3.000	1.102	0.019	129.199	0.896
5.000	0.829	0.019	104.725	2.133
7.000	0.551	0.031	78.318	2.178
10.000	0.347	0.002	56.333	0.715
30.000	0.197	0.014	54.033	3.301

frequency	hr amp	amp err	hr phase	phase err
0.100	0.183	0.009	252.388	5.135
0.300	0.424	0.022	231.738	2.388
0.500	0.537	0.036	223.878	2.766
0.700	0.581	0.016	224.688	2.896
1.000	0.788	0.012	217.300	2.131
3.000	1.163	0.057	185.627	2.641
5.000	1.137	0.080	168.600	3.071
7.000	1.196	0.079	152.136	4.925
10.000	0.906	0.011	142.833	1.302
30.000	0.777	0.006	114.667	1.303

frequency	ellipticity	ellip err	tilt angle	tilt err
0.100	-0.138	0.007	86.371	0.774
0.300	-0.301	0.016	75.634	1.152
0.500	-0.279	0.029	69.443	1.450
0.700	-0.295	0.013	70.974	1.300
1.000	-0.399	0.022	65.241	0.769
3.000	-0.530	0.034	43.522	2.878
5.000	-0.554	0.040	28.807	4.517
7.000	-0.421	0.038	9.817	3.594
10.000	-0.382	0.006	1.581	0.653
10.000	-0.374	0.004	4.100	0.466
25.000	-0.136	0.009	2.371	0.667
25.000	-0.115	0.011	3.053	1.364
30.000	-0.216	0.017	7.491	0.919
50.000	-0.105	0.006	0.930	0.441
100.000	-0.024	0.005	-0.717	1.071

station: mccoys tir7 seperation=550 meters
 number of turns=4 loop radius=50 meters
 hr mag const=7.936 hz mag const=7.092

frequency	hz amp	amp err	hz phase	phase err
1.000	1.000	0.001	171.833	0.167
3.000	0.993	0.000	178.770	0.000
5.000	1.000	0.001	180.600	0.000
7.000	1.007	0.002	182.500	0.000
10.000	1.012	0.000	183.000	0.000
30.000	1.220	0.000	186.200	0.000
50.000	1.533	0.000	181.800	0.000
100.000	1.356	0.001	166.000	0.000
200.000	0.485	0.003	179.100	0.000
300.000	0.387	0.037	180.800	0.645

frequency	hr amp	amp err	hr phase	phase err
1.000	0.064	0.000	247.333	0.333
3.000	0.180	0.000	255.770	0.000
5.000	0.295	0.000	253.267	0.333
7.000	0.404	0.001	250.000	0.289
10.000	0.549	0.000	244.000	0.000
30.000	1.041	0.001	216.867	0.333
50.000	1.075	0.001	206.133	0.333
100.000	1.339	0.000	208.333	0.333
200.000	0.647	0.004	222.100	0.000
300.000	0.587	0.010	226.725	0.813

frequency	ellipticity	ellip err	tilt angle	tilt err
1.000	-0.061	0.000	89.085	0.019
3.000	-0.177	0.000	87.584	0.006
5.000	-0.280	0.001	84.540	0.093
7.000	-0.361	0.001	79.940	0.093
10.000	-0.436	0.000	71.664	0.006
30.000	-0.270	0.003	50.260	0.034
50.000	-0.202	0.003	55.859	0.048
100.000	-0.387	0.003	45.478	0.029
200.000	-0.373	0.000	34.110	0.020
300.000	-0.371	0.021	29.107	3.012
500.000	-0.352	0.015	20.466	0.795
1000.000	-0.277	0.001	11.231	0.000

station: mccoys t2r1 seperation=2200 meters
 number of turns=4 loop radius=50 meters
 hr mag const=7.936 hz mag const=7.092

frequency	hz amp	amp err	hz phase	phase err
0.100	1.000	0.004	181.527	0.359
0.300	0.971	0.002	181.025	0.204
0.500	0.990	0.006	183.800	0.107
0.700	1.033	0.004	184.572	0.305
1.000	1.045	0.002	182.383	0.079
3.000	1.166	0.002	178.670	0.159
5.000	1.242	0.004	171.433	0.401
7.000	1.232	0.056	163.500	0.577
10.000	1.313	0.001	141.400	0.245
30.000	0.516	0.005	198.000	0.490

frequency	hr amp	amp err	hr phase	phase err
0.100	0.073	0.002	355.436	2.777
0.300	0.077	0.006	317.250	3.807
0.500	0.081	0.007	313.300	4.987
0.700	0.090	0.006	294.800	2.989
1.000	0.131	0.002	274.833	1.167
3.000	0.282	0.003	236.437	1.054
5.000	0.386	0.006	214.600	1.528
7.000	0.547	0.029	200.214	1.523
10.000	0.793	0.006	186.200	0.200
30.000	0.779	0.009	53.800	0.430

frequency	ellipticity	ellip err	tilt angle	tilt err
0.100	-0.007	0.004	94.084	0.125
0.300	-0.055	0.007	93.153	0.167
0.500	-0.064	0.008	92.756	0.233
0.700	-0.080	0.005	91.773	0.297
1.000	-0.125	0.002	90.312	0.152
3.000	-0.201	0.003	82.340	0.263
5.000	-0.211	0.008	75.662	0.504
7.000	-0.233	0.011	69.211	0.876
10.000	-0.350	0.002	63.270	0.184
30.000	-0.283	0.006	29.249	0.376
50.000	-0.222	0.002	15.249	0.333
100.000	-0.125	0.134	-9.882	6.377
200.000	-0.064	0.013	0.644	1.336

station: mccoys t2r2 seperation=448 meters
 number of turns=4 loop radius=50 meters
 hr mag const=7.936 hz mag const=7.092

frequency	hz amp	amp err	hz phase	phase err
1.000	1.001	0.000	171.000	0.000
3.000	0.994	0.000	176.770	0.000
5.000	1.004	0.000	177.400	0.200
7.000	1.011	0.001	177.700	0.200
10.000	1.034	0.001	175.000	0.000
30.000	1.359	0.000	160.400	0.122
50.000	1.959	0.002	130.020	0.020
100.000	1.726	0.001	128.250	0.250
200.000	1.893	0.017	101.300	0.374

frequency	hr amp	amp err	hr phase	phase err
1.000	0.118	0.000	185.860	0.040
3.000	0.124	0.000	196.770	0.000
5.000	0.136	0.000	206.060	0.160
7.000	0.154	0.000	213.800	0.184
10.000	0.183	0.000	220.600	0.164
30.000	0.461	0.001	223.154	0.039
50.000	0.811	0.002	212.100	0.063
100.000	1.425	0.001	205.000	0.000
200.000	1.799	0.015	179.300	0.374

frequency	ellipticity	ellip err	tilt angle	tilt err
1.000	-0.030	0.000	83.522	0.005
3.000	-0.042	0.000	83.324	0.006
5.000	-0.064	0.000	83.203	0.026
7.000	-0.088	0.001	82.934	0.033
10.000	-0.125	0.001	82.829	0.010
30.000	-0.294	0.001	80.321	0.032
50.000	-0.407	0.001	85.695	0.023
100.000	-0.738	0.002	65.069	0.278
200.000	-0.805	0.000	51.871	0.135
500.000	-0.585	0.006	4.033	0.274
1000.000	-0.189	0.001	-8.196	0.054

station: mccoys t2r3 seperation=1650 meters
 number of turns=4 loop radius=50 meters
 hr mag const=7.936 hz mag const=7.092

frequency	hz amp	amp err	hz phase	phase err
0.100	1.000	0.003	178.750	0.250
0.300	1.006	0.001	180.840	0.103
0.500	1.019	0.004	182.175	0.175
0.700	1.027	0.005	183.040	0.040
1.000	1.136	0.140	183.185	0.108
3.000	1.052	0.000	187.520	0.136
5.000	1.119	0.002	189.600	0.245
7.000	1.183	0.004	191.000	0.000
10.000	1.241	0.001	187.680	0.171
30.000	1.892	0.008	184.740	0.549
50.000	2.936	0.022	152.800	0.583
100.000	1.961	0.004	130.800	0.200
200.000	1.023	0.019	154.800	0.000

frequency	hr amp	amp err	hr phase	phase err
0.100	0.168	0.002	186.250	0.250
0.300	0.172	0.007	184.600	1.503
0.500	0.183	0.007	190.250	0.250
0.700	0.174	0.007	191.200	2.354
1.000	0.207	0.026	196.000	0.408
3.000	0.229	0.002	213.800	0.735
5.000	0.297	0.001	226.600	0.510
7.000	0.368	0.006	232.200	0.583
10.000	0.481	0.000	230.500	0.237
30.000	1.280	0.006	232.600	0.245
50.000	2.598	0.015	203.600	0.600
100.000	2.587	0.006	187.000	0.000
200.000	2.081	0.040	215.200	0.860

frequency	ellipticity	ellip err	tilt angle	tilt err
0.100	-0.021	0.001	80.560	0.132
0.300	-0.010	0.005	80.341	0.403
0.500	-0.024	0.001	79.942	0.357
0.700	-0.023	0.006	80.515	0.379
1.000	-0.039	0.001	79.931	0.118
3.000	-0.093	0.003	78.887	0.082
5.000	-0.153	0.003	77.733	0.091
7.000	-0.194	0.003	76.286	0.304
10.000	-0.243	0.001	73.113	0.045
30.000	-0.399	0.004	60.447	0.103
50.000	-0.469	0.002	50.496	0.072
100.000	-0.500	0.002	31.615	0.046
200.000	-0.399	0.002	16.307	0.079
200.000	-0.415	0.004	13.958	0.217
500.000	-0.169	0.006	2.537	0.699

station: mccoys t2r4 separation=1550 meters
 number of turns=4 loop radius=50 meters
 hr mag const=7.936 hz mag const=7.092

frequency	hz amp	amp err	hz phase	phase err
0.050	1.006	0.008	179.350	1.031
0.100	1.015	0.001	179.800	0.000
0.150	1.017	0.001	180.375	0.025
0.300	1.030	0.001	180.500	0.224
0.500	0.996	0.034	180.667	0.211
0.700	1.036	0.003	181.300	0.224
1.000	1.031	0.002	182.992	0.038
3.000	1.109	0.003	184.670	0.184
5.000	1.208	0.004	185.000	0.000
7.000	1.284	0.055	184.560	1.083
10.000	1.368	0.003	177.450	0.263
30.000	1.726	0.016	90.750	0.250
50.000	0.923	0.004	66.000	0.000

frequency	hr amp	amp err	hr phase	phase err
0.050	0.035	0.004	177.850	4.589
0.100	0.043	0.001	186.467	2.539
0.150	0.043	0.002	192.025	1.675
0.300	0.046	0.004	195.000	3.679
0.500	0.052	0.003	203.833	1.424
0.700	0.052	0.002	203.133	3.242
1.000	0.057	0.001	215.600	0.748
3.000	0.112	0.001	234.980	0.436
5.000	0.169	0.001	236.520	0.700
7.000	0.230	0.011	236.740	1.392
10.000	0.295	0.000	227.125	0.125
30.000	0.609	0.010	140.500	0.500
50.000	0.393	0.003	120.000	0.000

frequency	ellipticity	ellip err	tilt angle	tilt err
0.050	0.000	0.002	88.044	0.241
0.100	-0.005	0.002	87.596	0.080
0.150	-0.008	0.001	87.616	0.110
0.300	-0.011	0.002	87.539	0.220
0.500	-0.020	0.001	87.234	0.154
0.700	-0.018	0.003	87.349	0.130
1.000	-0.030	0.001	87.347	0.038
3.000	-0.078	0.001	86.276	0.051
5.000	-0.109	0.002	84.966	0.053
7.000	-0.140	0.005	83.607	0.123
10.000	-0.161	0.001	81.836	0.061
30.000	-0.255	0.004	76.237	0.103
50.000	-0.322	0.003	74.266	0.188
100.000	-0.471	0.002	67.241	0.408
200.000	-0.799	0.012	4.104	1.819

station: mccoys t2r5 seperation=2150 meters
 number of turns=50 loop radius=4 meters
 hr mag const=7.936 hz mag const=7.092

frequency	ellipticity	ellip err	tilt angle	tilt err
0.100	-0.016	0.007	84.519	0.355
0.300	-0.044	0.006	83.045	0.471
0.500	-0.082	0.016	82.030	0.690
0.700	-0.102	0.011	82.458	0.298
1.000	-0.133	0.001	81.989	0.228
3.000	-0.283	0.004	75.457	0.093
5.000	-0.364	0.003	69.323	0.194
7.000	-0.418	0.007	64.390	0.899
10.000	-0.447	0.003	56.394	0.026
30.000	-0.520	0.003	30.514	0.146
50.000	-0.462	0.015	16.560	1.335
100.000	-0.276	0.001	1.076	0.071
200.000	-0.078	0.004	0.734	0.290

station: mccoys t2r6 seperation=3000 meters
 number of turns=4 loop radius=50 meters
 hr mag const=7.936 hz mag const=7.092

frequency	ellipticity	ellip err	tilt angle	tilt err
0.100	-0.005	0.013	84.535	0.986
0.300	-0.042	0.004	81.572	0.522
0.500	-0.026	0.019	82.239	0.688
0.700	-0.028	0.014	82.682	0.646
1.000	-0.096	0.003	81.736	0.289
1.000	-0.120	0.010	81.787	0.330
3.000	-0.222	0.022	75.606	0.720
5.000	-0.267	0.008	73.027	1.084
7.000	-0.306	0.008	66.519	1.803
10.000	-0.385	0.004	61.330	0.259
30.000	-0.527	0.007	43.333	0.587
50.000	-0.558	0.008	28.265	0.994
100.000	-0.425	0.002	4.619	0.318
200.000	-0.205	0.004	4.261	0.316
500.000	-0.306	0.030	6.460	1.998

station: mccoys t3r1 seperation=548 meters
 number of turns=4 loop radius=50 meters
 hr mag const=7.936 hz mag const=7.092

frequency	hz amp	amp err	hz phase	phase err
1.000	0.999	0.001	180.680	0.000
3.000	1.011	0.001	181.793	0.008
5.000	1.031	0.000	182.406	0.006
10.000	1.054	0.010	181.669	0.014
30.000	1.181	0.001	180.377	0.017
50.000	1.375	0.000	176.750	0.150
70.000	1.322	0.004	174.000	0.000
100.000	1.738	0.012	200.500	0.645
200.000	1.033	0.002	227.200	0.200

frequency	hr amp	amp err	hr phase	phase err
1.000	0.069	0.000	348.750	0.854
3.000	0.077	0.001	329.500	1.258
5.000	0.094	0.002	314.200	1.393
10.000	0.117	0.005	288.250	0.750
30.000	0.305	0.016	259.500	0.866
50.000	0.538	0.000	249.000	0.000
70.000	0.474	0.038	234.000	1.732
100.000	1.368	0.009	266.750	0.854
200.000	1.192	0.003	289.400	0.245

frequency	ellipticity	ellip err	tilt angle	tilt err
1.000	-0.014	0.001	93.851	0.006
3.000	-0.041	0.002	93.702	0.007
5.000	-0.067	0.003	93.463	0.011
10.000	-0.106	0.004	91.827	0.013
30.000	-0.253	0.014	87.057	0.067
50.000	-0.367	0.000	82.125	0.061
70.000	-0.300	0.028	78.878	0.486
100.000	-0.611	0.003	60.471	0.127
200.000	-0.591	0.002	36.475	0.060
300.000	-0.559	0.004	21.775	4.305
500.000	-0.383	0.001	16.181	0.076
1000.000	-0.232	0.001	8.576	0.048

station: mccoys t3r2 separation=1350 meters
 number of turns=4 loop radius=50 meters
 hr mag const=7.936 hz mag const=7.092

frequency	hz amp	amp err	hz phase	phase err
0.100	1.008	0.029	182.520	0.183
0.300	0.990	0.007	182.160	0.160
0.500	0.997	0.008	182.414	0.296
0.700	0.999	0.008	182.620	0.353
1.000	1.000	0.000	182.980	0.012
3.000	1.114	0.000	182.098	0.026
5.000	1.188	0.001	178.940	0.051
7.000	1.245	0.001	174.500	0.000
10.000	1.409	0.001	169.600	0.245
30.000	1.471	0.015	128.600	2.462
50.000	1.317	0.010	71.400	0.400
100.000	0.593	0.002	6.200	0.200

frequency	hr amp	amp err	hr phase	phase err
0.100	0.068	0.004	191.000	2.510
0.300	0.073	0.002	196.200	1.281
0.500	0.081	0.002	203.000	1.949
0.700	0.082	0.003	211.200	1.778
1.000	0.099	0.000	216.800	0.200
3.000	0.194	0.000	226.770	0.000
5.000	0.274	0.001	225.600	0.447
7.000	0.350	0.002	222.100	0.510
10.000	0.478	0.001	217.200	0.200
30.000	0.904	0.009	177.600	0.245
50.000	1.114	0.011	123.000	0.663
100.000	0.838	0.001	35.700	0.200

frequency	ellipticity	ellip err	tilt angle	tilt err
0.100	-0.011	0.003	86.220	0.165
0.300	-0.018	0.001	85.926	0.142
0.500	-0.020	0.002	85.626	0.150
0.700	-0.039	0.003	85.867	0.182
1.000	-0.055	0.000	85.277	0.023
3.000	-0.121	0.000	82.834	0.014
5.000	-0.163	0.001	80.764	0.078
7.000	-0.200	0.001	78.813	0.153
10.000	-0.237	0.002	76.321	0.094
30.000	-0.387	0.021	63.973	0.645
50.000	-0.473	0.004	52.581	0.190
100.000	-0.246	0.003	33.952	0.116
200.000	-0.236	0.010	21.937	0.185
500.000	-0.128	0.024	16.748	1.357

station: mccoys t3r3 seperation=2200 meters
 number of turns=4 loop radius=50 meters
 hr mag const=7.936 hz mag const=7.092

frequency	ellipticity	ellip err	tilt angle	tilt err
1.000	-0.075	0.004	83.769	0.138
3.000	-0.065	0.005	78.527	0.215
5.000	-0.067	0.013	74.109	0.910
7.000	-0.145	0.025	68.271	3.532
10.000	-0.154	0.003	75.800	0.269
10.000	-0.066	0.003	108.354	0.510
30.000	-0.280	0.047	119.842	1.255
30.000	-0.306	0.031	119.836	1.899
50.000	-0.338	0.043	-37.235	1.262
50.000	-0.362	0.014	-7.266	34.626
100.000	-0.236	0.019	-16.493	0.644

station: mccoys t3r4 seperation=3200 meters
 number of turns=4 loop radius=50 meters
 hr mag const=7.936 hz mag const=7.092

frequency	ellipticity	ellip err	tilt angle	tilt err
0.050	0.000	0.007	88.977	0.532
0.100	-0.090	0.016	88.367	0.679
0.300	-0.125	0.024	69.756	1.424
0.500	-0.105	0.011	67.000	1.448
1.000	-0.154	0.004	79.454	0.178
3.000	-0.241	0.005	70.397	0.249
5.000	-0.252	0.004	65.879	0.526
7.000	-0.299	0.014	64.056	0.639
10.000	-0.335	0.005	59.079	0.145
30.000	-0.474	0.006	42.596	0.272
50.000	-0.521	0.007	26.593	1.049
100.000	-0.429	0.008	4.758	0.421
200.000	-0.360	0.021	-1.914	1.596
300.000	-0.718	0.096	3.297	28.777

station: mccoys t3r5 seperation=2450 meters
 number of turns=4 loop radius=50 meters
 hr mag const=7.936 hz mag const=7.092

frequency	ellipticity	ellip err	tilt angle	tilt err
0.050	-0.019	0.008	92.673	0.609
0.100	0.006	0.003	92.426	0.144
0.300	-0.015	0.004	87.496	0.326
0.500	-0.028	0.004	87.160	0.207
0.700	-0.036	0.005	87.220	0.328
1.000	-0.122	0.000	79.269	0.023
3.000	-0.217	0.006	72.603	0.325
5.000	-0.242	0.002	67.671	0.098
7.000	-0.257	0.003	64.117	0.240
50.000	-0.252	0.008	44.254	0.135
100.000	-0.585	0.003	27.091	0.168
200.000	-0.587	0.009	-8.294	0.658

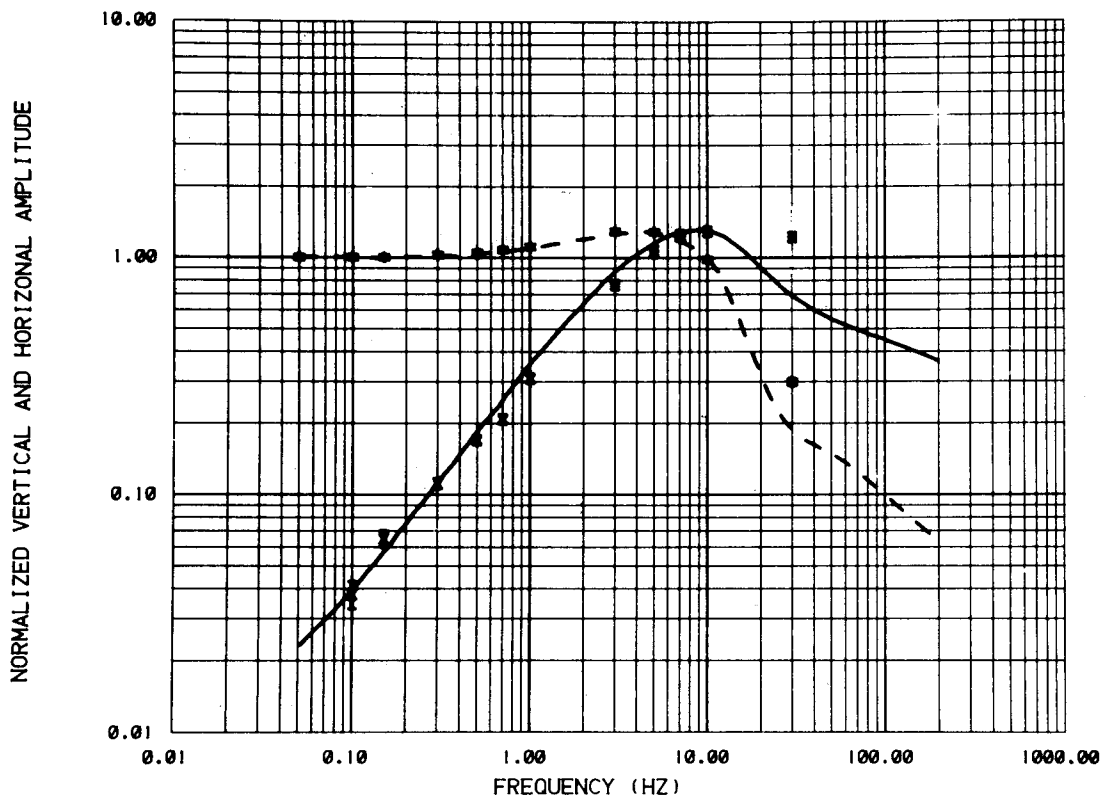
station: mccoys t3r6 seperation=1750 meters
 number of turns=4 loop radius=50 meters
 hr mag const=7.936 hz mag const=7.092

frequency	ellipticity	ellip err	tilt angle	tilt err
0.100	-0.006	0.001	83.911	0.179
0.300	-0.011	0.002	83.678	0.135
0.500	-0.025	0.004	84.026	0.110
0.700	-0.023	0.005	83.745	0.094
10.000	-0.330	0.020	63.992	2.490
30.000	-0.312	0.005	49.577	2.950
50.000	-0.335	0.006	42.999	3.173
100.000	-0.060	0.002	3.476	0.177
200.000	-0.006	0.000	0.519	0.011
500.000	-0.018	0.001	0.072	0.070

APPENDIX C

LAYERED-MODEL INVERSIONS OF SOUNDINGS

COMPARISON OF CALCULATED AND MEASURED DATA



MCCOY TIRI

CALCULATED DATA

HR —————
 HZ — — — — —

MEASURED DATA

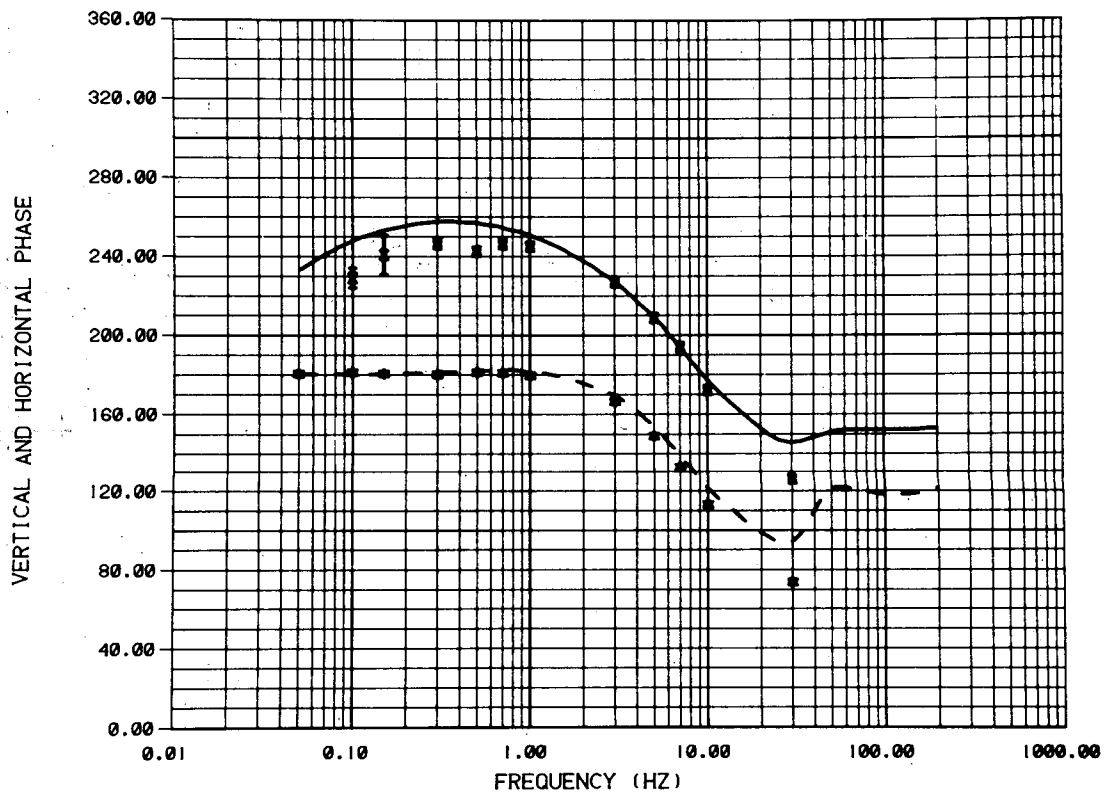
HR X
 HZ *

LAYER	RESISTIVITY(OHM-M)	THICKNESS(M)
1	54.50 ± .1066E-02	73.12 ± 2.
2	10.31 ± .6520E-01	469.1 ± 6.
3	598.2 ± 294.3	.1000E+11 ± 0.

DATA VARIANCE ESTIMATE 117.8

XBL 812-7951

COMPARISON OF CALCULATED AND MEASURED DATA



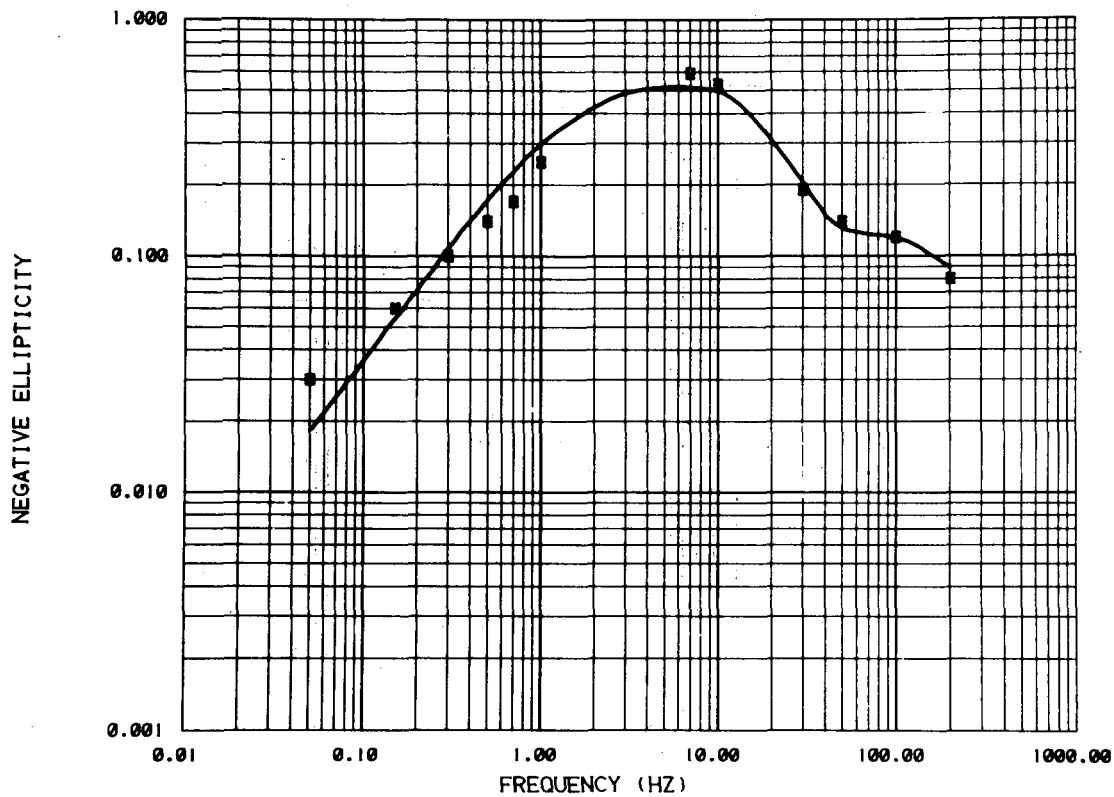
MCCOY TIRI

CALCULATED DATA		MEASURED DATA		LAYER	RESISTIVITY(OHM-M)	THICKNESS(M)
HR	—————	HR	X	1	54.50 ± .1066E-02	73.12 ± 2.
HZ	- - - - -	HZ	*	2	10.31 ± .6520E-01	469.1 ± 6.
				3	598.2 ± 294.3	.1000E+11 ± 0.

DATA VARIANCE ESTIMATE 117.8

XBL 812-7952

COMPARISON OF CALCULATED AND MEASURED DATA



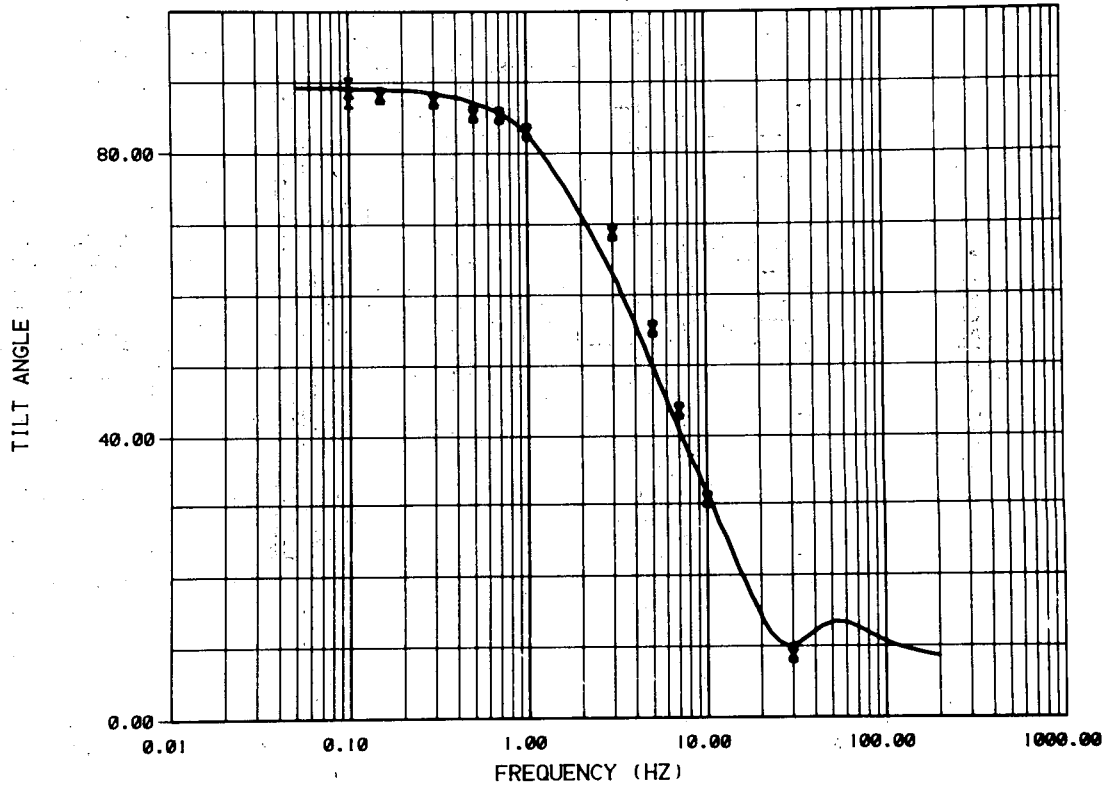
MCCOY TIRI

CALCULATED DATA	MEASURED DATA	LAYER	RESISTIVITY(OHM-M)	THICKNESS(M)
ELLIPTICITY	ELLIPTICITY	X		
		1	54.50 ± .1066E-02	73.12 ± 2.
		2	10.31 ± .6520E-01	469.1 ± 6.
		3	598.2 ± 294.3	.1000E+11 ± 0.

DATA VARIANCE ESTIMATE 117.8

XBL 812-7953

COMPARISON OF CALCULATED AND MEASURED DATA



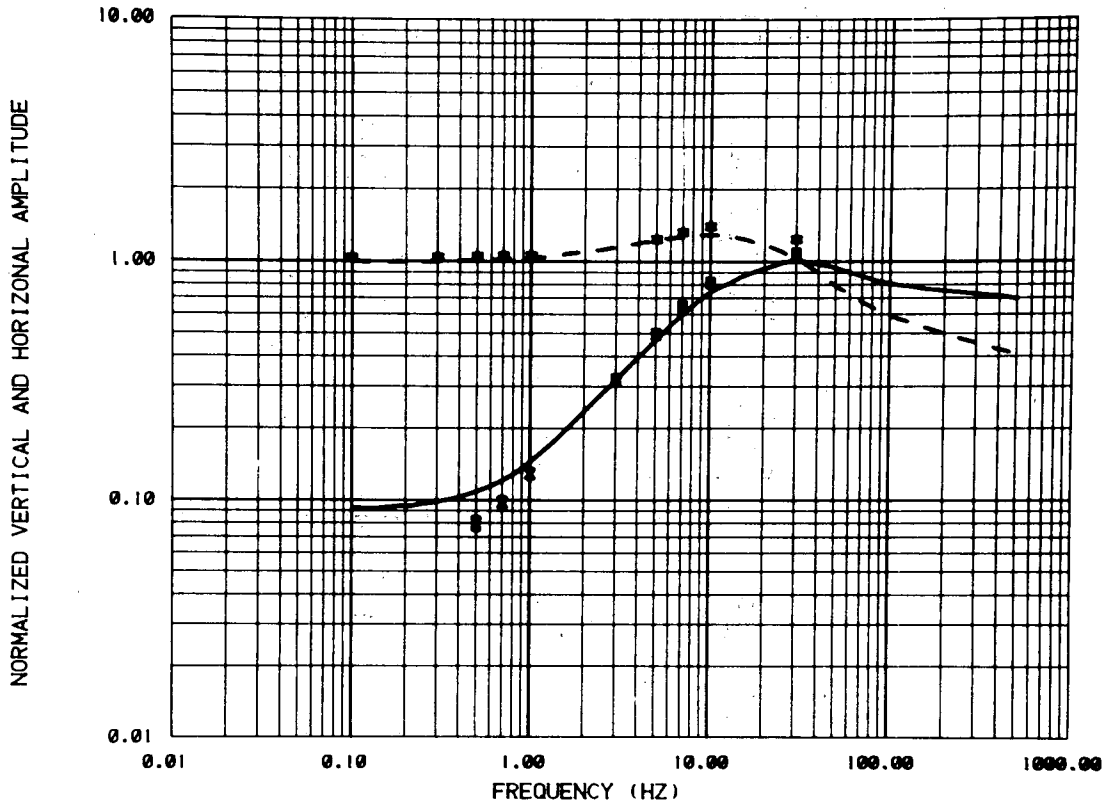
MCCOY TIRI

CALCULATED DATA	MEASURED DATA	LAYER	RESISTIVITY(OHM-M)	THICKNESS(M)
TILT ANGLE ———	TILT ANGLE X	1	54.50 ± .1066E-02	73.12 ± .2.
		2	10.31 ± .6520E-01	469.1 ± 6.
		3	598.2 ± 294.3	.1000E+11 ± 0.

DATA VARIENCE ESTIMATE 117.8

XBL 812-7954

COMPARISON OF CALCULATED AND MEASURED DATA

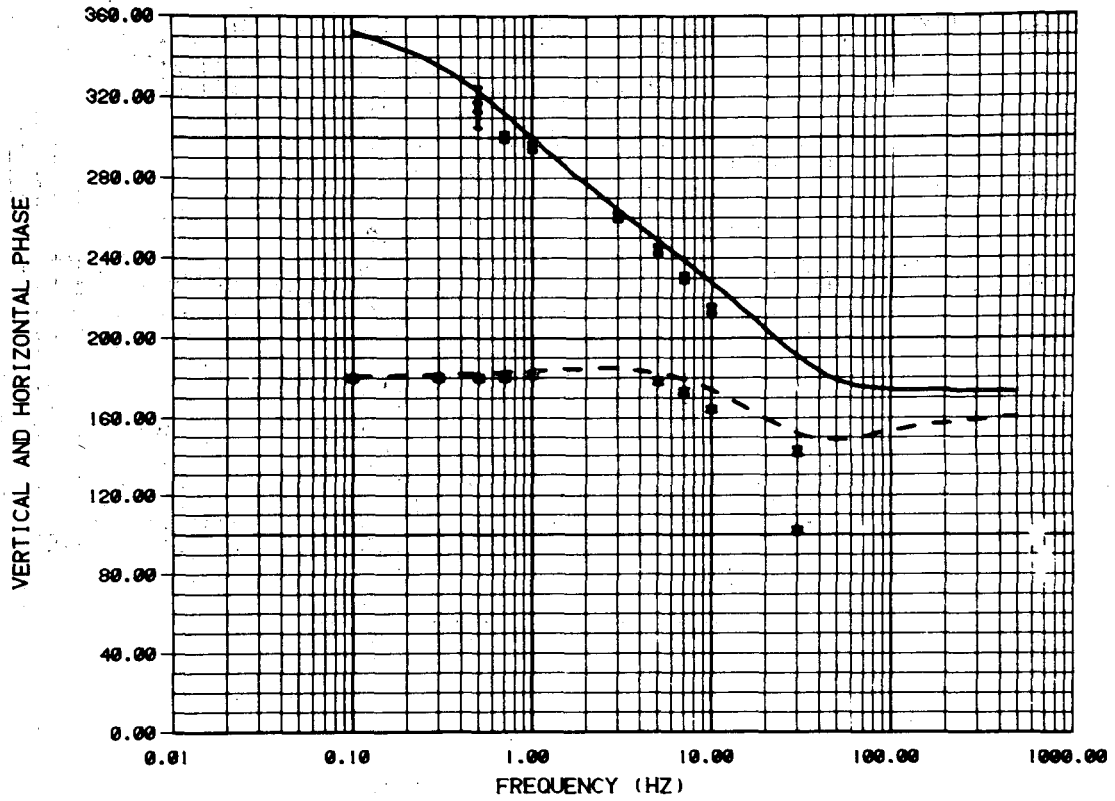


MCCOY TIR2

CALCULATED DATA		MEASURED DATA		LAYER	RESISTIVITY(OHM-M)	THICKNESS(M)
HR	—————	HR	X	1	883.9 ± .1141E-02	142.5 ± 1.
HZ	—————	HZ	*	2	8.666 ± .5815E-01	263.2 ± 9.
				3	29.16 ± 1.944	.1000E+11 ± 0.
DATA VARIANCE ESTIMATE				156.4		

XBL 812-7955

COMPARISON OF CALCULATED AND MEASURED DATA



MCCOY TIR2

CALCULATED DATA

HR _____
 HZ - - - - -

MEASURED DATA

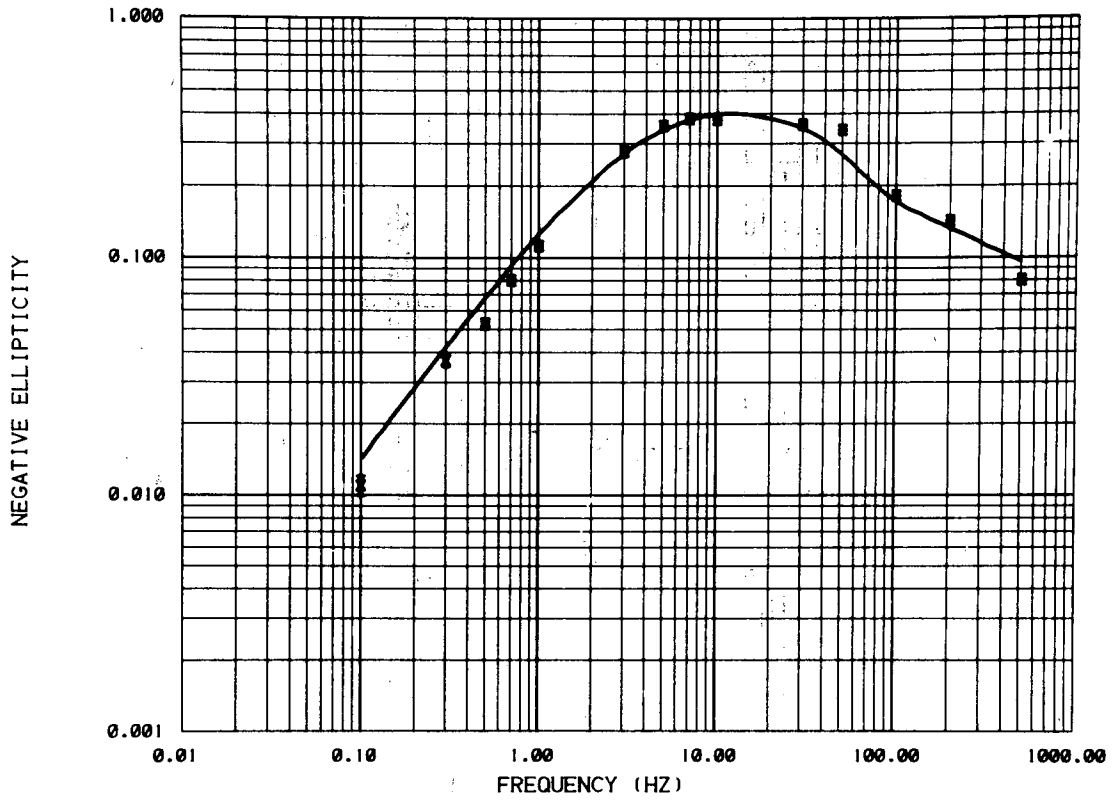
HR X
 HZ *

LAYER	RESISTIVITY(OHM-M)	THICKNESS(M)
1	803.9 ± .1141E-02	142.5 ± 1.
2	8.666 ± .5815E-01	263.2 ± 9.
3	29.16 ± 1.944	.1000E+11 ± 0.

DATA VARIENCE ESTIMATE 156.4

XBL 812-7956

COMPARISON OF CALCULATED AND MEASURED DATA



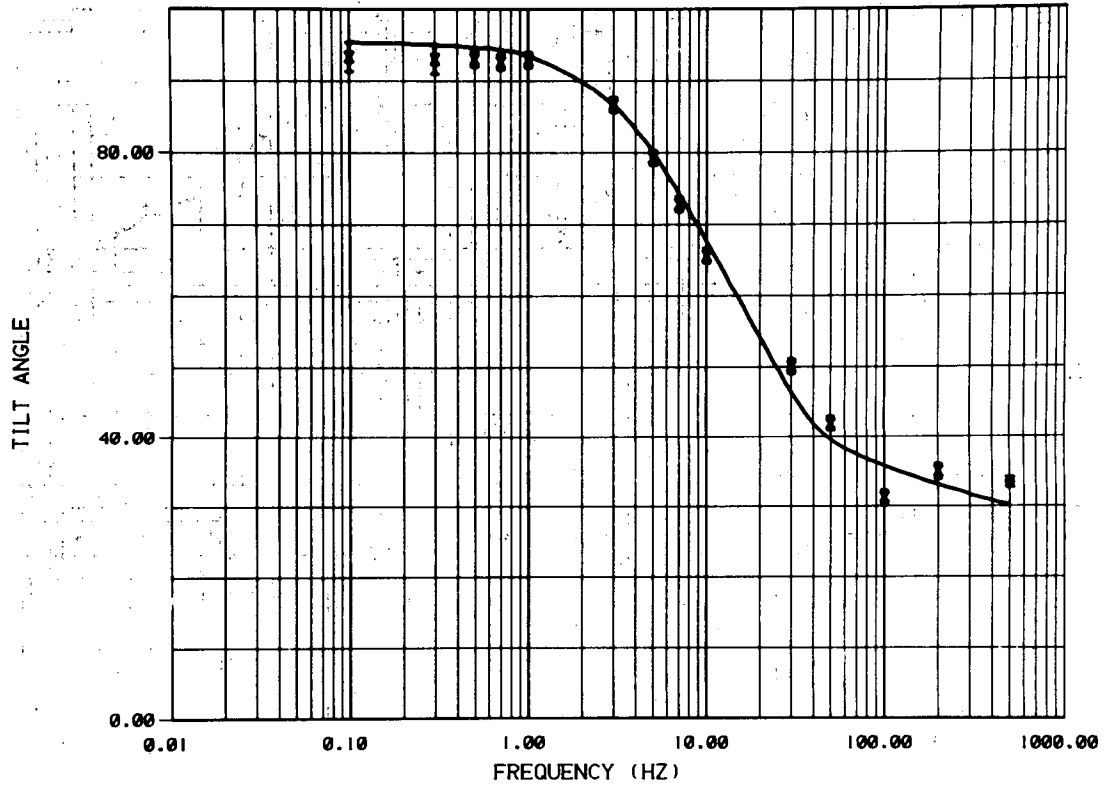
MCCOY TIR2

CALCULATED DATA	MEASURED DATA	LAYER	RESISTIVITY(OHM-M)	THICKNESS(M)
ELLIPTICITY	ELLIPTICITY	X 1	803.9 ± .1141E-02	142.5 ± 1.
		2	8.666 ± .5815E-01	263.2 ± 9.
		3	29.16 ± 1.944	.1000E+11 ± 0.

DATA VARIENCE ESTIMATE 156.4

XBL 812-7957

COMPARISON OF CALCULATED AND MEASURED DATA

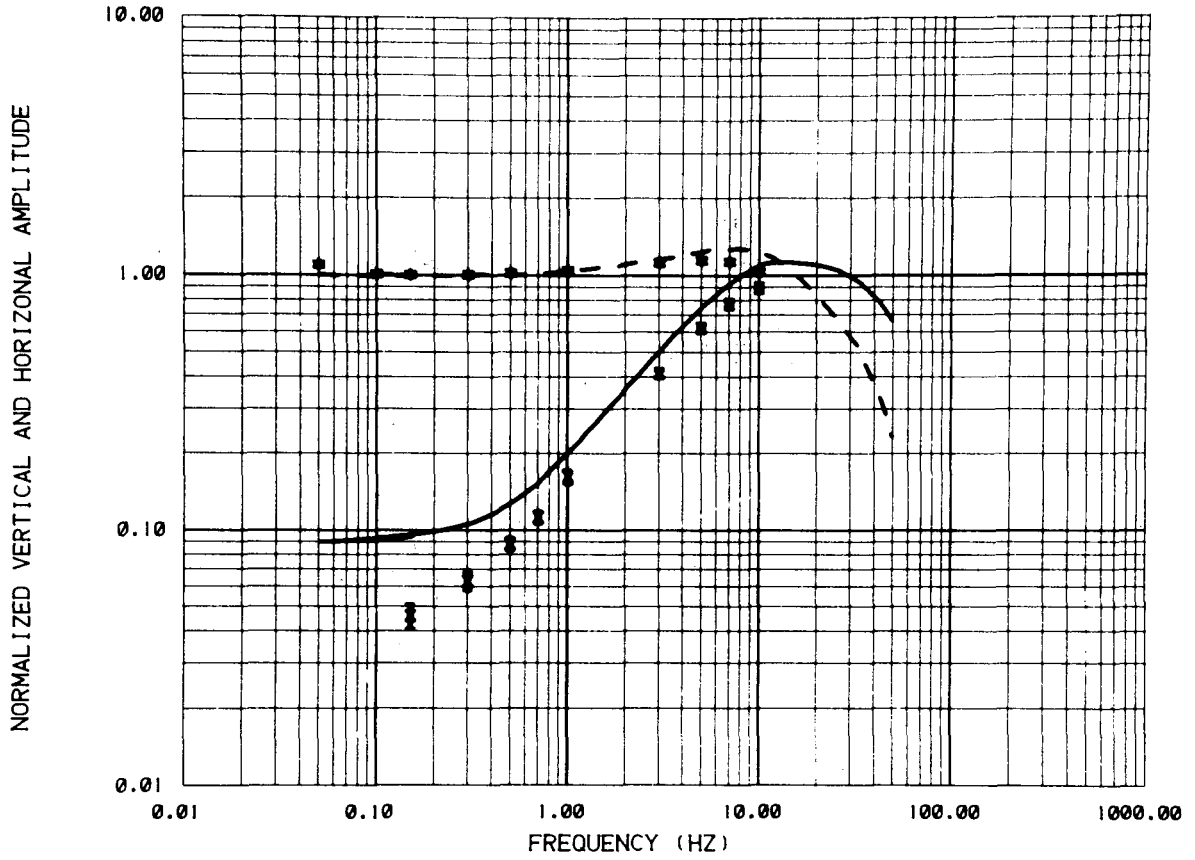


MCCOY TIR2

CALCULATED DATA	MEASURED DATA	LAYER	RESISTIVITY(OHM-M)	THICKNESS(M)
TILT ANGLE ———	TILT ANGLE X	1	803.9 * .1141E-02	142.5 * .1.
		2	8.666 * .5815E-01	263.2 * 9.
		3	29.16 * 1.944	.1000E+11 * 0.
DATA VARIENCE ESTIMATE	156.4			

XBL 812-7958

COMPARISON OF CALCULATED AND MEASURED DATA



MCCOY TIR3

CALCULATED DATA

HR —————
 HZ — — — — —

MEASURED DATA

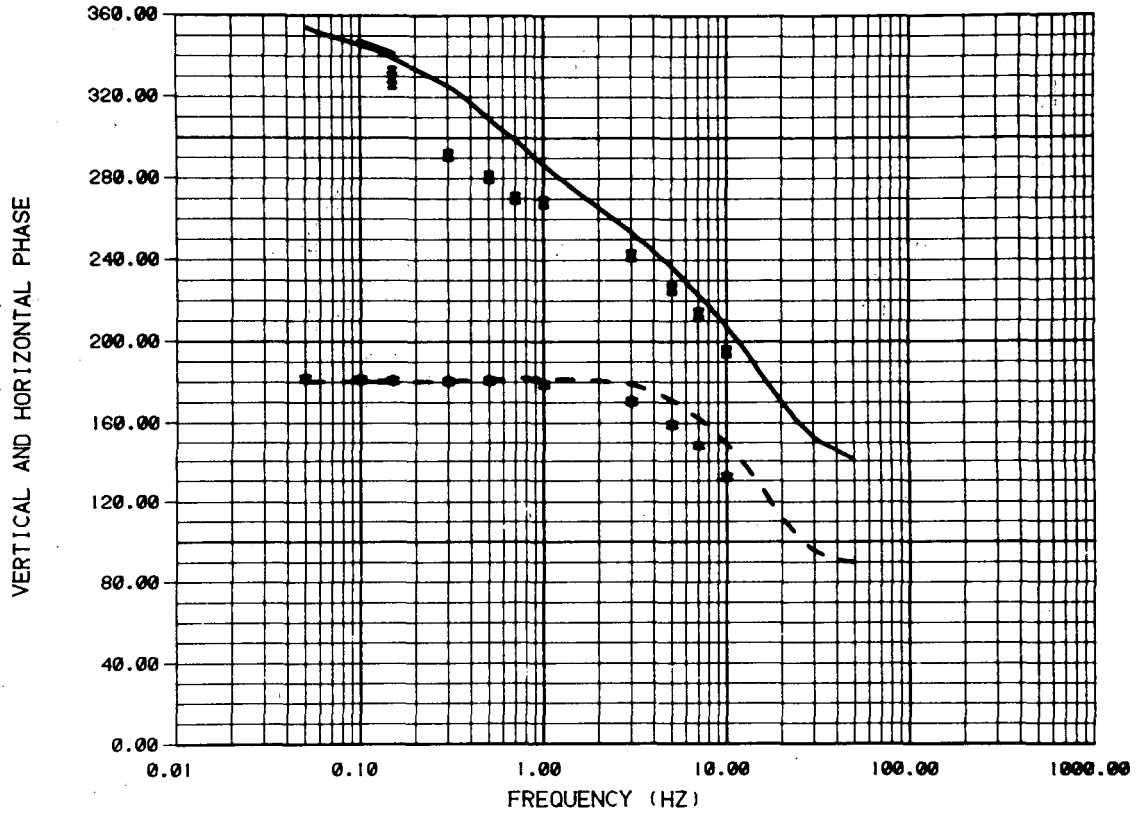
HR X
 HZ *

LAYER	RESISTIVITY(OHM-M)	THICKNESS(M)
1	21.50 ± .1034E-02	205.7 ± 38.
2	9.300 ± 2.485	165.1 ± 63.
3	1566. ± 1332.	.1000E+11 ± 0.

DATA VARIANCE ESTIMATE 184.1

XBL 8012-12988

COMPARISON OF CALCULATED AND MEASURED DATA



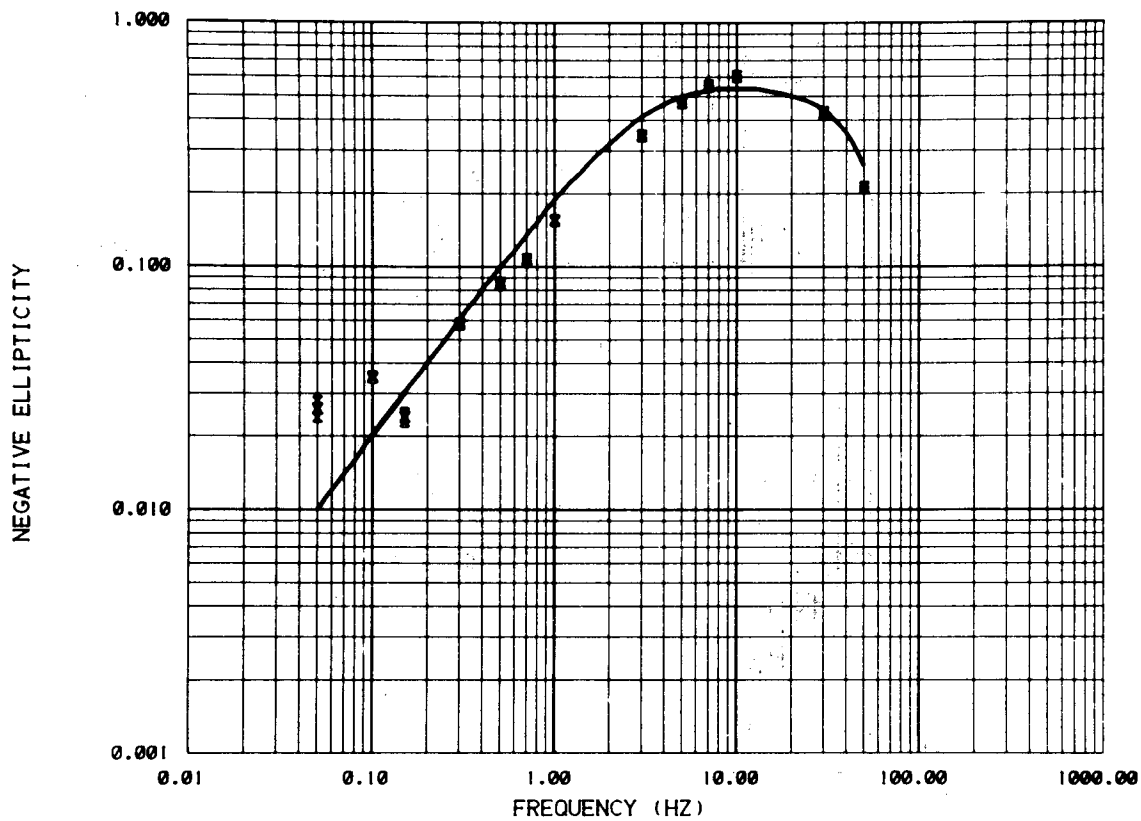
MCCOY TIR3

CALCULATED DATA		MEASURED DATA		LAYER	RESISTIVITY(OHM-M)	THICKNESS(M)
HR	—————	HR	X	1	21.50 ± .1034E-02	205.7 ± 38.
HZ	- - - - -	HZ	*	2	9.300 ± 2.485	165.1 ± 63.
				3	1566. ± 1332.	.1000E+11 ± 0.

DATA VARIANCE ESTIMATE 184.1

XBL 812-7959

COMPARISON OF CALCULATED AND MEASURED DATA



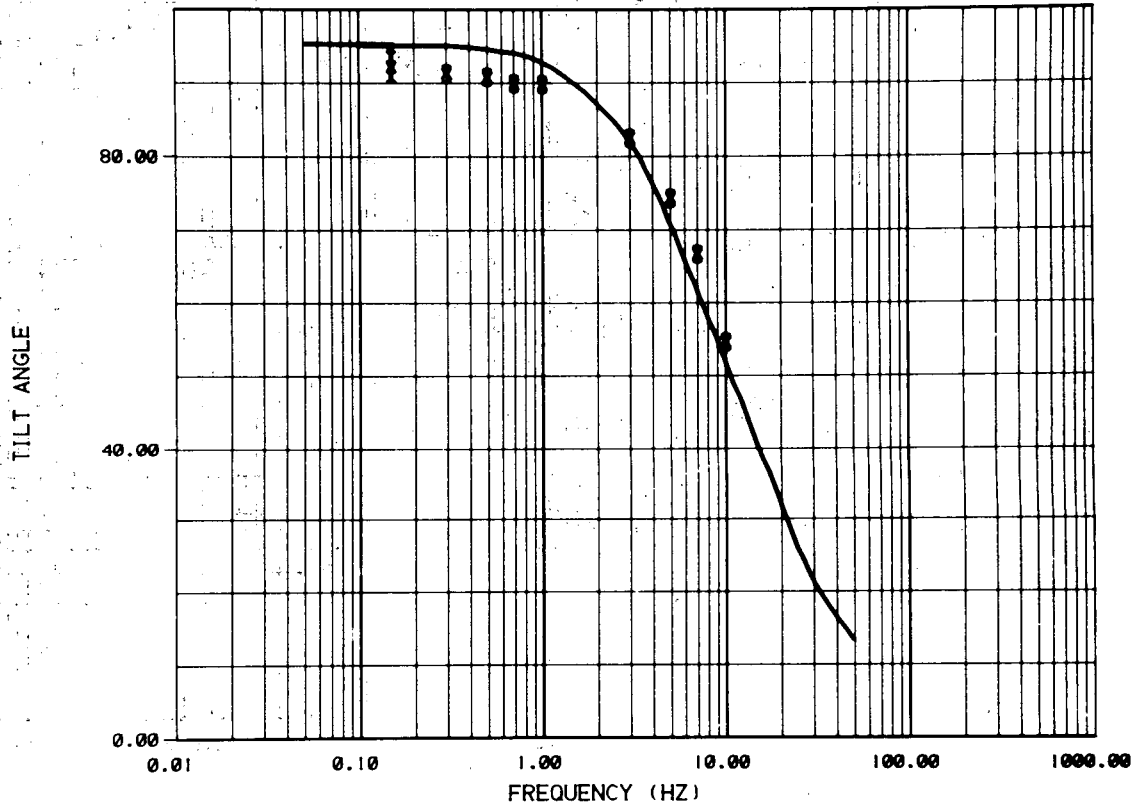
MCCOY TIR3

CALCULATED DATA	MEASURED DATA	LAYER	RESISTIVITY(OHM-M)	THICKNESS(M)
ELLIPTICITY	ELLIPTICITY	X 1	21.50 ± .1034E-02	205.7 ± 38.
		2	9.300 ± 2.485	165.1 ± 63.
		3	1566. ± 1332.	.1000E+11 ± 0.

DATA VARIANCE ESTIMATE 184.1

XBL 812-7960

COMPARISON OF CALCULATED AND MEASURED DATA



MCCOY TIR3

CALCULATED DATA

MEASURED DATA

LAYER RESISTIVITY(OHM-M) THICKNESS(M)

TILT ANGLE

TILT ANGLE

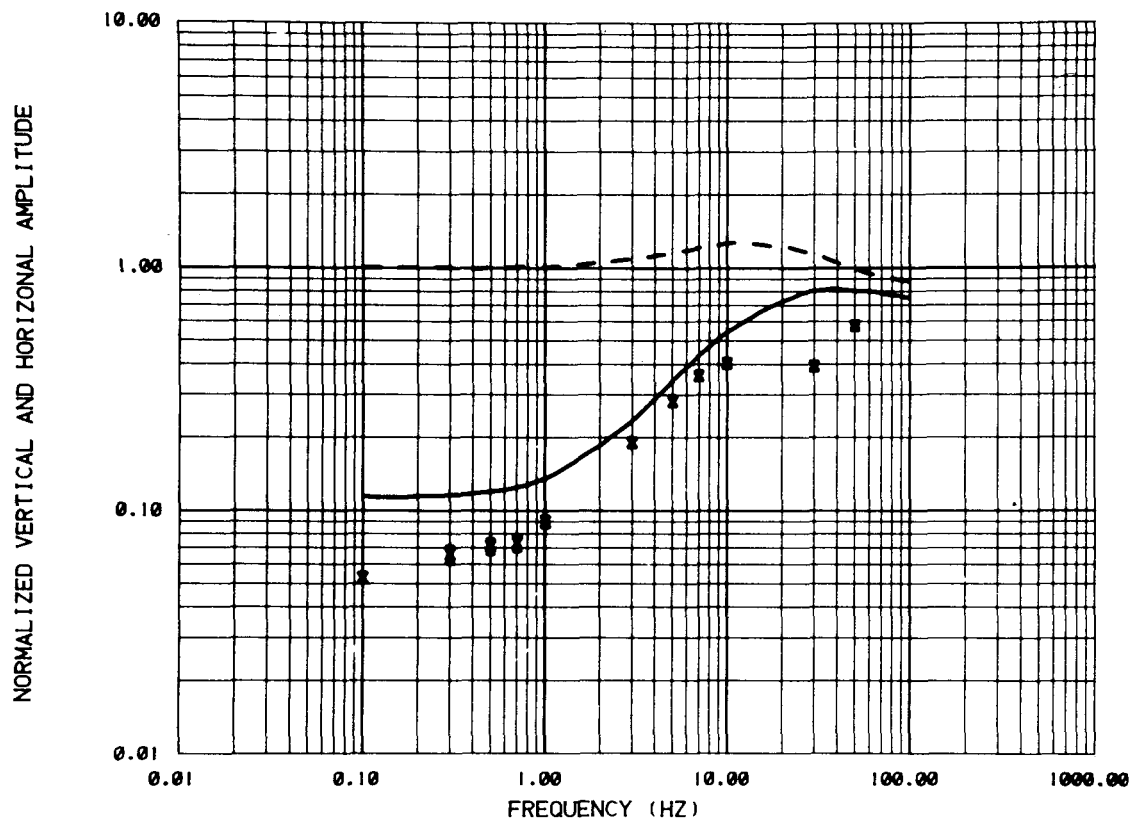
X

1	21.50	± .1034E-02	205.7	± 38.
2	9.300	± 2.485	165.1	± 63.
3	1566.	± 1332.	.1000E+11	± 0.

DATA VARIANCE ESTIMATE 184.1

XBL 812-7961

COMPARISON OF CALCULATED AND MEASURED DATA



MCCOY TIR4

CALCULATED DATA

HR _____
 HZ _____

MEASURED DATA

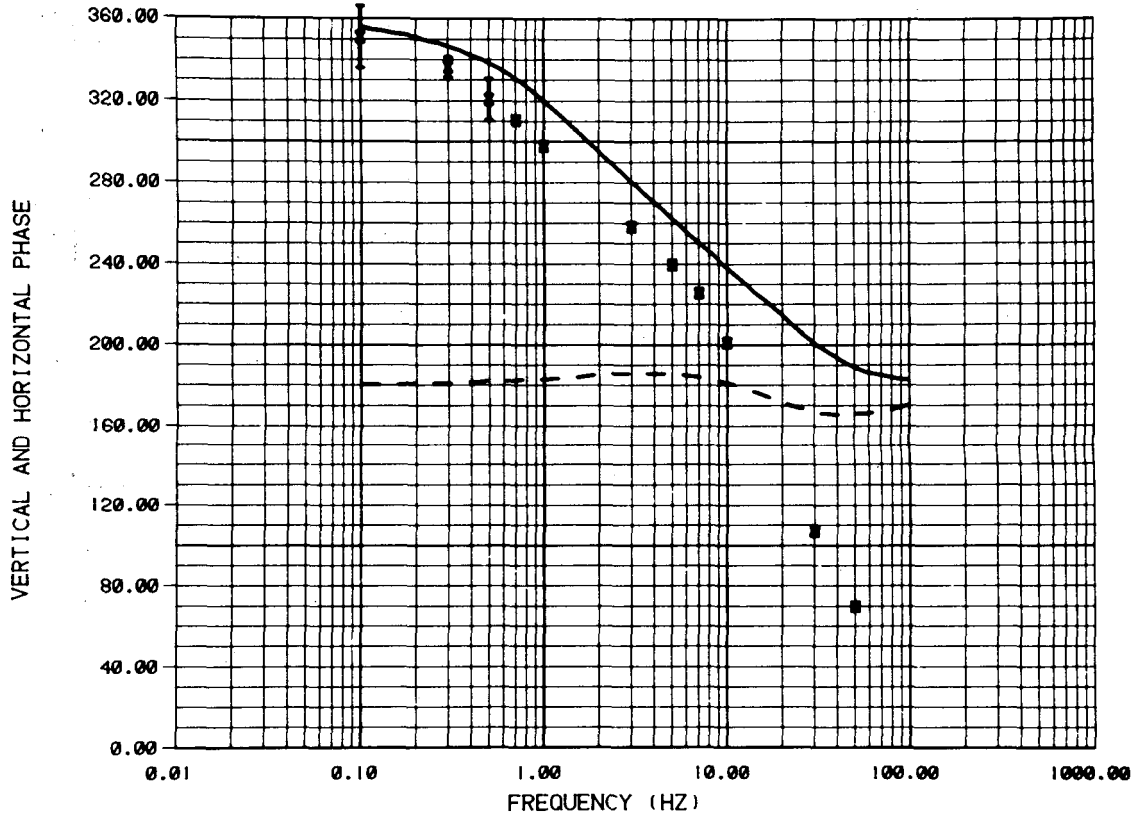
HR X
 HZ *

LAYER	RESISTIVITY(OHM-M)	THICKNESS(M)
1	.2309E+45 ± 1.097E-02	341.8 ± 10.
2	7.400 ± 1.576	160.3 ± 44.
3	141.6 ± 43.30	.1000E+11 ± 0.

DATA VARIENCE ESTIMATE 874.6

XBL 812-7962

COMPARISON OF CALCULATED AND MEASURED DATA



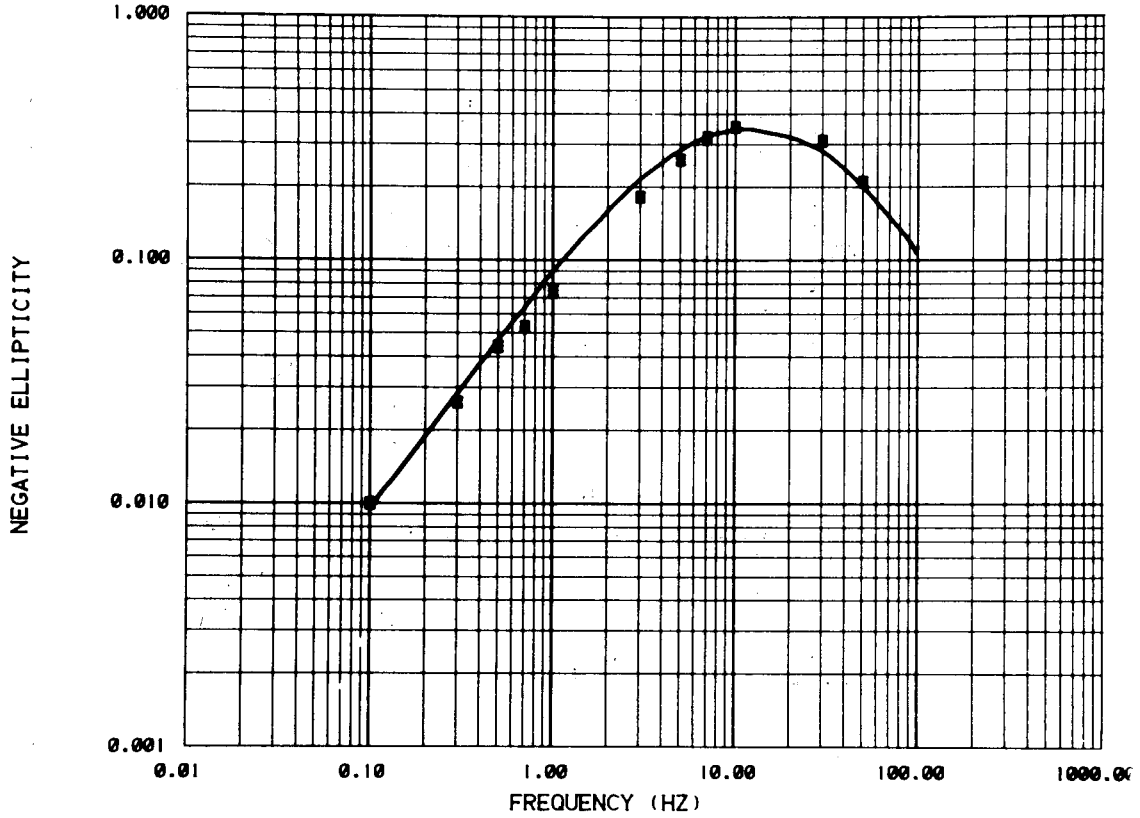
MCCOY TIR4

CALCULATED DATA		MEASURED DATA		LAYER	RESISTIVITY(OHM-M)	THICKNESS(M)
HR	—————	HR	X	1	.2309E+45 ± .1097E-02	341.8 ± 10.
HZ	—————	HZ	*	2	7.400 ± 1.576	160.3 ± 44.
				3	141.6 ± 43.30	.1000E+11 ± 0.

DATA VARIANCE ESTIMATE 874.6

XBL 812-7963

COMPARISON OF CALCULATED AND MEASURED DATA



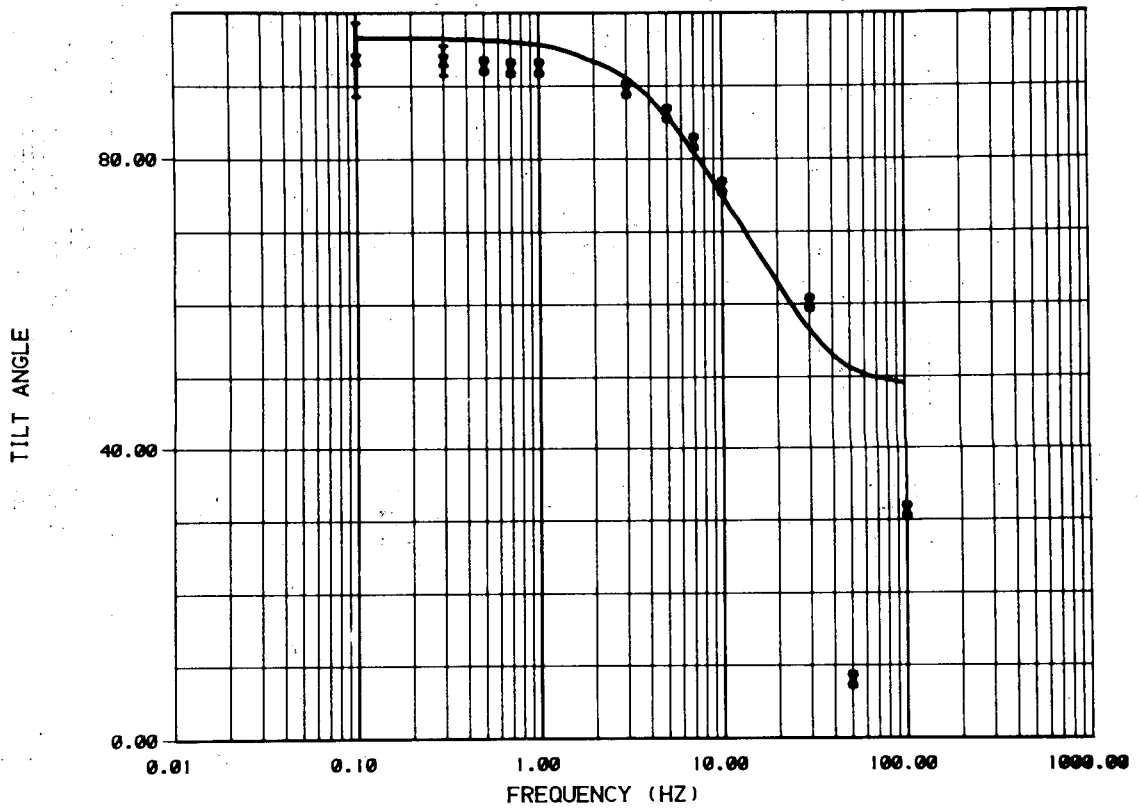
MCCOY TIR4

CALCULATED DATA	MEASURED DATA	LAYER	RESISTIVITY(OHM-M)	THICKNESS(M)
ELLIPTICITY	ELLIPTICITY	X 1	.2309E+45 ± .1097E-02	341.8 ± 10.
		2	7.400 ± 1.576	160.3 ± 44.
		3	.141.6 ± 43.30	.1000E+11 ± 0.

DATA VARIENCE ESTIMATE 874.6

XBL 812-7964

COMPARISON OF CALCULATED AND MEASURED DATA



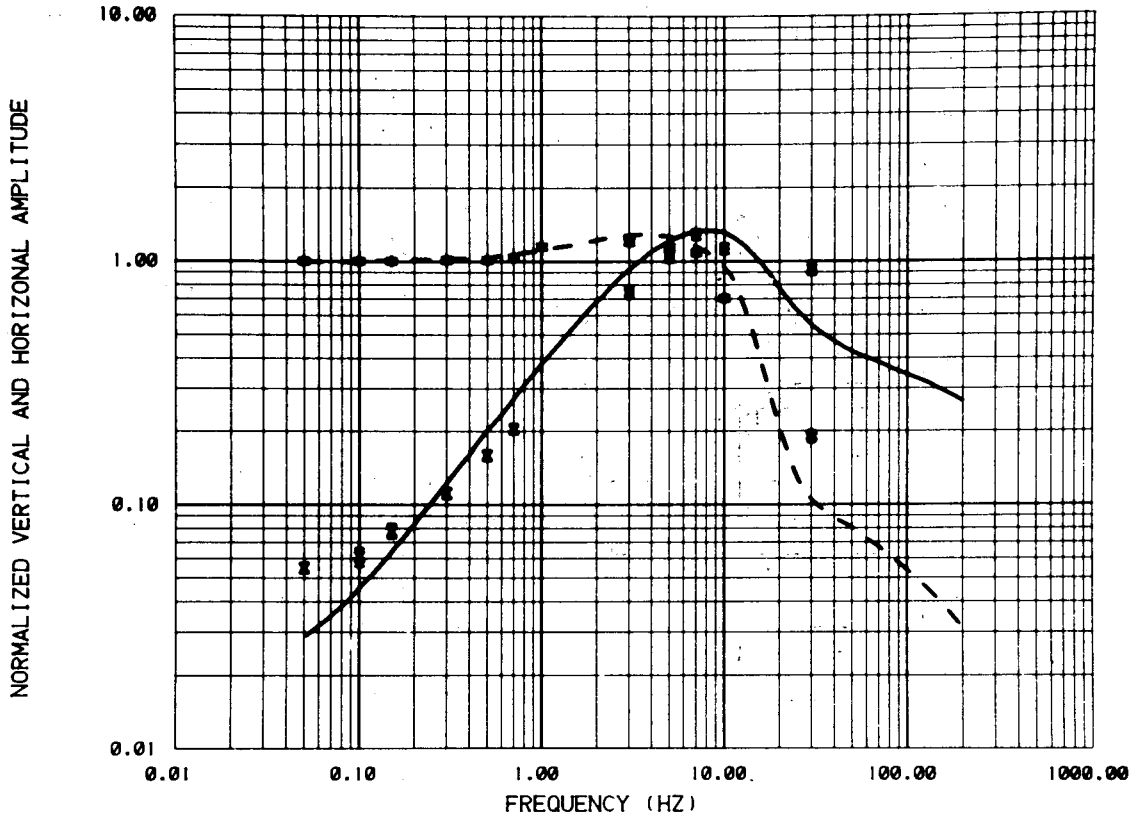
MCCOY TIR4

CALCULATED DATA	MEASURED DATA	LAYER	RESISTIVITY(OHM-M)	THICKNESS(N)
TILT ANGLE	TILT ANGLE	X		
		1	.2309E+45 ± .1097E-02	341.8 ± 10.
		2	7.400 ± 1.576	160.3 ± 44.
		3	141.6 ± 43.30	.1000E+11 ± 0.

DATA VARIANCE ESTIMATE 874.6

XBL 812-7965

COMPARISON OF CALCULATED AND MEASURED DATA

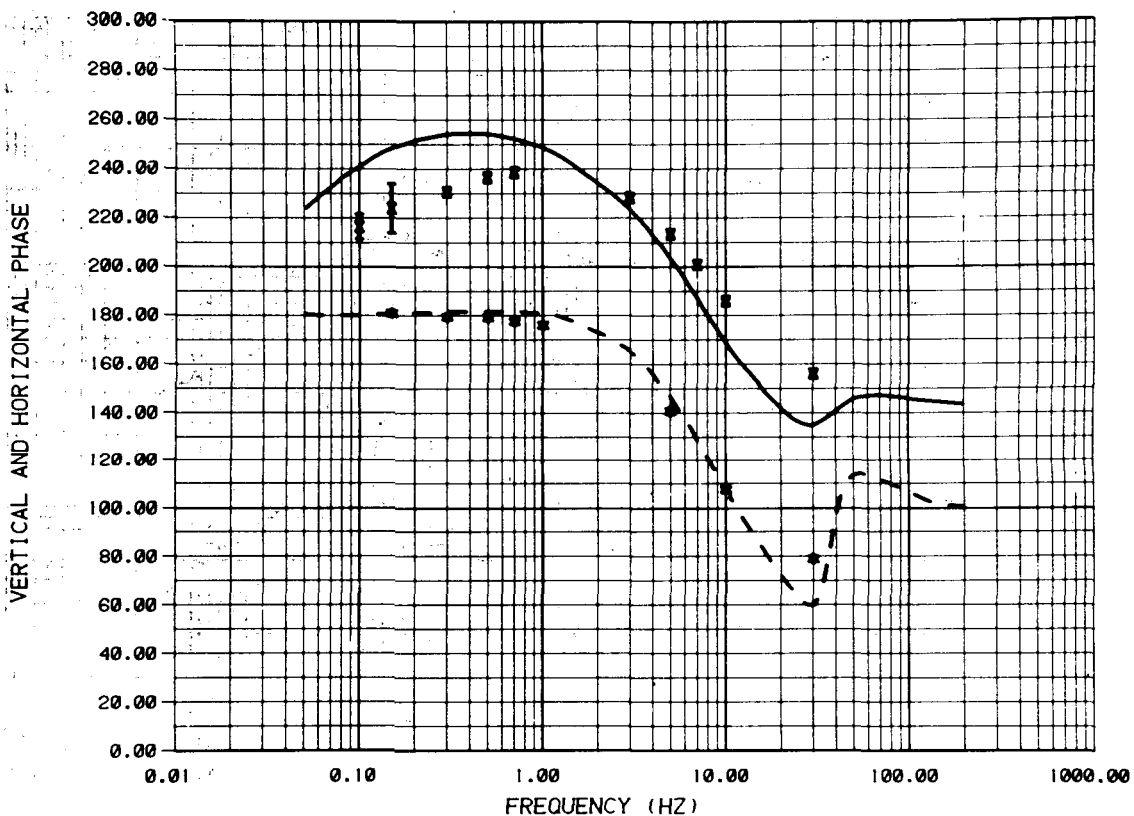


MCCOY TIR5

CALCULATED DATA		MEASURED DATA		LAYER	RESISTIVITY (OHM-M)	THICKNESS (M)
HR	—————	HR	X	1	11.36 ± .1172E-02	107.4 ± 6.
HZ	—————	HZ	*	2	6.989 ± .1875	243.2 ± 11.
				3	189.0 ± 26.15	.1000E+11 ± 0.
DATA VARIANCE ESTIMATE					180.3	

XBL 812-7966

COMPARISON OF CALCULATED AND MEASURED DATA



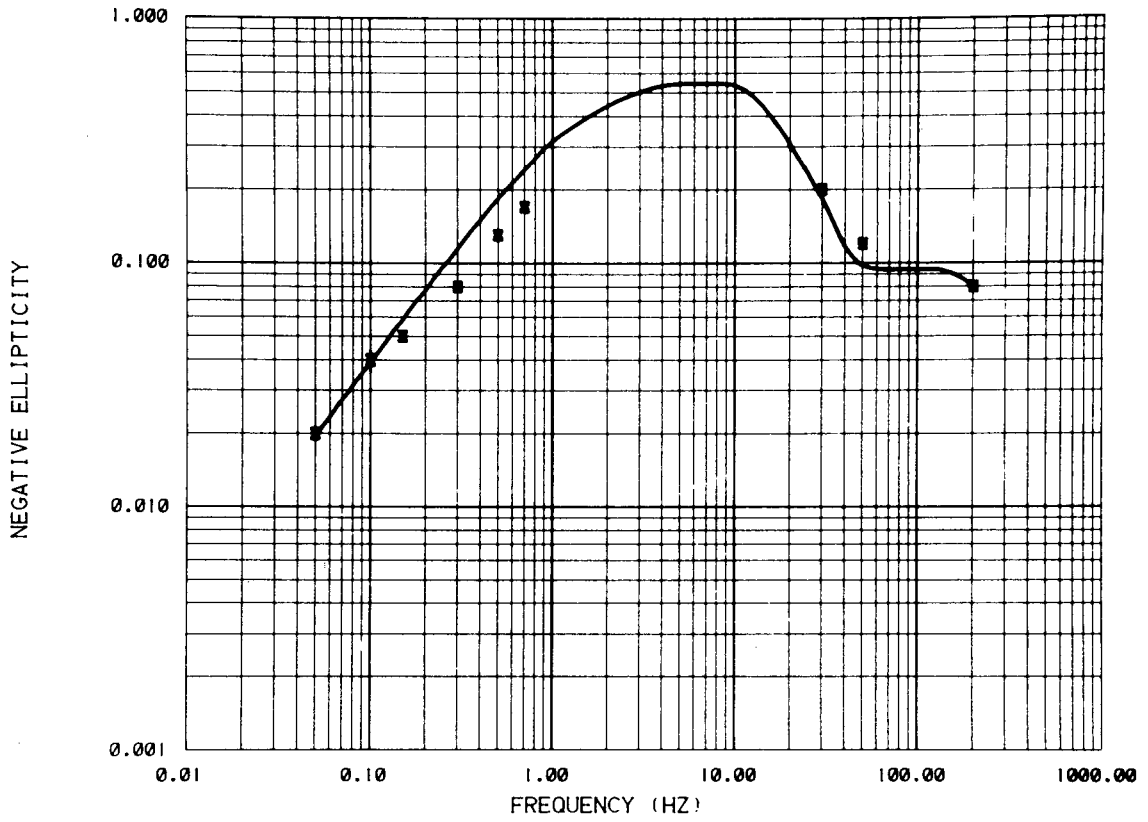
MCCOY TIR5

CALCULATED DATA		MEASURED DATA		LAYER	RESISTIVITY(OHM-M)	THICKNESS(M)
HR	—————	HR	X	1	11.36 ± .1172E-02	107.4 ± 6.
HZ	—————	HZ	*	2	6.989 ± .1875	243.2 ± 11.
				3	189.0 ± 26.15	.1000E+11 ± 0.

DATA VARIENCE ESTIMATE 180.3

XBL 812-7967

COMPARISON OF CALCULATED AND MEASURED DATA



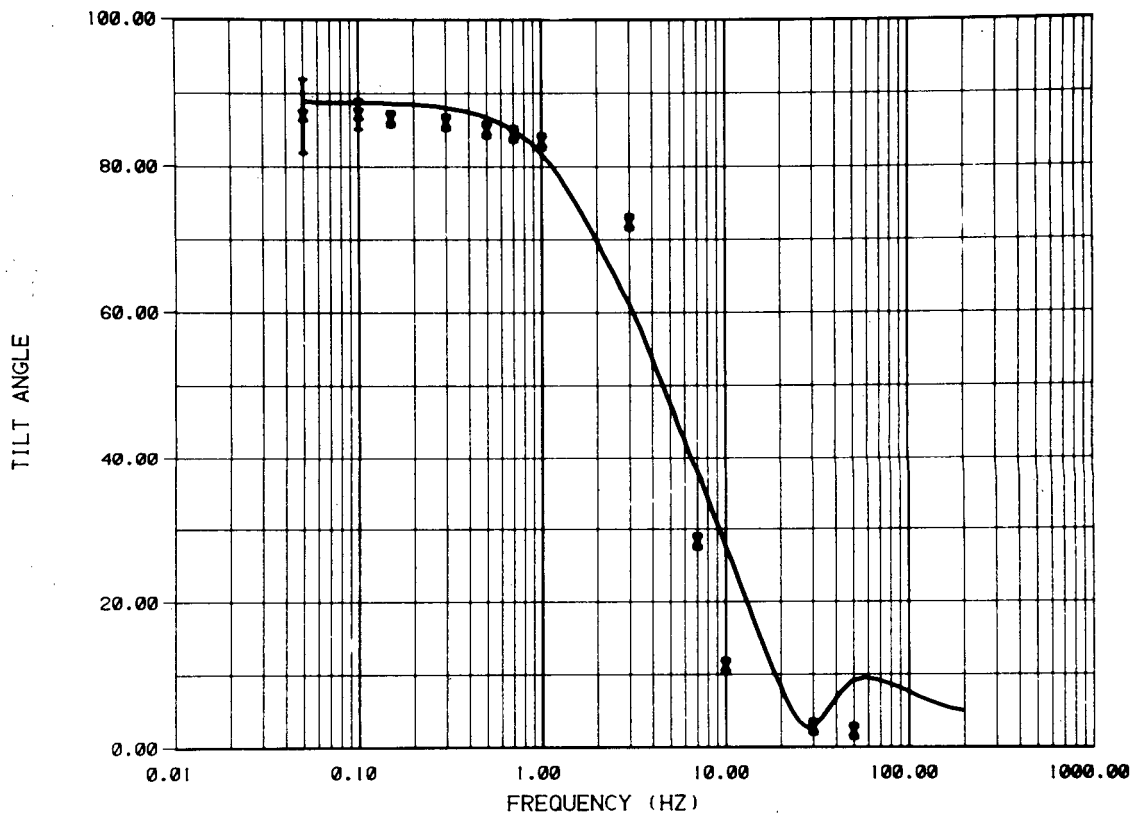
MCCOY T1R5

CALCULATED DATA	MEASURED DATA	LAYER	RESISTIVITY(OHM-M)	THICKNESS(M)
ELLIPTICITY	ELLIPTICITY	X	1 11.36 ± .1172E-02	107.4 ± 6.
			2 6.989 ± .1875	243.2 ± 11.
			3 189.0 ± 26.15	.1000E+11 ± 0.

DATA VARIANCE ESTIMATE 180.3

XBL 812-7968

COMPARISON OF CALCULATED AND MEASURED DATA



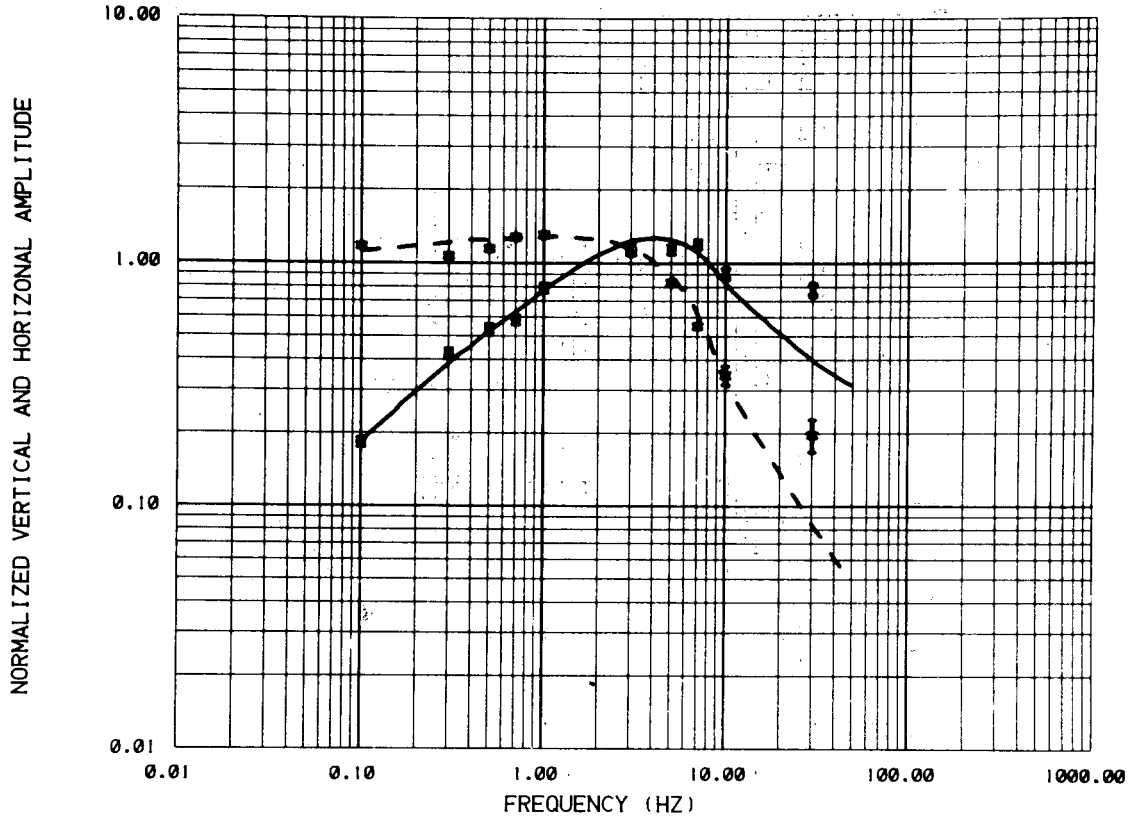
MCCOY TIR5

CALCULATED DATA	MEASURED DATA	LAYER	RESISTIVITY(OHM-M)	THICKNESS(M)
TILT ANGLE	TILT ANGLE	X 1	11.36 ± .1172E-02	107.4 ± 6.
		2	6.989 ± .1875	243.2 ± 11.
		3	189.0 ± 26.15	.1000E+11 ± 0.

DATA VARIENCE ESTIMATE 180.3

XBL 812-7969

COMPARISON OF CALCULATED AND MEASURED DATA



MCCOY TIR6

CALCULATED DATA

HR —————
 HZ — — — — —

MEASURED DATA

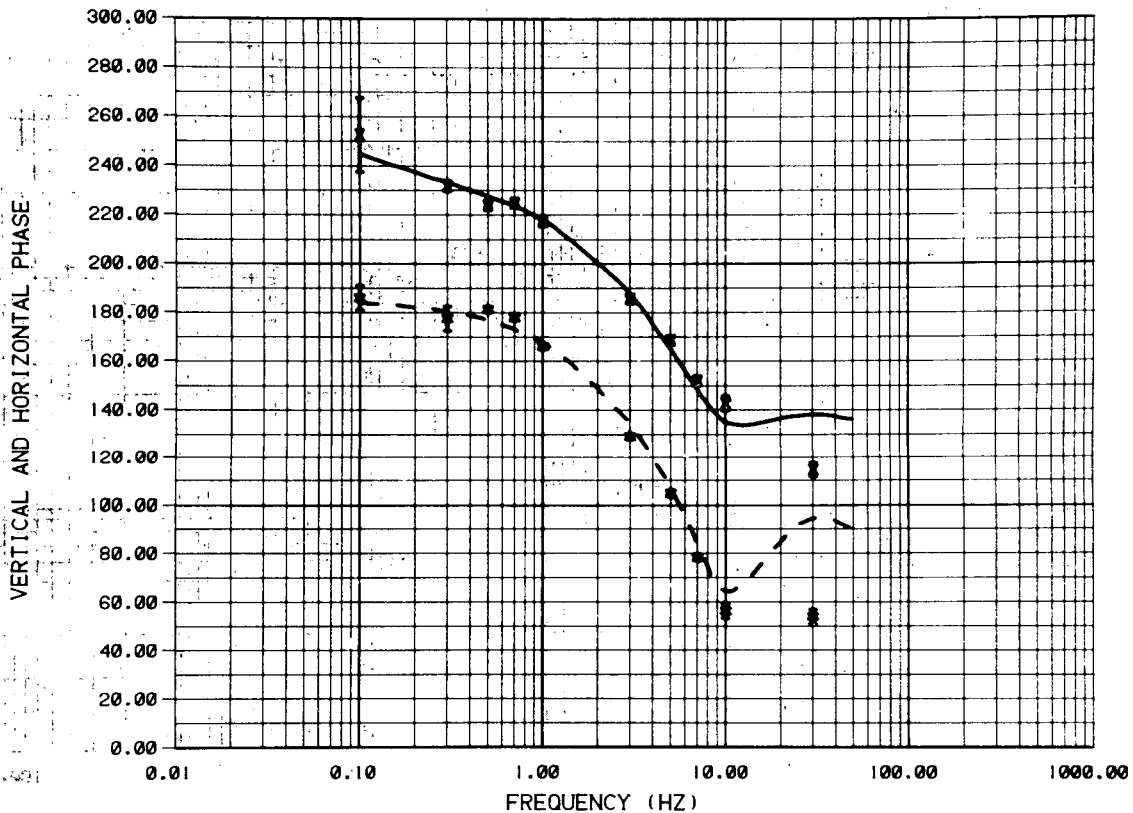
HR : X
 HZ : *

LAYER	RESISTIVITY(OHM-M)	THICKNESS(M)
1	17.44 ± .1315E-02	928.9 ± 61.
2	111.9 ± 82.12	1256. ± 99.
3	4.178 ± .1814	.1000E+11 ± 0.

DATA VARIANCE ESTIMATE 60.22

XBL 812-7970

COMPARISON OF CALCULATED AND MEASURED DATA



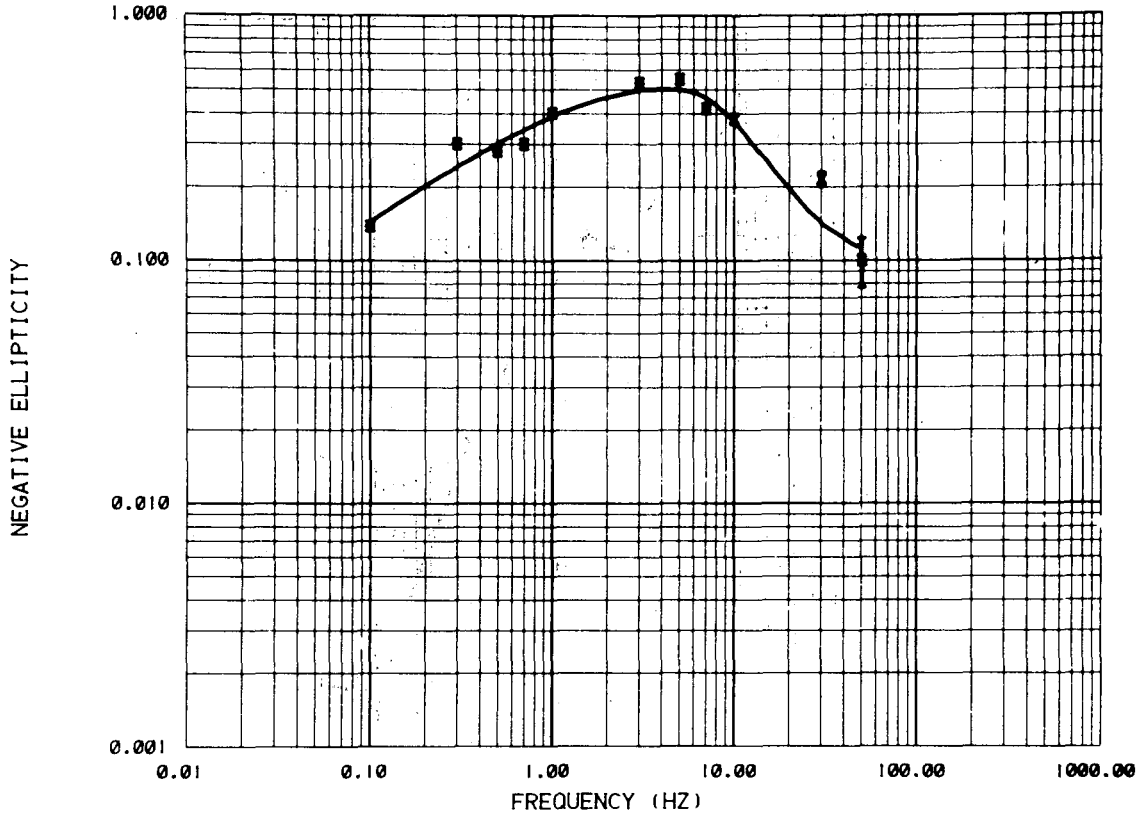
MCCOY TIR6

CALCULATED DATA		MEASURED DATA		LAYER	RESISTIVITY(OHM-M)	THICKNESS(M)
HR	—————	HR	X	1	17.44 ± .1315E-02	928.9 ± 61.
HZ	—————	HZ	*	2	111.9 ± 82.12	1256. ± 99.
				3	4.178 ± .1814	.1000E+11 ± 0.

DATA VARIANCE ESTIMATE 60.22

XBL 812-7971

COMPARISON OF CALCULATED AND MEASURED DATA



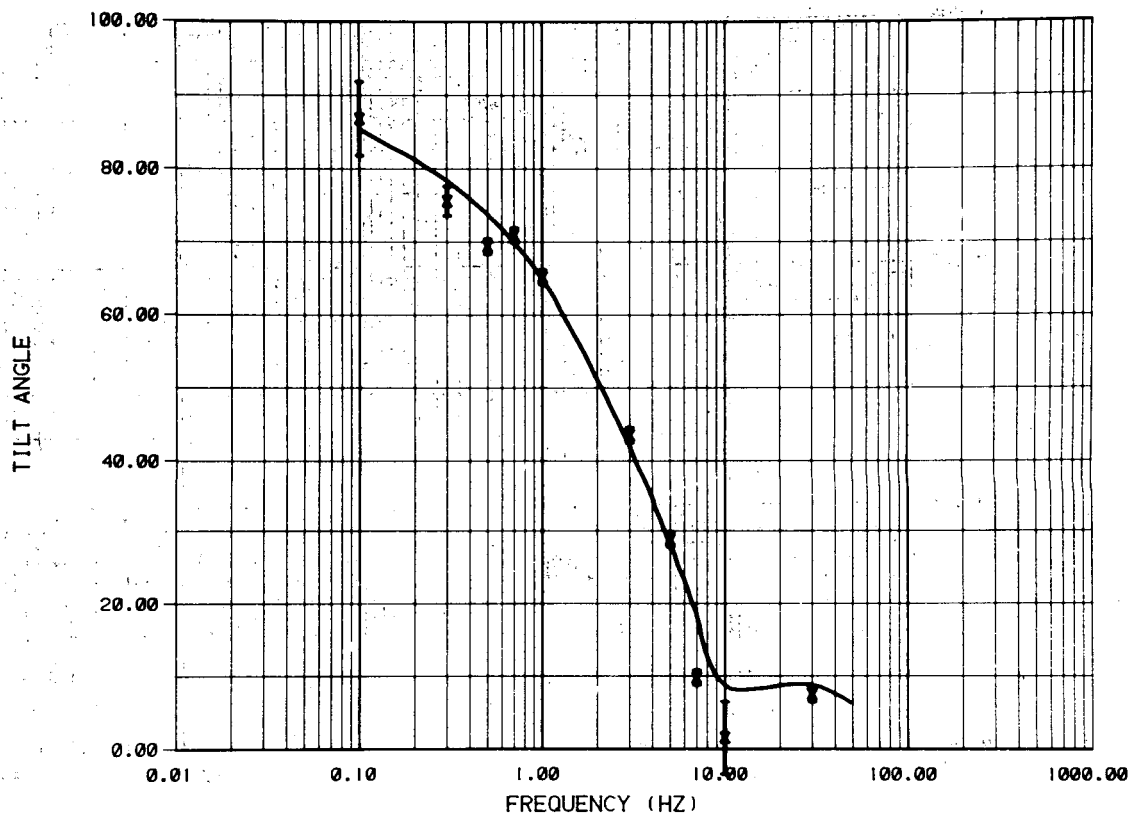
MCCOY TIR6

CALCULATED DATA	MEASURED DATA	LAYER	RESISTIVITY(OHM-M)	THICKNESS(M)
ELLIPTICITY	ELLIPTICITY	X 1	17.44 ± .1315E-02	928.9 ± 61.
		2	111.9 ± 82.12	1256. ± 99.
		3	4.178 ± .1814	.1000E+11 ± 0.

DATA VARIENCE ESTIMATE 60.22

XBL 812-7972

COMPARISON OF CALCULATED AND MEASURED DATA



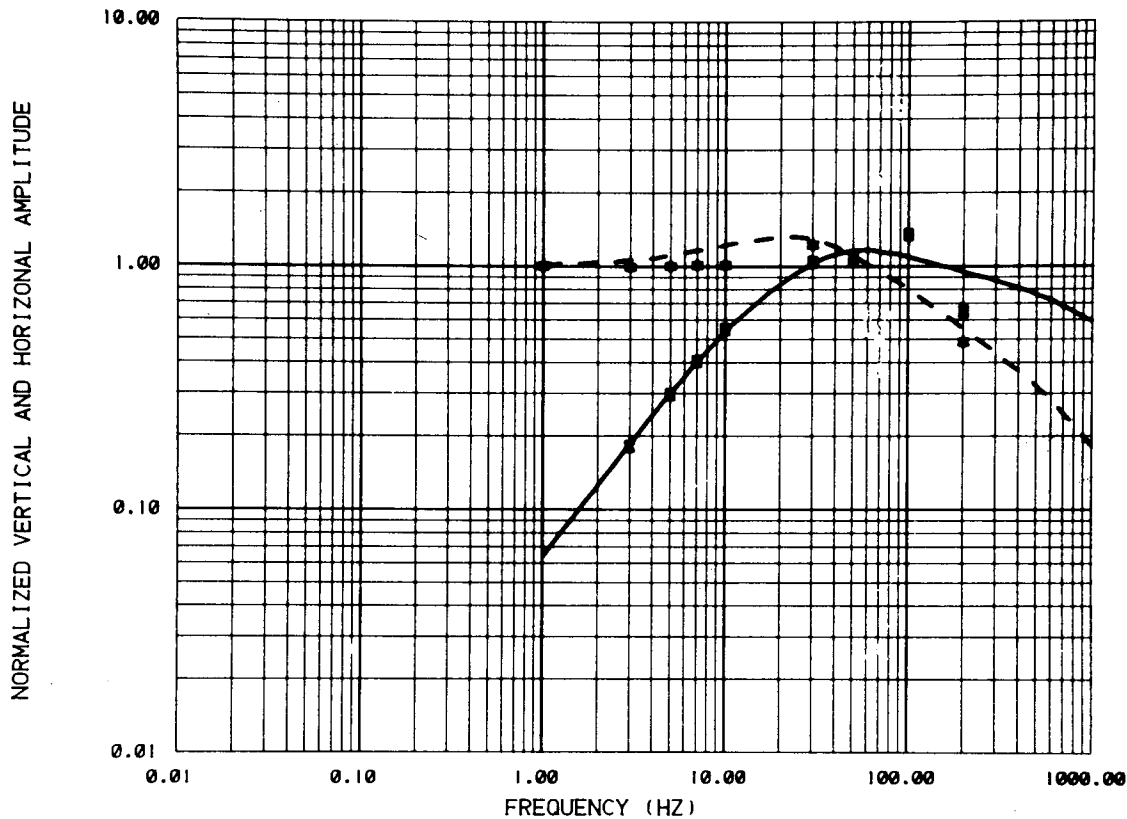
MCCOY TIR6

CALCULATED DATA	MEASURED DATA	LAYER	RESISTIVITY(OHM-M)	THICKNESS(M)
TILT ANGLE ———	TILT ANGLE X	1	17.44 ± .1315E-02	928.9 ± 61.
		2	111.9 ± 82.12	1256. ± 99.
		3	4.178 ± .1814	.1000E+11 ± 0.

DATA VARIANCE ESTIMATE 60.22

XBL 812-7973

COMPARISON OF CALCULATED AND MEASURED DATA



MCCOY T1R7

CALCULATED DATA

HR _____
 HZ — — —

MEASURED DATA

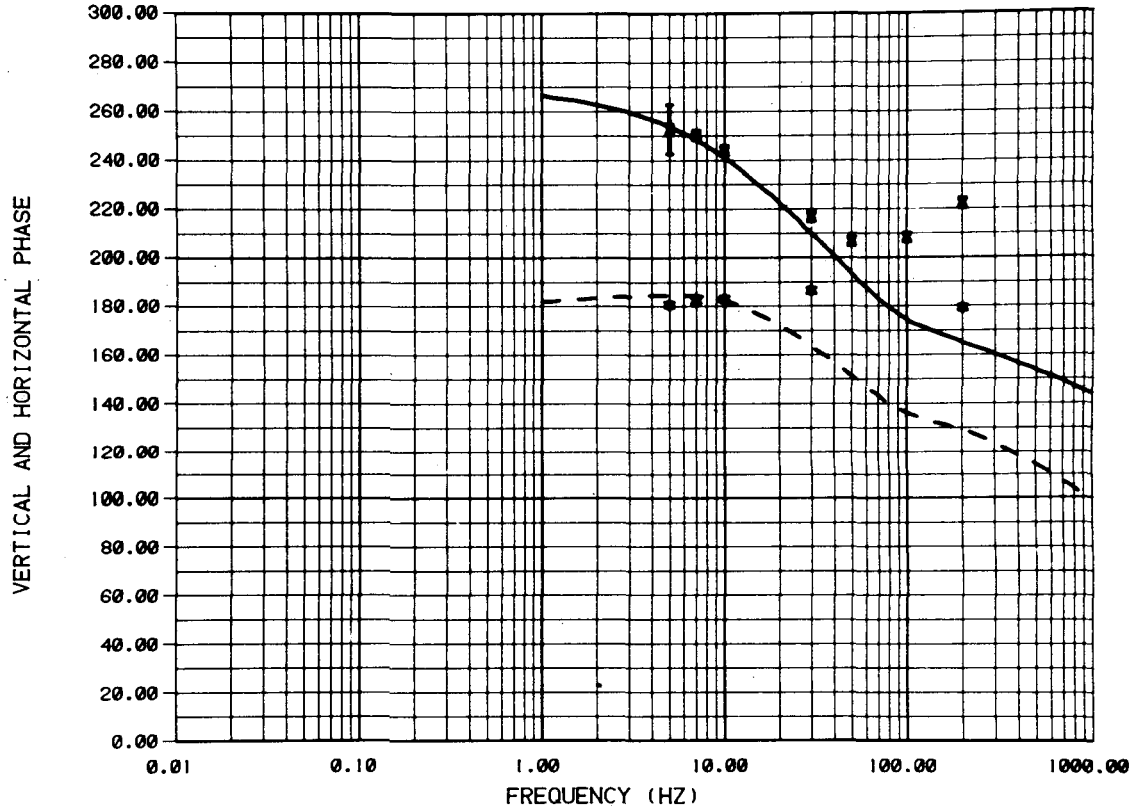
HR X
 HZ *

LAYER	RESISTIVITY(OHM-M)	THICKNESS(M)
1	19.97 ± .1467E-02	78.30 ± 2.
2	4.601 ± .1004	189.3 ± 10.
3	362.8 ± 843.7	.1000E+11 ± 0.

DATA VARIENCE ESTIMATE 510.4

XBL 812-7974

COMPARISON OF CALCULATED AND MEASURED DATA



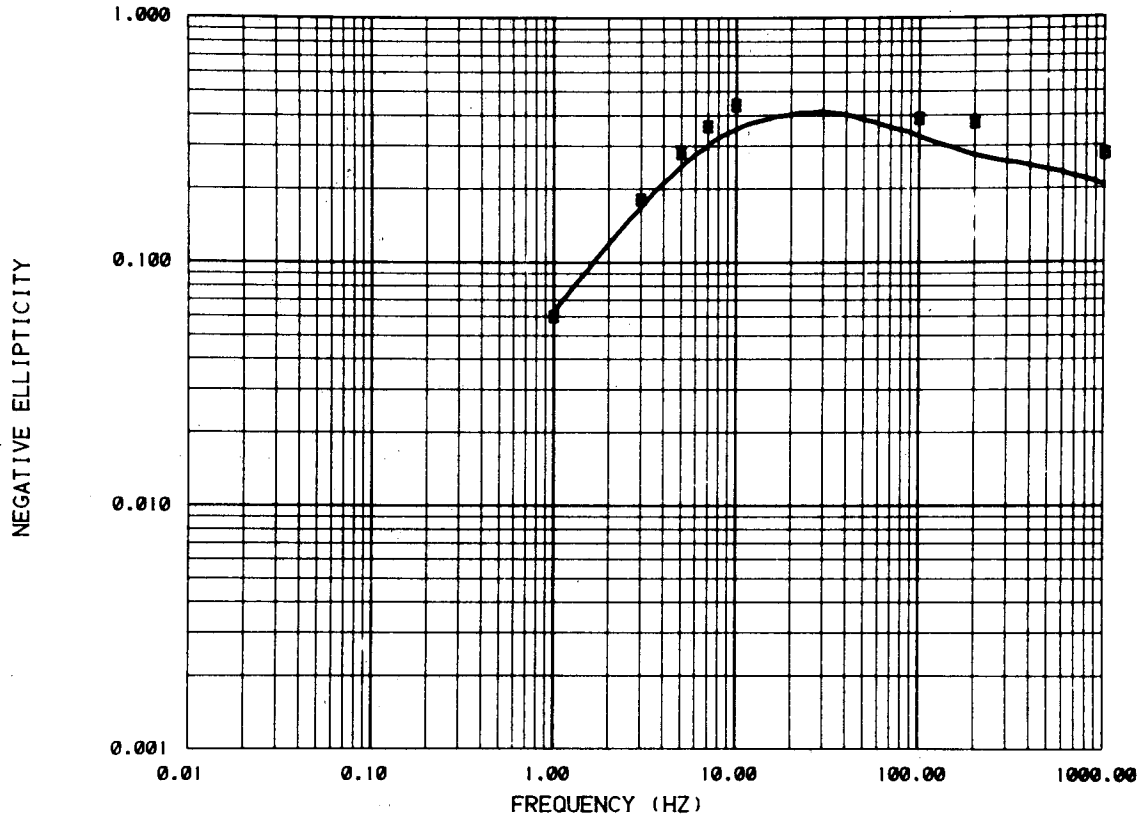
MCCOY T1R7

CALCULATED DATA		MEASURED DATA		LAYER	RESISTIVITY(OHM-M)	THICKNESS(M)
HR	—————	HR	X	1	19.97 ± .1467E-02	78.30 ± 2.
HZ	— — — —	HZ	*	2	4.601 ± .1004	189.3 ± 10.
				3	362.8 ± 843.7	.1000E+11 ± 0.

DATA VARIENCE ESTIMATE 510.4

XBL 812-7975

COMPARISON OF CALCULATED AND MEASURED DATA



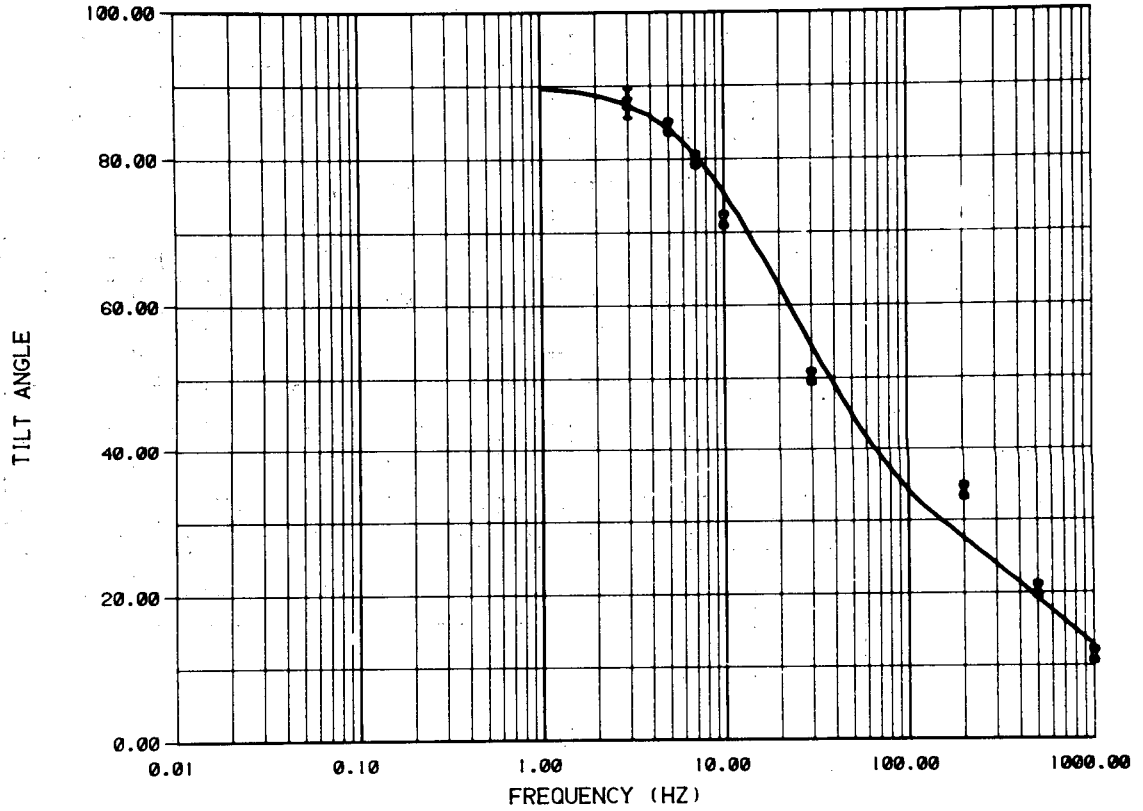
MCCOY TIR7

CALCULATED DATA	MEASURED DATA	LAYER	RESISTIVITY(OHM-M)	THICKNESS(M)
ELLIPTICITY	ELLIPTICITY	X 1	19.97 ± .1467E-02	78.30 • 2.
		2	4.601 ± .1004	189.3 • 10.
		3	362.8 ± 843.7	.1000E+11 • 0.

DATA VARIENCE ESTIMATE 510.4

XBL 812-7976

COMPARISON OF CALCULATED AND MEASURED DATA



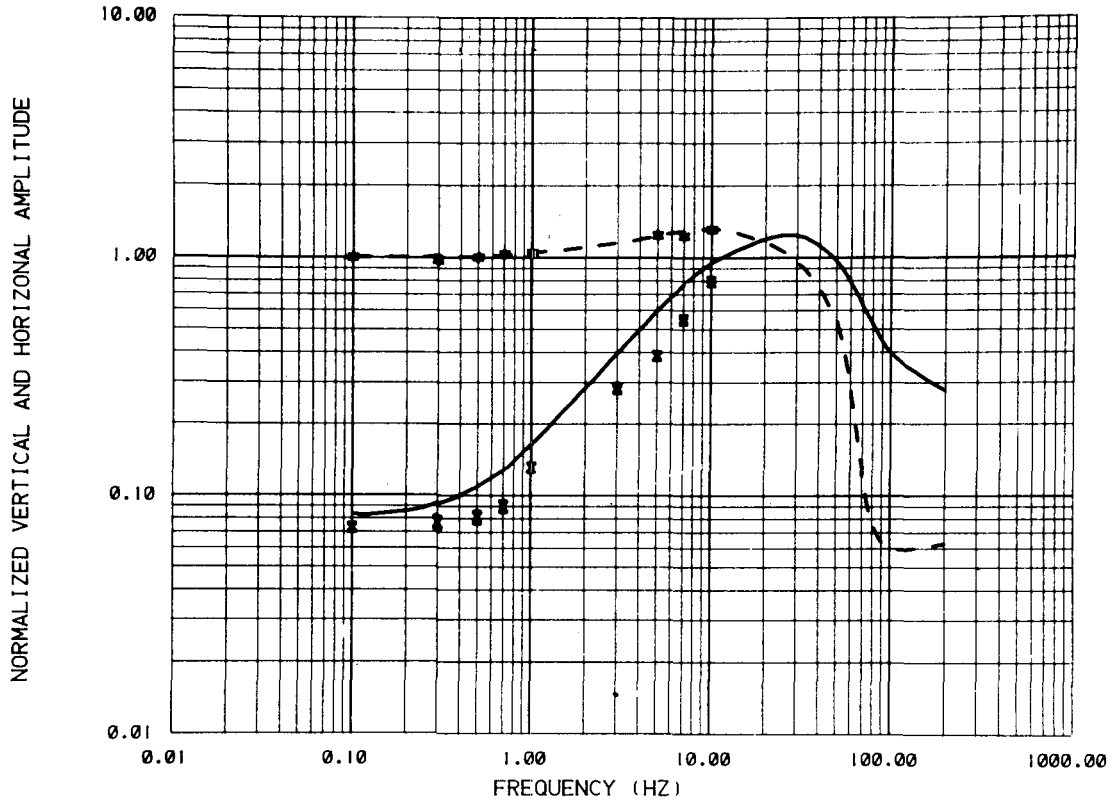
MCCOY TIR7

CALCULATED DATA	MEASURED DATA	LAYER	RESISTIVITY(OHM-M)	THICKNESS(M)
TILT ANGLE ———	TILT ANGLE X	1	19.97 ± .1467E-02	78.30 ± 2.
		2	4.601 ± .1004	189.3 ± 10.
		3	362.8 ± 843.7	.1000E+11 ± 0.

DATA VARIENCE ESTIMATE 510.4

XBL 812-7977

COMPARISON OF CALCULATED AND MEASURED DATA



MCCOY T2R1

CALCULATED DATA

HR —————
 HZ — — — — —

MEASURED DATA

HR X
 HZ *

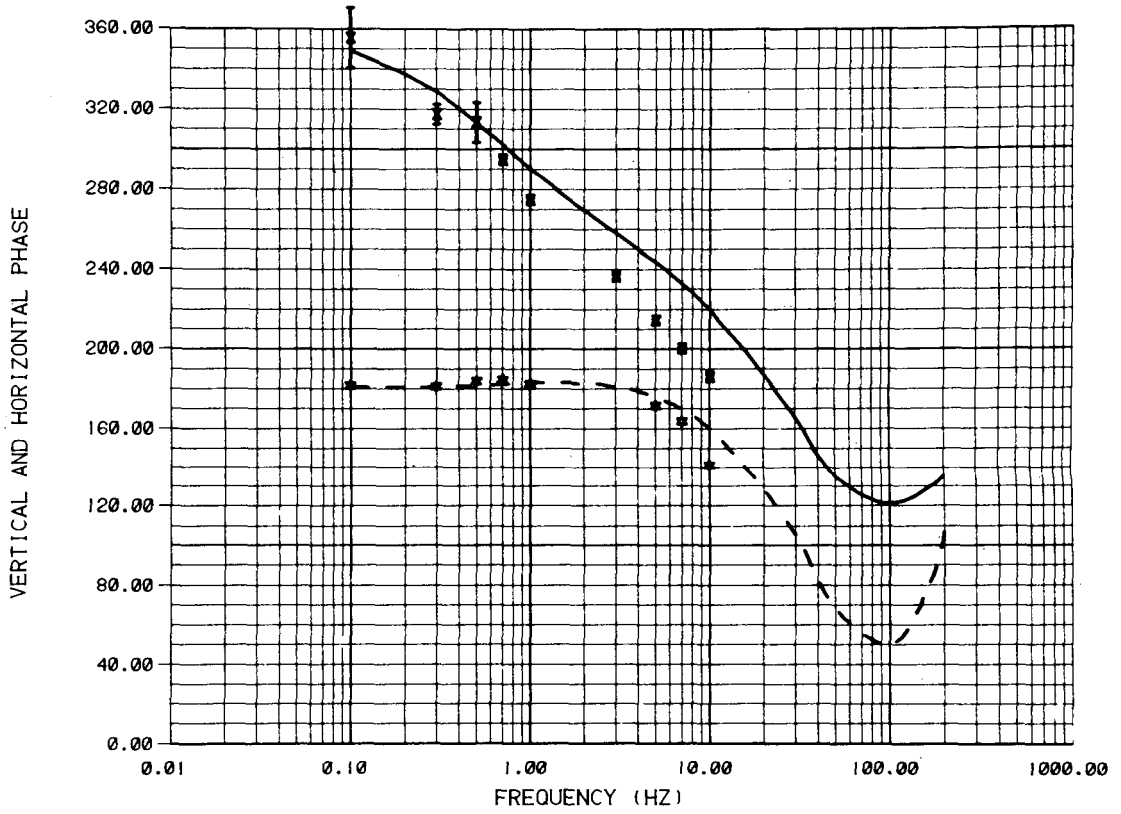
LAYER RESISTIVITY(OHM-M) THICKNESS(M)

1	19.59 ± .1013E-02	203.4 ± 2.
2	101.0 ± 2.066	.1000E+11 ± 0.

DATA VARIENCE ESTIMATE 217.5

XBL 812-7978

COMPARISON OF CALCULATED AND MEASURED DATA



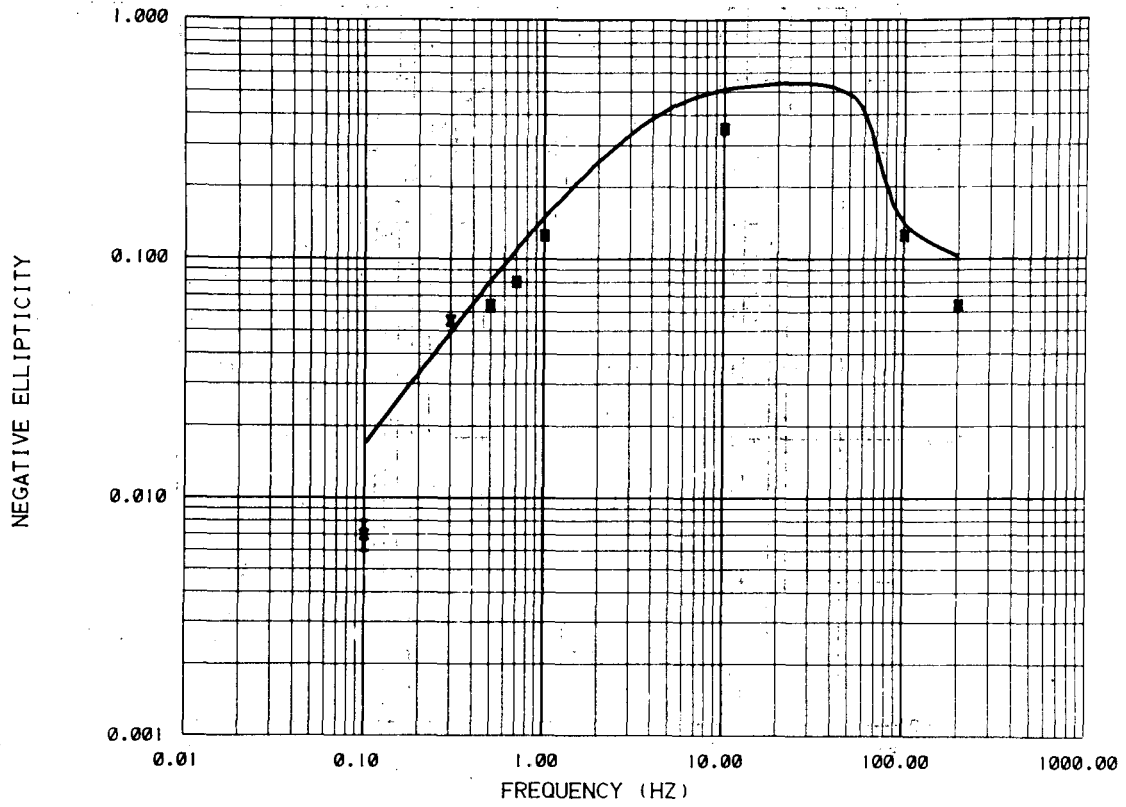
MCCOY T2R1

CALCULATED DATA		MEASURED DATA		LAYER	RESISTIVITY(OHM-M)	THICKNESS(M)
HR	—————	HR	X	1	19.59 ± .1013E-02	203.4 ± 2.
HZ	- - - - -	HZ	*	2	101.0 ± 2.066	.1000E+11 ± 0.

DATA VARIANCE ESTIMATE 217.5

XBL 812-7979

COMPARISON OF CALCULATED AND MEASURED DATA



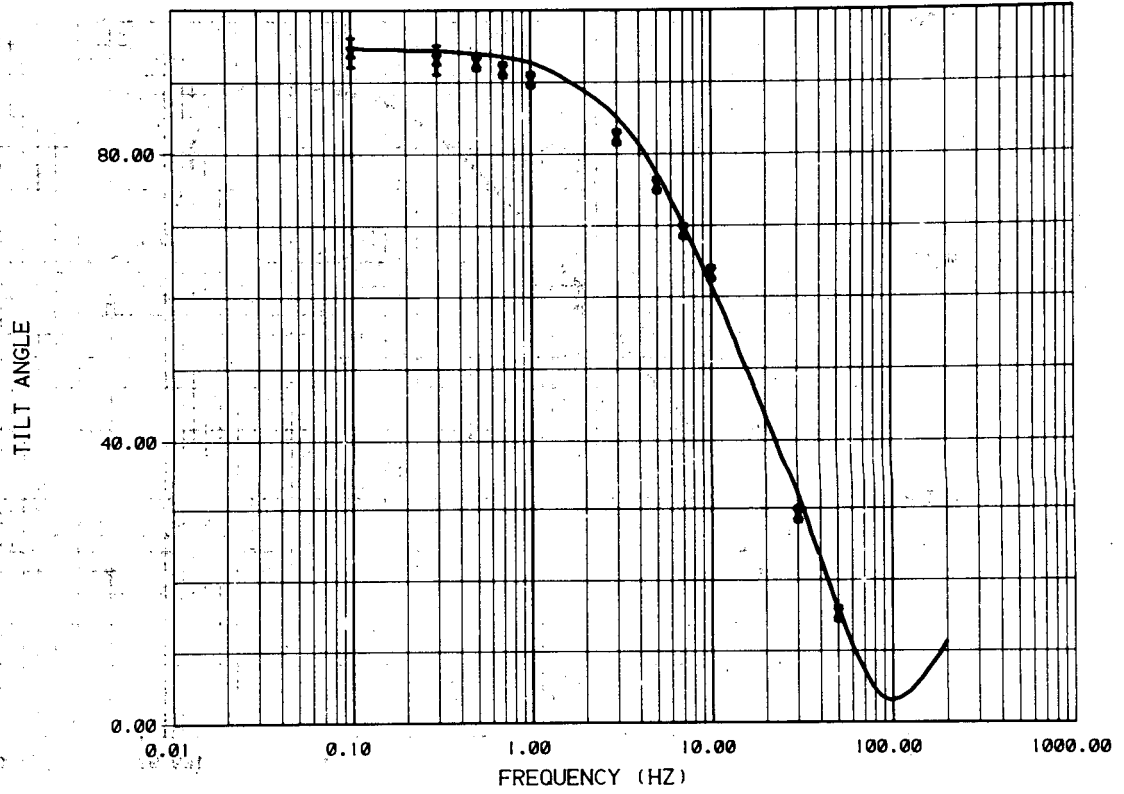
MCCOY T2R1

CALCULATED DATA	MEASURED DATA	LAYER	RESISTIVITY(OHM-M)	THICKNESS(M)
ELLIPTICITY	ELLIPTICITY	X 1	19.59 ± .1013E-02	203.4 ± 2.
		2	101.0 ± 2.066	.1000E+11 ± 0.

DATA VARIANCE ESTIMATE 217.5

XBL 812-7980

COMPARISON OF CALCULATED AND MEASURED DATA



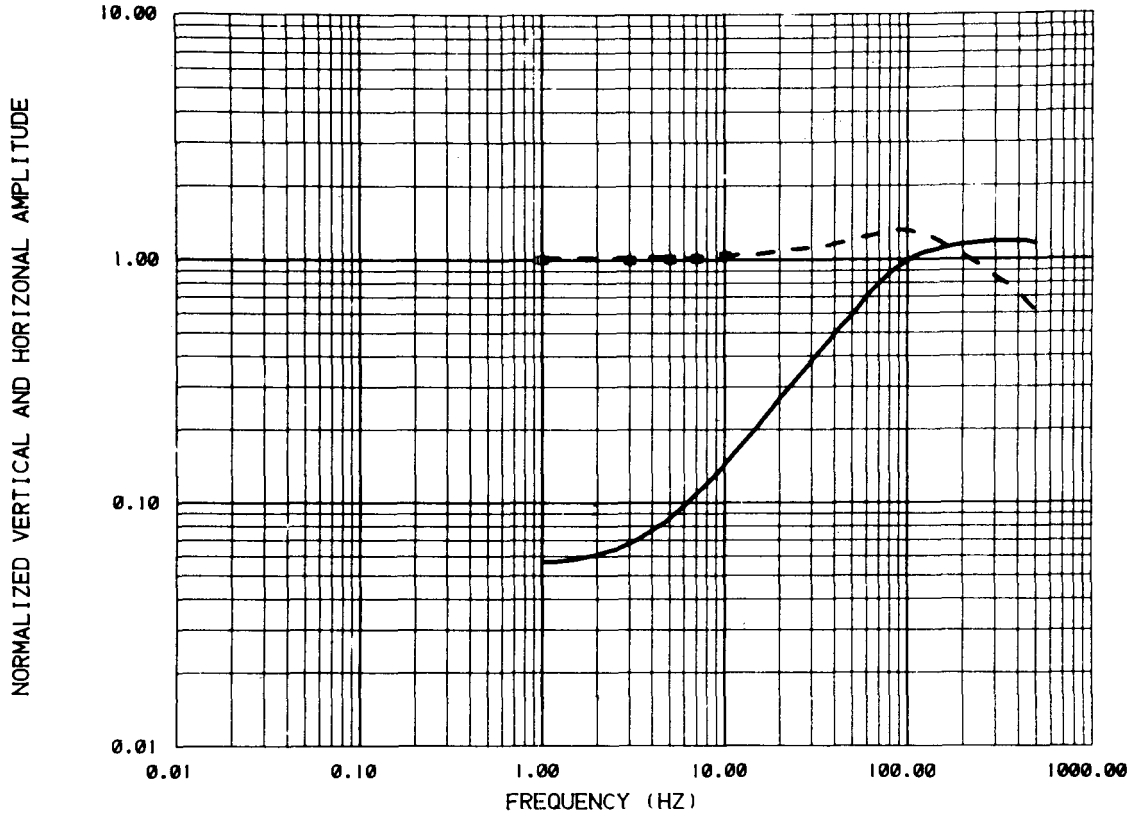
MCCOY T2R1

CALCULATED DATA	MEASURED DATA	LAYER	RESISTIVITY(OHM-M)	THICKNESS(M)
TILT ANGLE	TILT ANGLE	X 1	19.59 ± .1013E-02	203.4 ± 2.
		2	101.0 ± 2.066	.1000E+11 ± 0.

DATA VARIENCE ESTIMATE 217.5

XBL 812-7981

COMPARISON OF CALCULATED AND MEASURED DATA



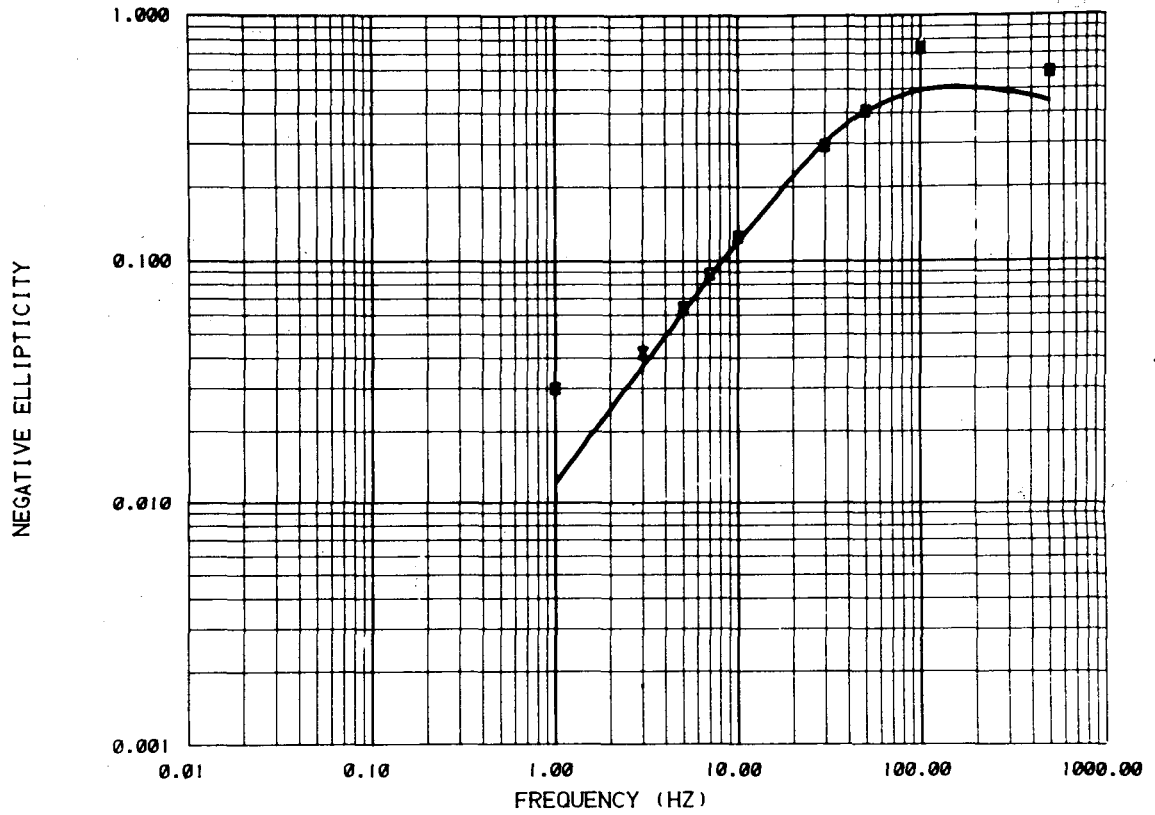
MCCOY T2R2

CALCULATED DATA		MEASURED DATA		LAYER	RESISTIVITY(OHM-M)	THICKNESS(M)
HR	—————	HR	X	1	14.03 ± .4155	110.2 ± 3.
HZ	— — —	HZ	*	2	511.7 ± 382.8	.1000E+11 ± 0.

DATA VARIANCE ESTIMATE 407.1

XBL 812-7982

COMPARISON OF CALCULATED AND MEASURED DATA



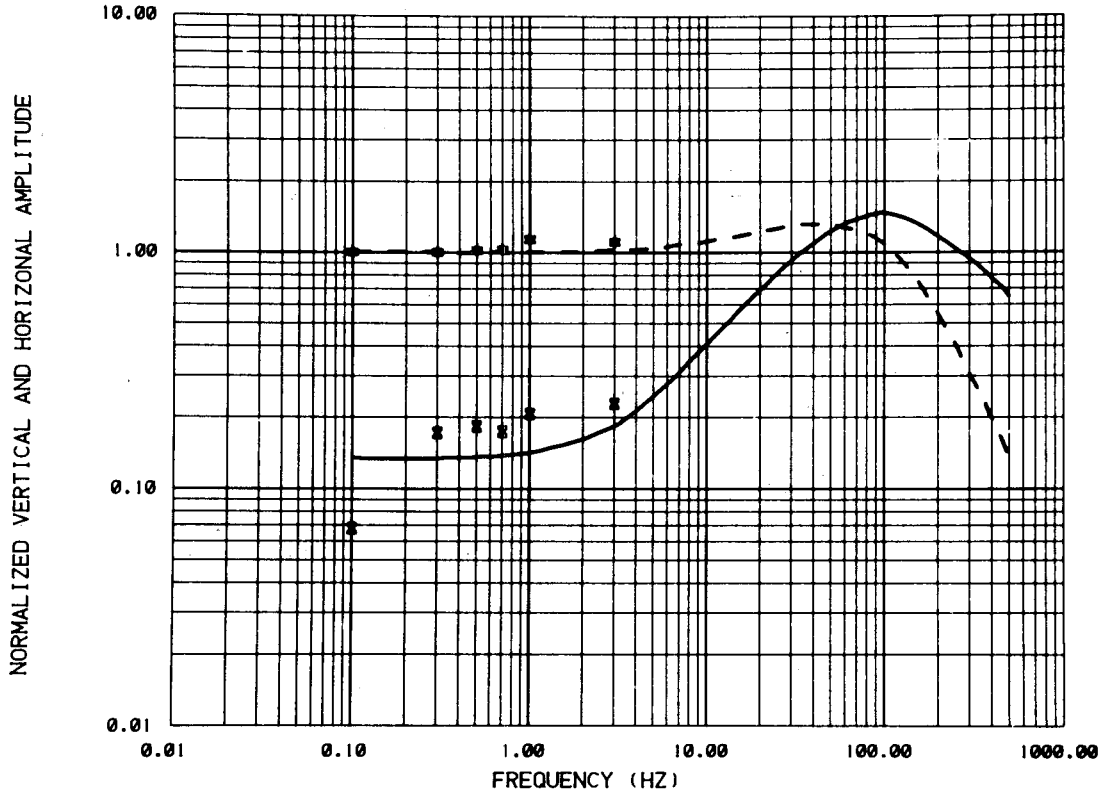
MCCOY T2R2

CALCULATED DATA	MEASURED DATA	LAYER	RESISTIVITY(OHM-M)	THICKNESS(M)
ELLIPTICITY ———	ELLIPTICITY	X 1	14.03 ± .4155	110.2 ± 3.
		2	511.7 ± 382.8	.1000E+11 ± 0.

DATA VARIENCE ESTIMATE 407.1

XBL 812-7983

COMPARISON OF CALCULATED AND MEASURED DATA



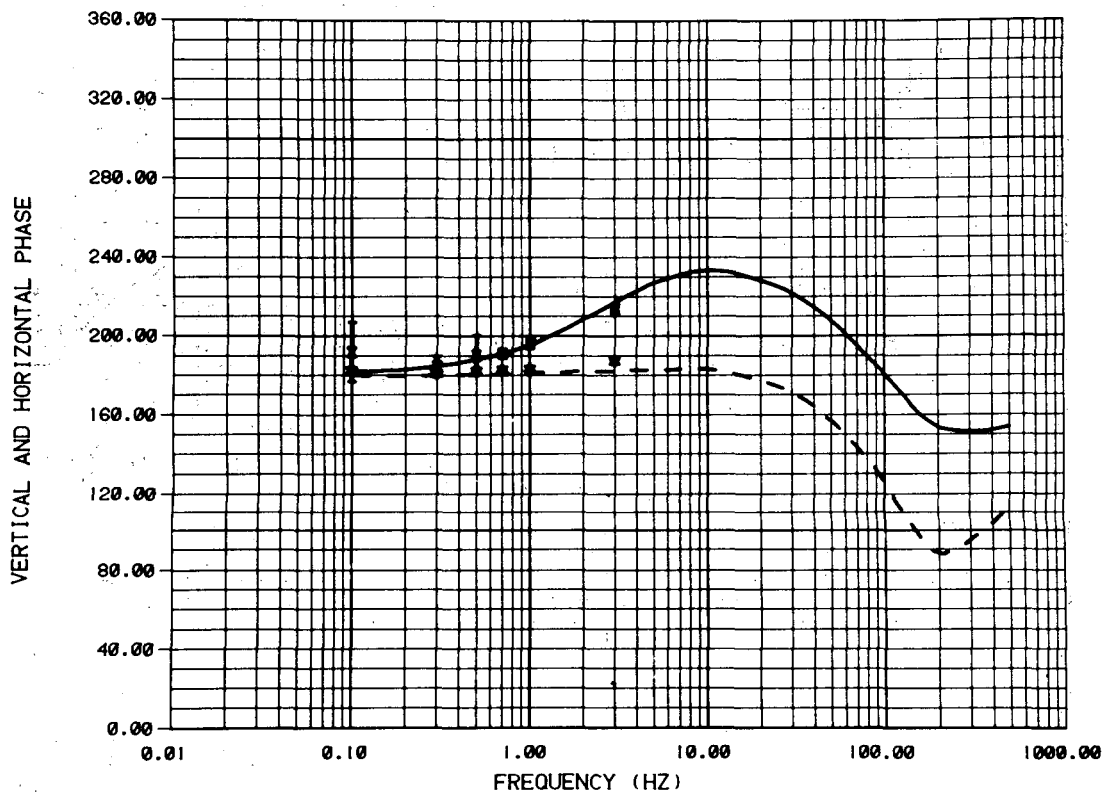
MCCOY T2R3

CALCULATED DATA		MEASURED DATA		LAYER	RESISTIVITY(OHM-M)	THICKNESS(M)
HR	—————	HR	X	1	68.60 ± .1450E-02	312.7 ± 13.
HZ	-----	HZ	*	2	295.6 ± 29.06	.1000E+11 ± 0.

DATA VARIENCE ESTIMATE 91.27

XBL 812-7984

COMPARISON OF CALCULATED AND MEASURED DATA



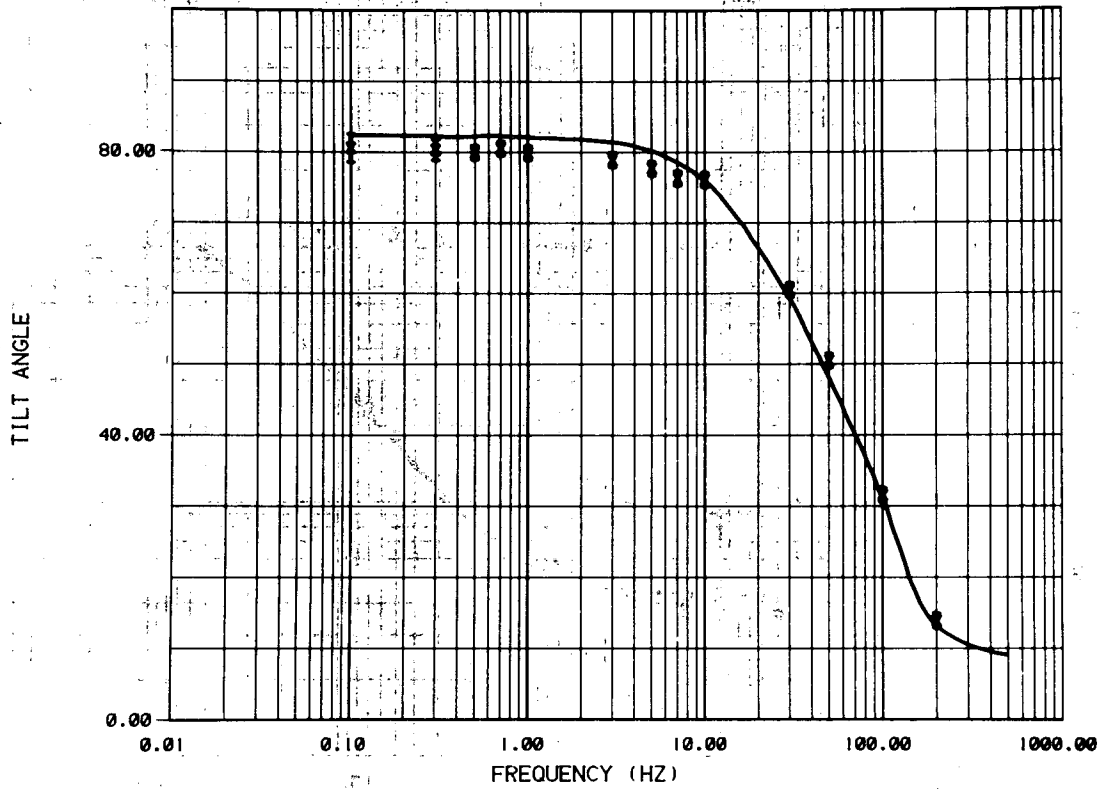
MCCOY T2R3

CALCULATED DATA		MEASURED DATA		LAYER	RESISTIVITY(OHM-M)	THICKNESS(M)
HR	—————	HR	X	1	68.60	* .1450E-02 312.7 * 13.
HZ	- - - - -	HZ	*	2	295.6	* 29.06 .1000E+11 * 0.

DATA VARIANCE ESTIMATE 91.27

XBL 812-7985

COMPARISON OF CALCULATED AND MEASURED DATA



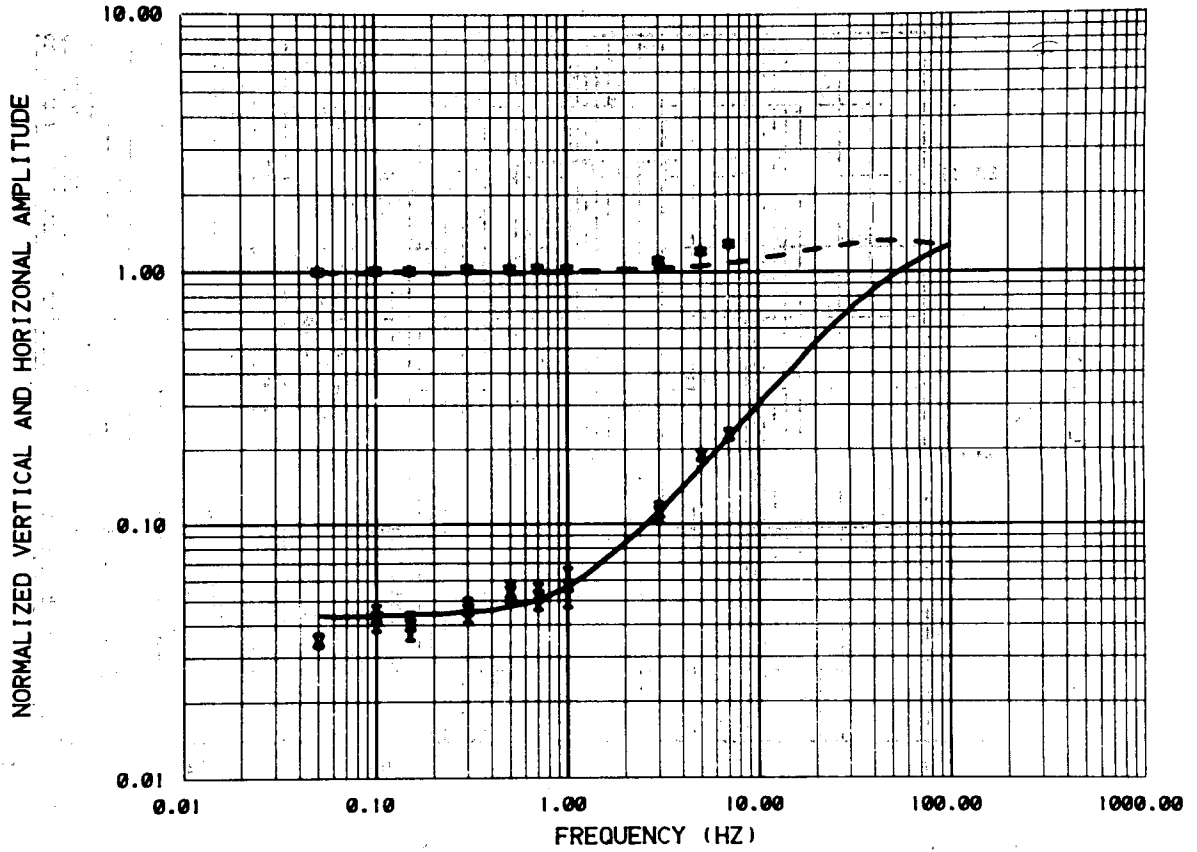
MCCOY T2R3

CALCULATED DATA	MEASURED DATA	LAYER	RESISTIVITY(OHM-M)	THICKNESS(M)
TILT ANGLE	TILT ANGLE	X 1	68.60 ± .1450E-02	312.7 ± 13.
		2	295.6 ± 29.06	.1000E+11 ± 0.

DATA VARIENCE ESTIMATE 91.27

XBL 812-7986

COMPARISON OF CALCULATED AND MEASURED DATA



MCCOY T2R4 VARIABLE DIPOLE

CALCULATED DATA

HR _____
 HZ _____

MEASURED DATA

HR X
 HZ *

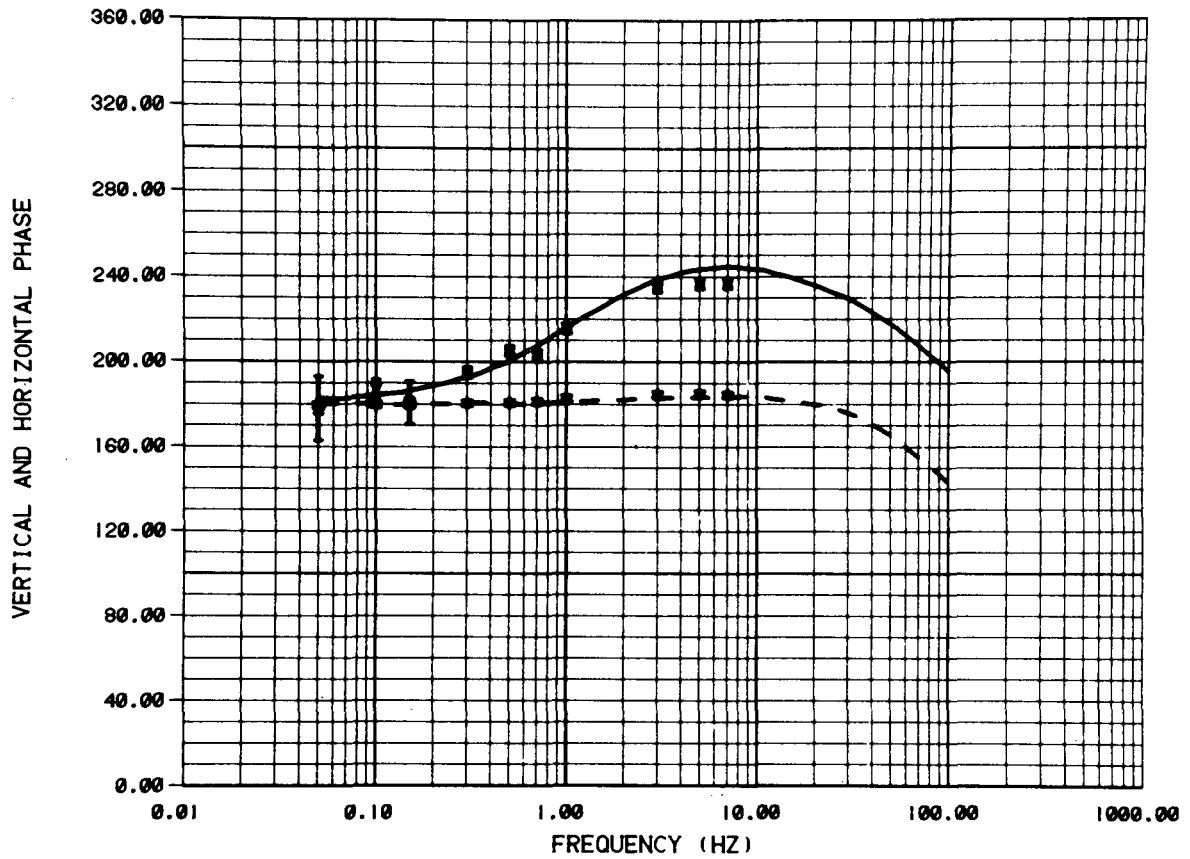
LAYER RESISTIVITY(OHM-M) THICKNESS(M)

1	81.00	± .1077E-02	67.00	± 3.
2	150.0	± 1.325	.1000E+11	± 0.

DATA VARIANCE ESTIMATE 1422.

XBL 8012-12985

COMPARISON OF CALCULATED AND MEASURED DATA



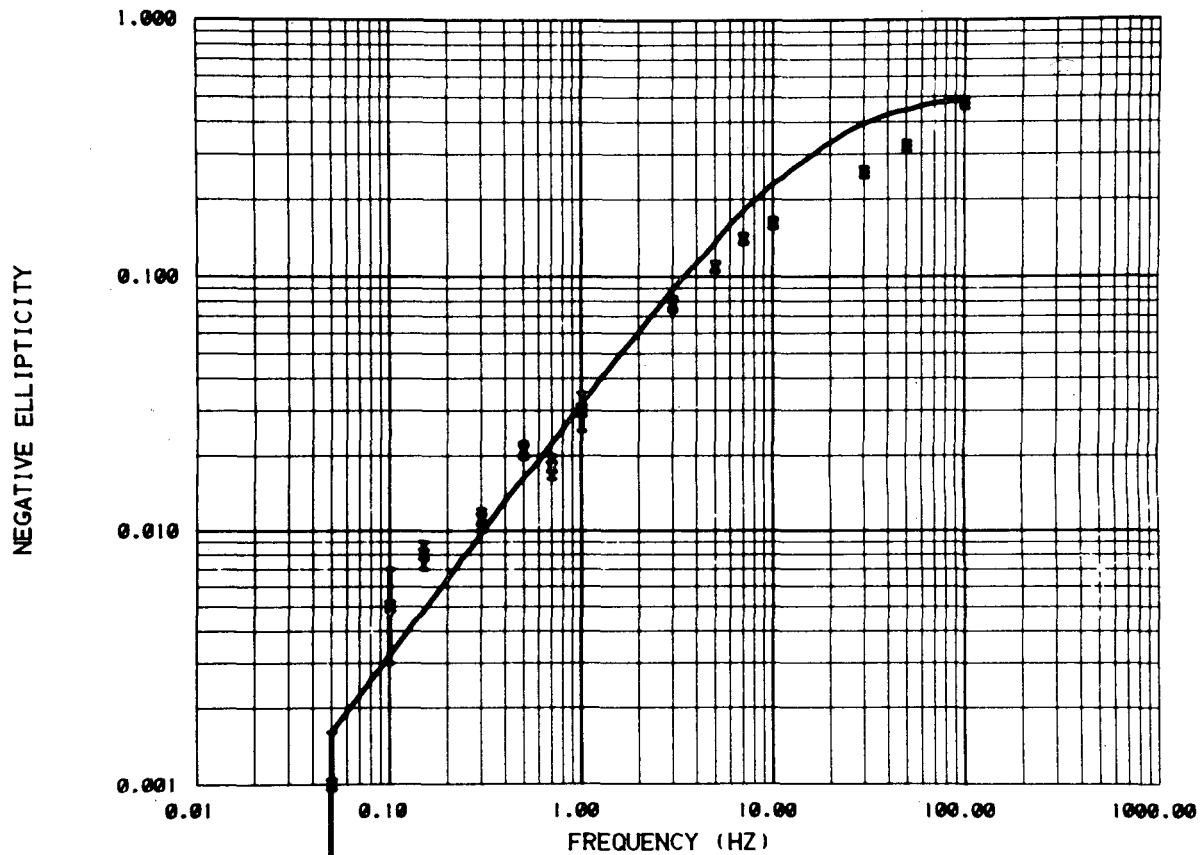
MCCOY T2R4 VARIABLE DIPOLE

CALCULATED DATA		MEASURED DATA		LAYER	RESISTIVITY(OHM-M)	THICKNESS(M)
HR	—————	HR	X	1	81.00 ± .1077E-02	67.00 ± 3.
HZ	- - - - -	HZ	*	2	150.0 ± 1.325	.1000E+11 ± 0.

DATA VARIANCE ESTIMATE 1422.

XBL 8012-12984

COMPARISON OF CALCULATED AND MEASURED DATA



MCOY T2R4 VARIABLE DIPOLE

CALCULATED DATA
ELLIPTICITY



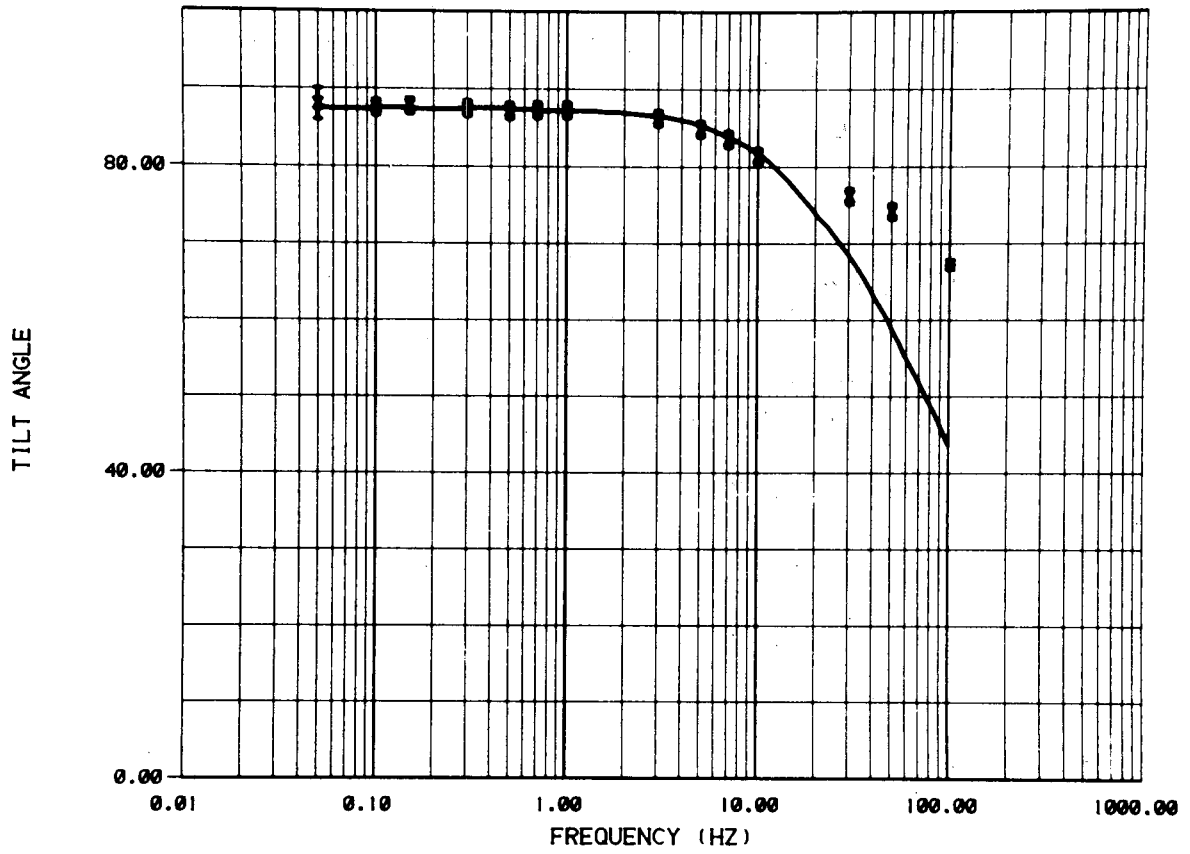
MEASURED DATA
ELLIPTICITY

LAYER	RESISTIVITY(OHM-M)	THICKNESS(M)
X 1	81.00 ± .1077E-02	67.00 ± 3.
2	150.0 ± 1.325	.1000E+11 ± 0.

DATA VARIANCE ESTIMATE 1422.

XBL 8012-12990

COMPARISON OF CALCULATED AND MEASURED DATA



MCCOY T2R4 VARIABLE DIPOLE

CALCULATED DATA

TILT ANGLE

————

MEASURED DATA

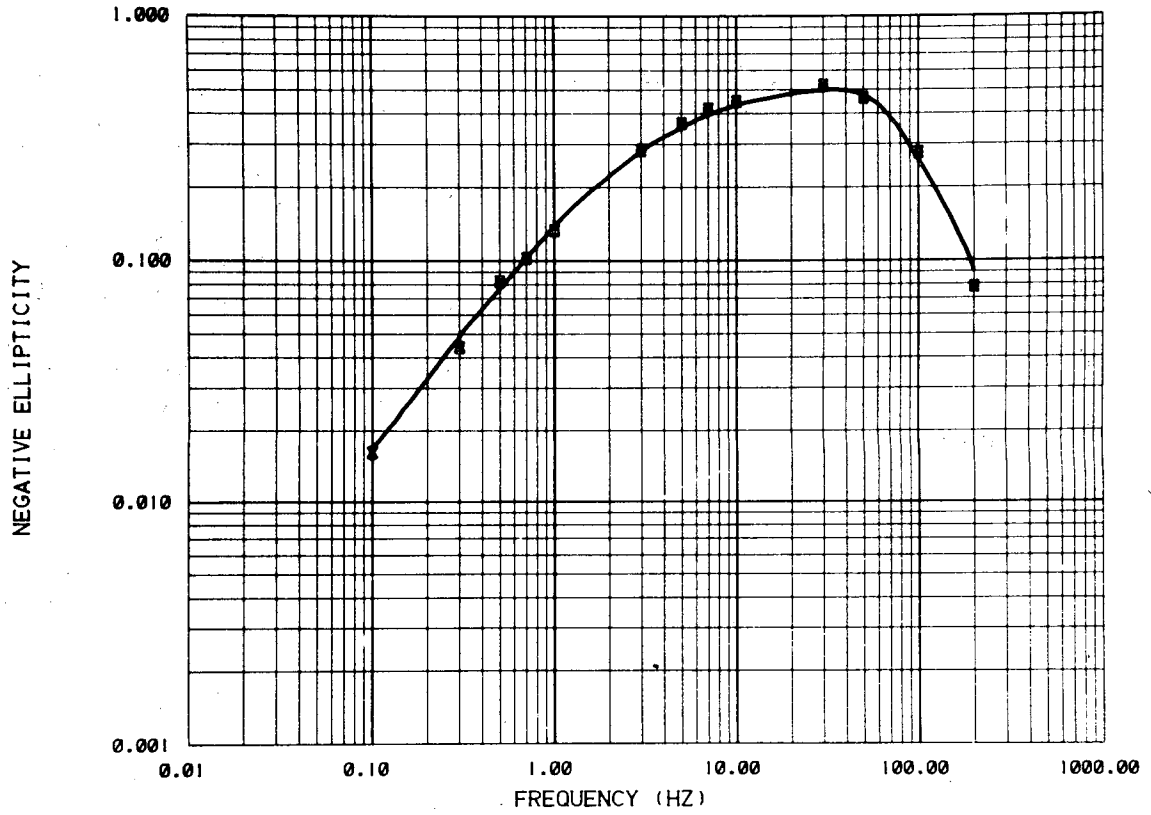
TILT ANGLE

LAYER	RESISTIVITY(OHM-M)	THICKNESS(M)
X 1	81.00 ± .1077E-02	67.00 ± 3.
2	150.0 ± 1.325	.1000E+11 ± 0.

DATA VARIANCE ESTIMATE 1422.

XBL 8012-12986

COMPARISON OF CALCULATED AND MEASURED DATA



MCCOY T2R5

CALCULATED DATA
ELLIPTICITY

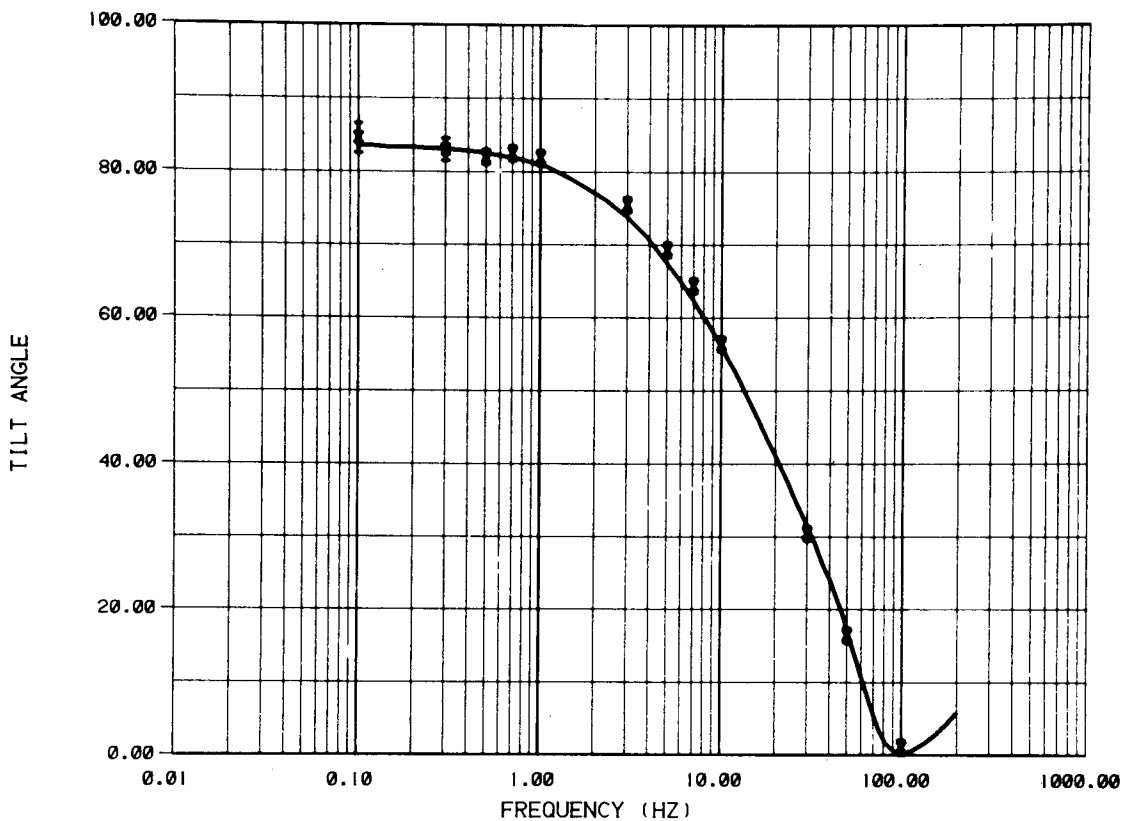
MEASURED DATA
ELLIPTICITY

LAYER	RESISTIVITY(OHM-M)	THICKNESS(M)
1	20.61 ± .4402E-02	165.1 ± 4.
2	126.3 ± 10.72	594.6 ± 48.
3	38.43 ± 1.894	.1000E+11 ± 0.

DATA VARIANCE ESTIMATE 23.81

XBL 812-7987

COMPARISON OF CALCULATED AND MEASURED DATA



MCCOY T2R5

CALCULATED DATA

TILT ANGLE

—————

MEASURED DATA

TILT ANGLE

LAYER X

RESISTIVITY(OHM-M)

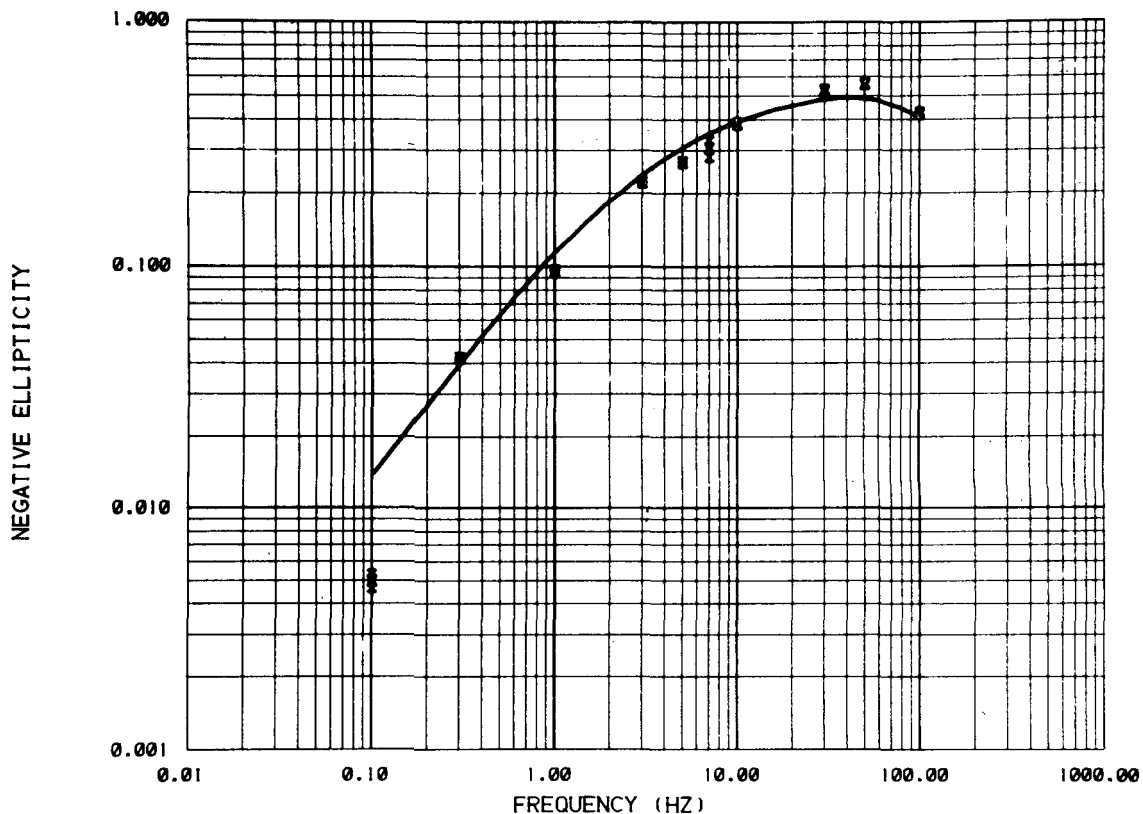
THICKNESS(M)

1	20.61 ± .4402E-02	165.1 ± 4.
2	126.3 ± 10.72	594.6 ± 48.
3	38.43 ± 1.894	.1000E+11 ± 0.

DATA VARIENCE ESTIMATE 23.81

XBL 812-7988

COMPARISON OF CALCULATED AND MEASURED DATA



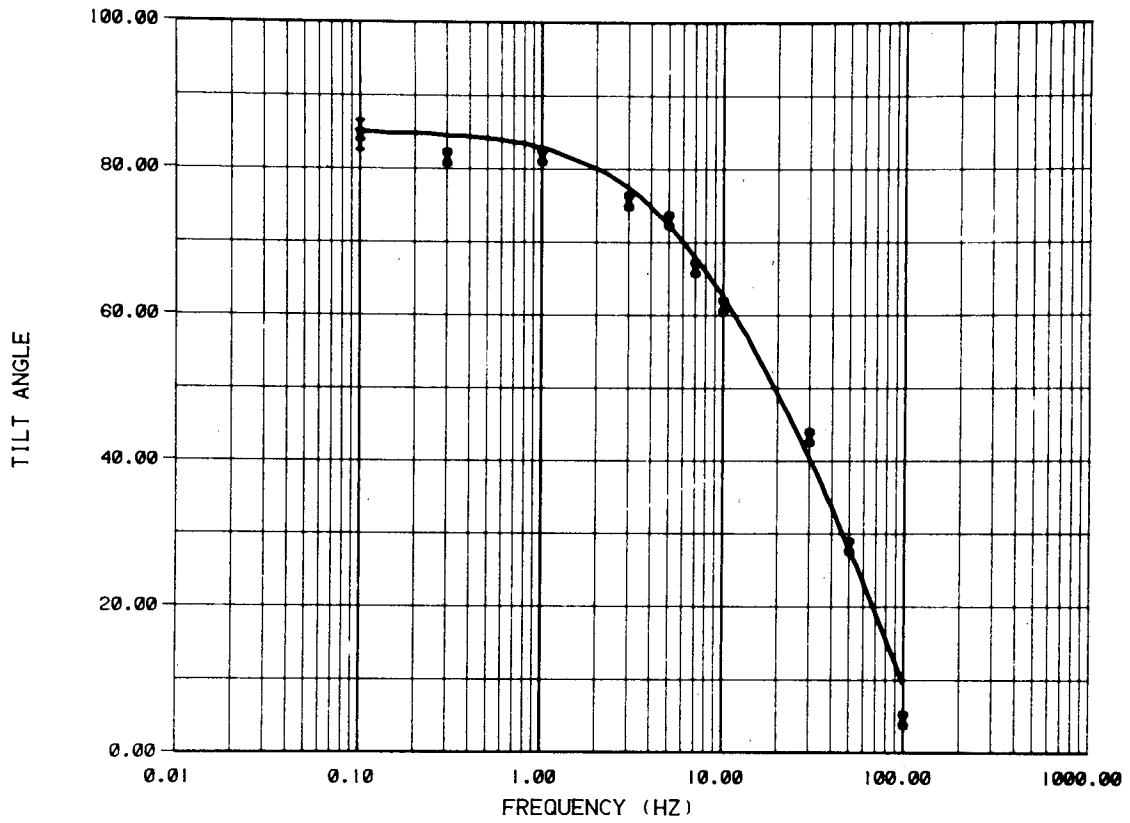
MCCOY T2R6

CALCULATED DATA	MEASURED DATA	LAYER	RESISTIVITY(OHM-M)	THICKNESS(M)
ELLIPTICITY ———	ELLIPTICITY	X 1	44.46 ± .4833E-02	88.66 ± 11.
		2	167.2 ± 9.746	1522. ± 182.
		3	72.36 ± 6.498	.1000E+11 ± 0.

DATA VARIANCE ESTIMATE 142.6

XBL 812-7989

COMPARISON OF CALCULATED AND MEASURED DATA



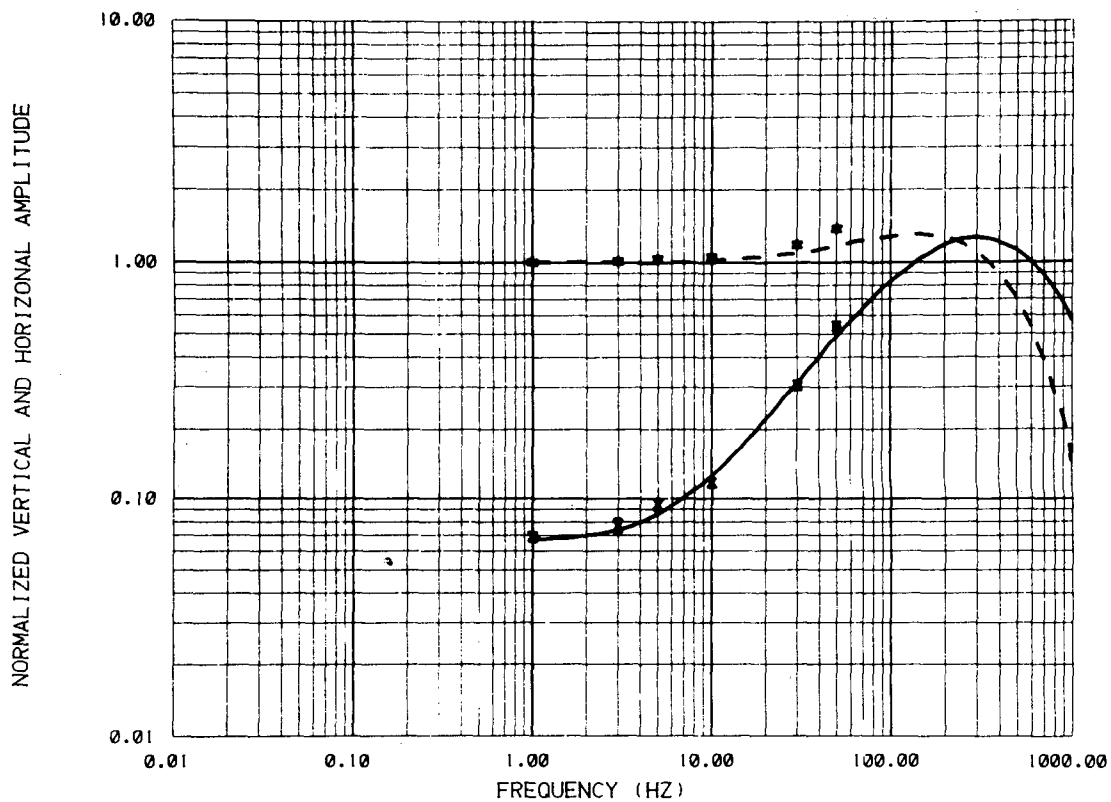
MCCOY T2R6

CALCULATED DATA	MEASURED DATA	LAYER	RESISTIVITY(OHM-M)	THICKNESS(M)
TILT ANGLE ———	TILT ANGLE X	1	44.46 ± .4833E-02	88.66 ± 11.
		2	167.2 ± 9.746	1522. ± 182.
		3	72.36 ± 6.498	.1000E+11 ± 0.

DATA VARIENCE ESTIMATE 142.6

XBL 812-7990

COMPARISON OF CALCULATED AND MEASURED DATA



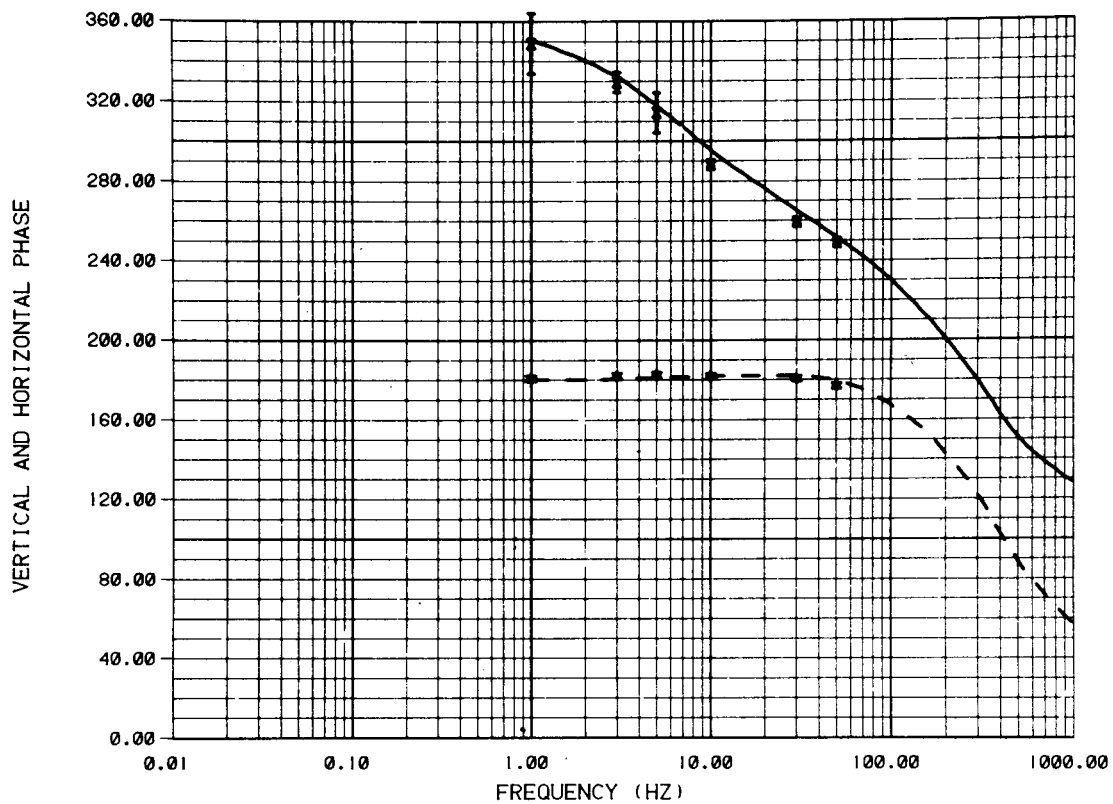
MCCOY T3R1

CALCULATED DATA		MEASURED DATA		LAYER	RESISTIVITY(OHM-M)	THICKNESS(M)
HR	—————	HR	X	1	20.30 ± .1131E-02	97.96 ± 2.
HZ	— — — — —	HZ	*	2	210.2 ± 24.86	.1000E+11 ± 0.

DATA VARIANCE ESTIMATE 60.72

XBL 812-7991

COMPARISON OF CALCULATED AND MEASURED DATA



MCCOY T3R1

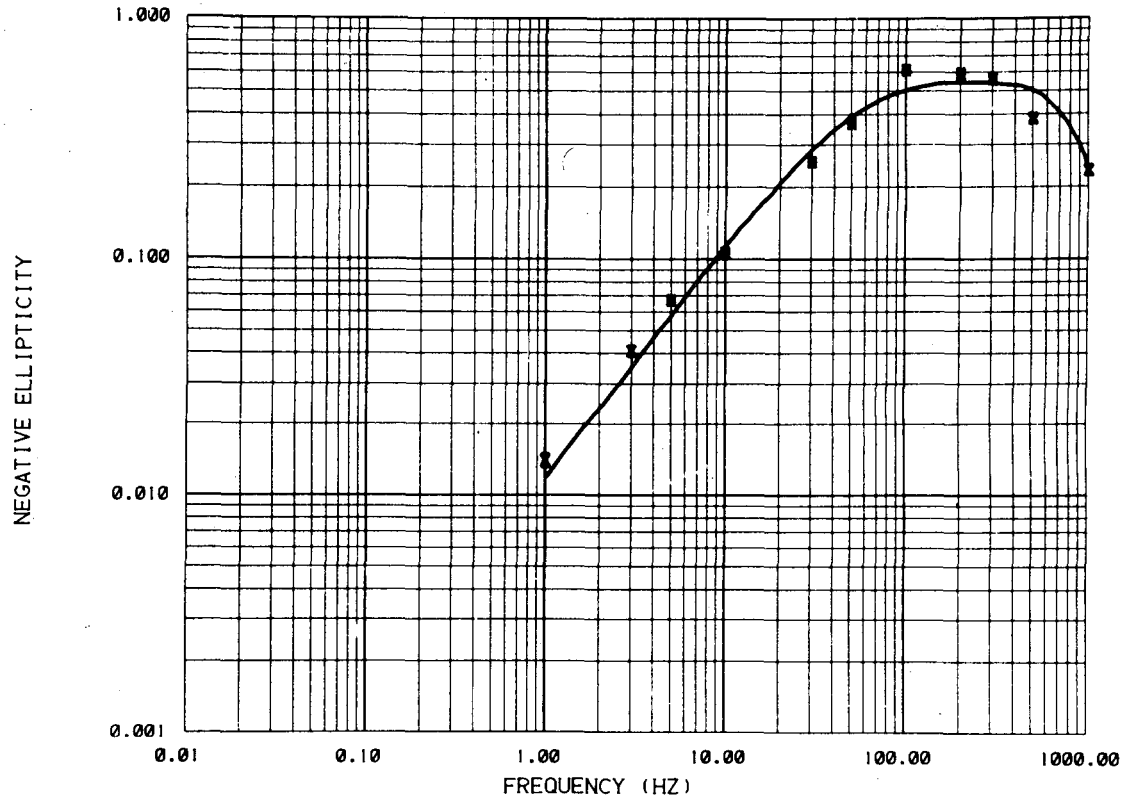
CALCULATED DATA		MEASURED DATA		LAYER	RESISTIVITY(OHM-M)	THICKNESS(M)
HR	—————	HR	X	1	20.30 ± .1131E-02	97.96 ± 2.
HZ	— — — — —	HZ	*	2	210.2 ± 24.86	.1000E+11 ± 0.

DATA VARIANCE ESTIMATE 60.72

XBL 812-7992

L

COMPARISON OF CALCULATED AND MEASURED DATA



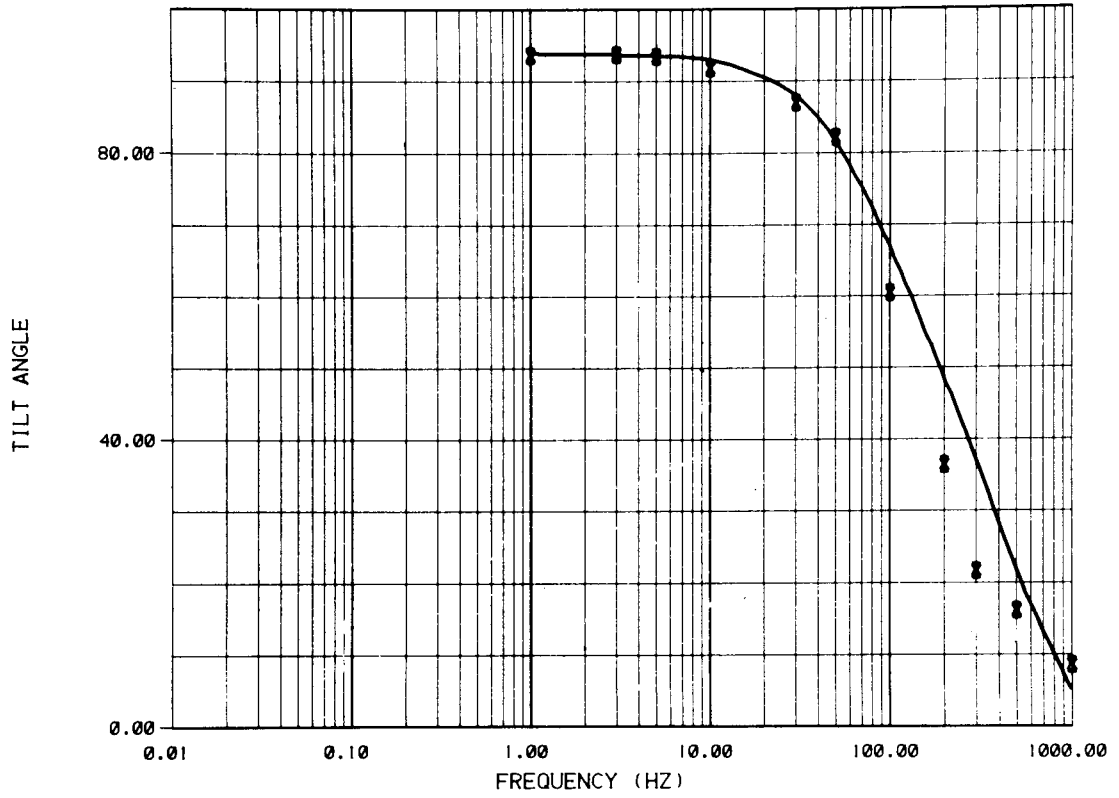
MCCOY T3R1

CALCULATED DATA	MEASURED DATA	LAYER	RESISTIVITY(OHM-M)	THICKNESS(M)
ELLIPTICITY	ELLIPTICITY	X 1	20.30 ± .1131E-02	97.96 ± 2.
		2	210.2 ± 24.86	.1000E+11 ± 0.

DATA VARIENCE ESTIMATE 60.72

XBL 812-7993

COMPARISON OF CALCULATED AND MEASURED DATA



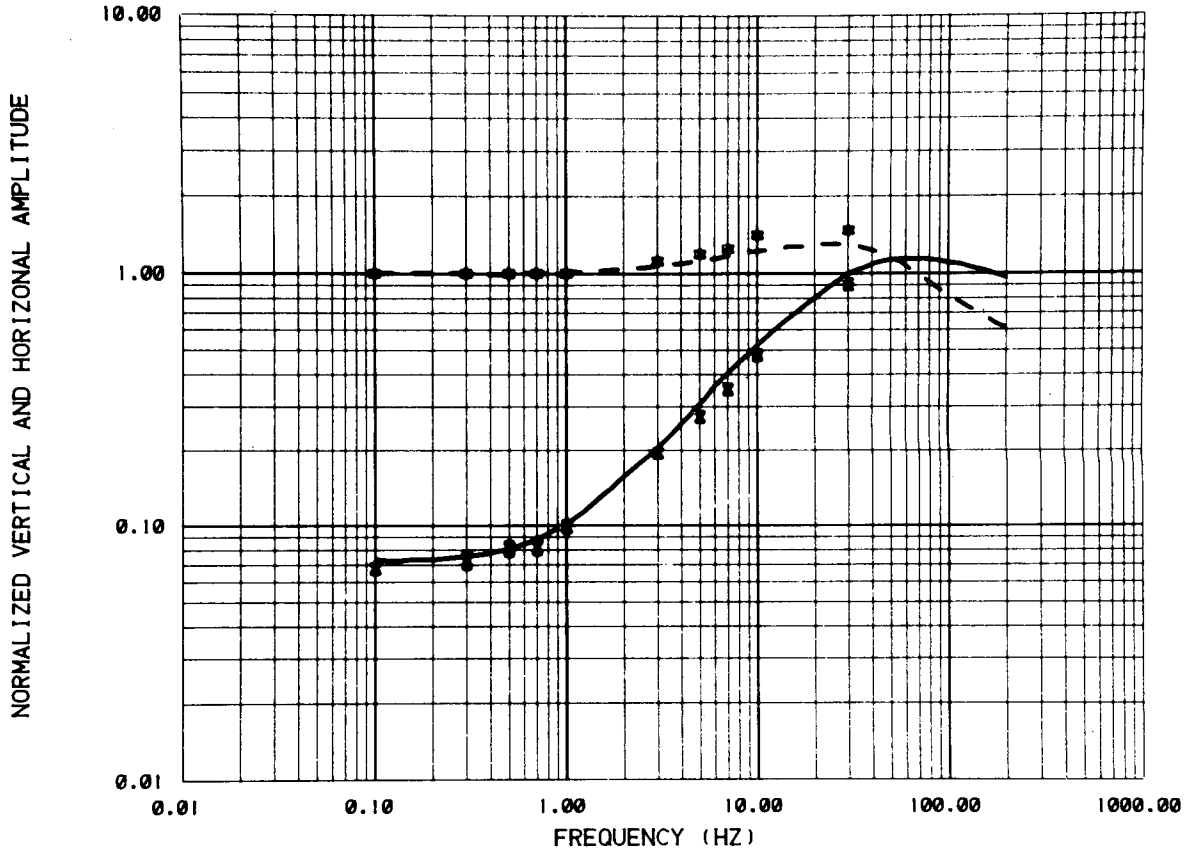
MCCOY T3R1

CALCULATED DATA	MEASURED DATA	LAYER	RESISTIVITY(OHM-M)	THICKNESS(M)
TILT ANGLE	TILT ANGLE	X 1	20.30 ± .1131E-02	97.96 ± 2.
		2	210.2 ± 24.86	.1000E+11 ± 0.

DATA VARIANCE ESTIMATE 60.72

XBL 812-7994

COMPARISON OF CALCULATED AND MEASURED DATA



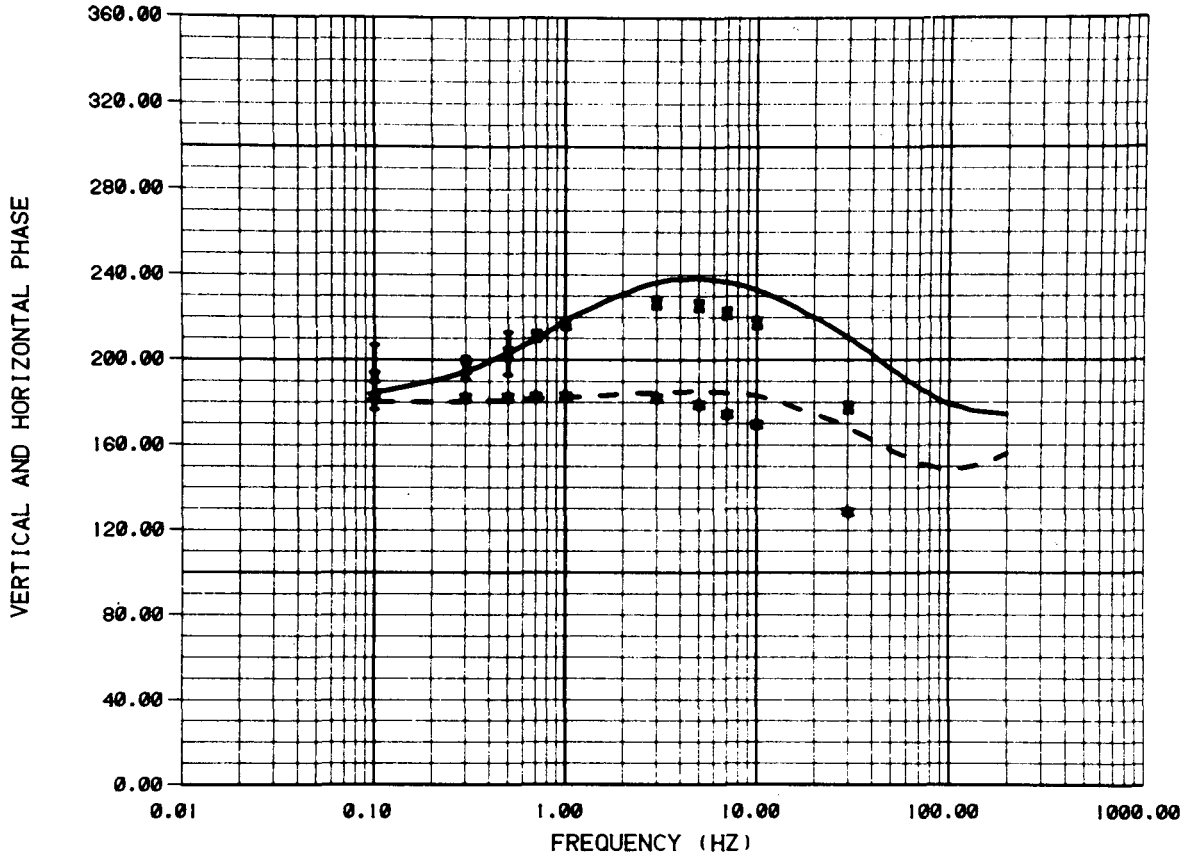
MCCOY T3R2 VARIABLE DIPOLE

CALCULATED DATA		MEASURED DATA		LAYER	RESISTIVITY(OHM-M)	THICKNESS(M)
HR	—————	HR	X	1	200.0 ± 0.	100.0 ± 0.
HZ	- - - - -	HZ	*	2	100.0 ± 0.	.1000E+12 ± 0.

DATA VARIENCE ESTIMATE 135.6

XBL 8012-12974

COMPARISON OF CALCULATED AND MEASURED DATA



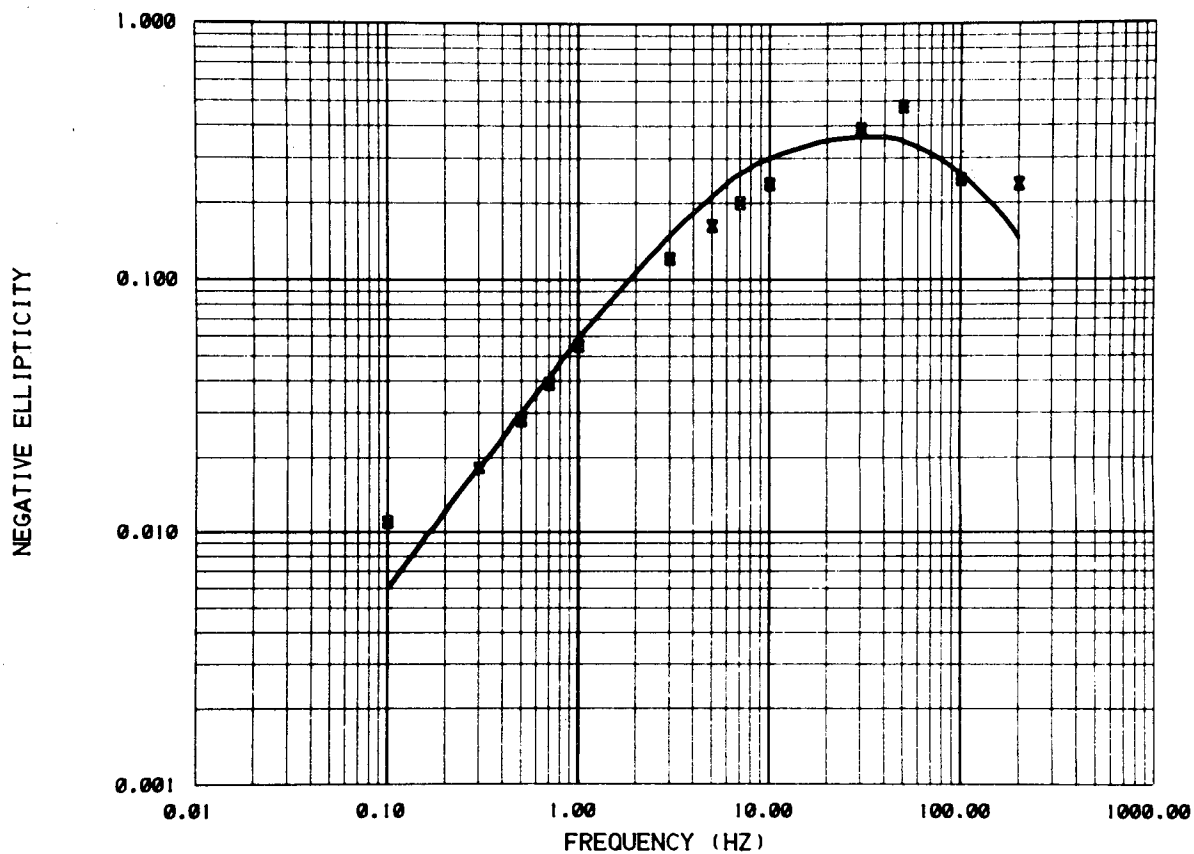
MCCOY T3R2 VARIABLE DIPOLE

CALCULATED DATA		MEASURED DATA		LAYER	RESISTIVITY(OHM-M)	THICKNESS(M)
HR	—————	HR	X	1	200.0 ± 0.	100.0 ± 0.
HZ	— — — — —	HZ	*	2	100.0 ± 0.	.1000E+12 ± 0.

DATA VARIANCE ESTIMATE 135.6

XBL 8012-12970

COMPARISON OF CALCULATED AND MEASURED DATA



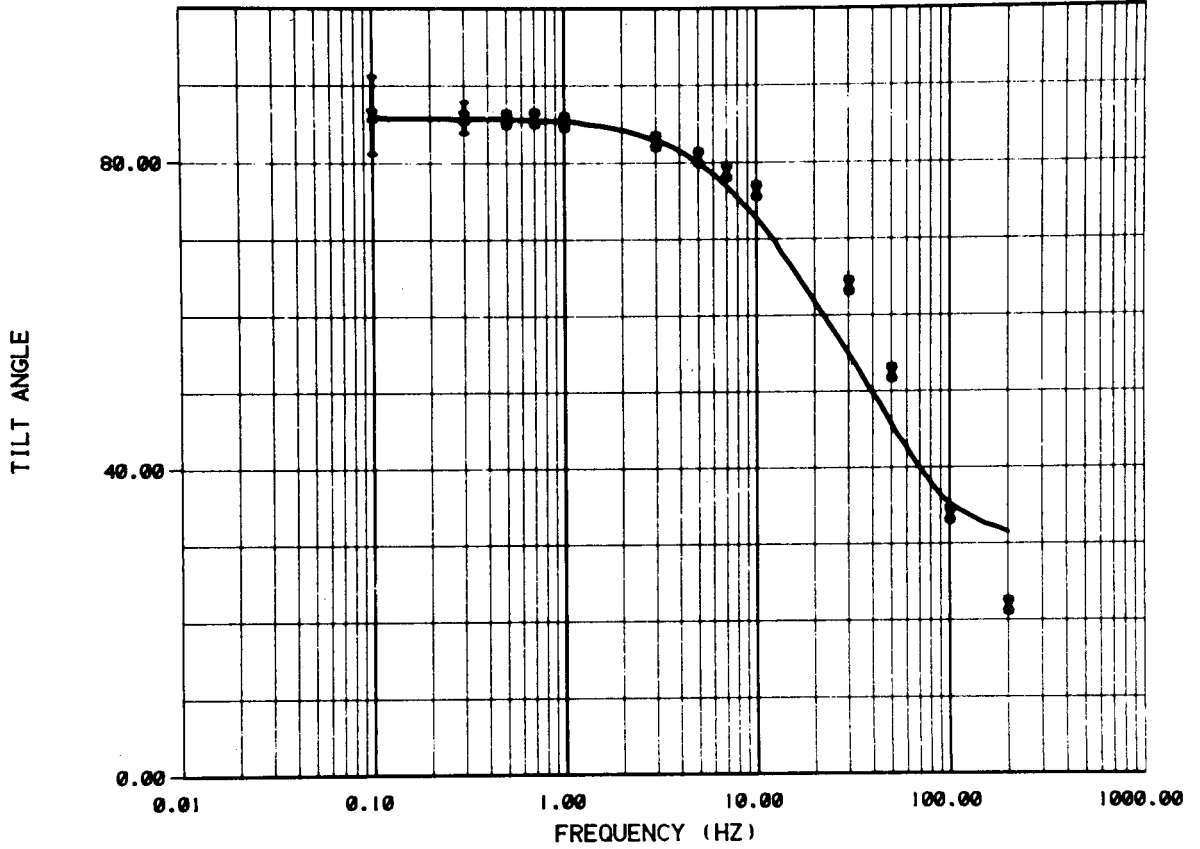
MCCOY T3R2 VARIABLE DIPOLE

CALCULATED DATA	MEASURED DATA	LAYER	RESISTIVITY(OHM-M)	THICKNESS(M)
ELLIPTICITY ———	ELLIPTICITY	X 1	200.0 ± 0.	100.0 ± 0.
		2	100.0 ± 0.	.1000E+12 ± 0.

DATA VARIENCE ESTIMATE 135.6

XBL 8012-12977

COMPARISON OF CALCULATED AND MEASURED DATA



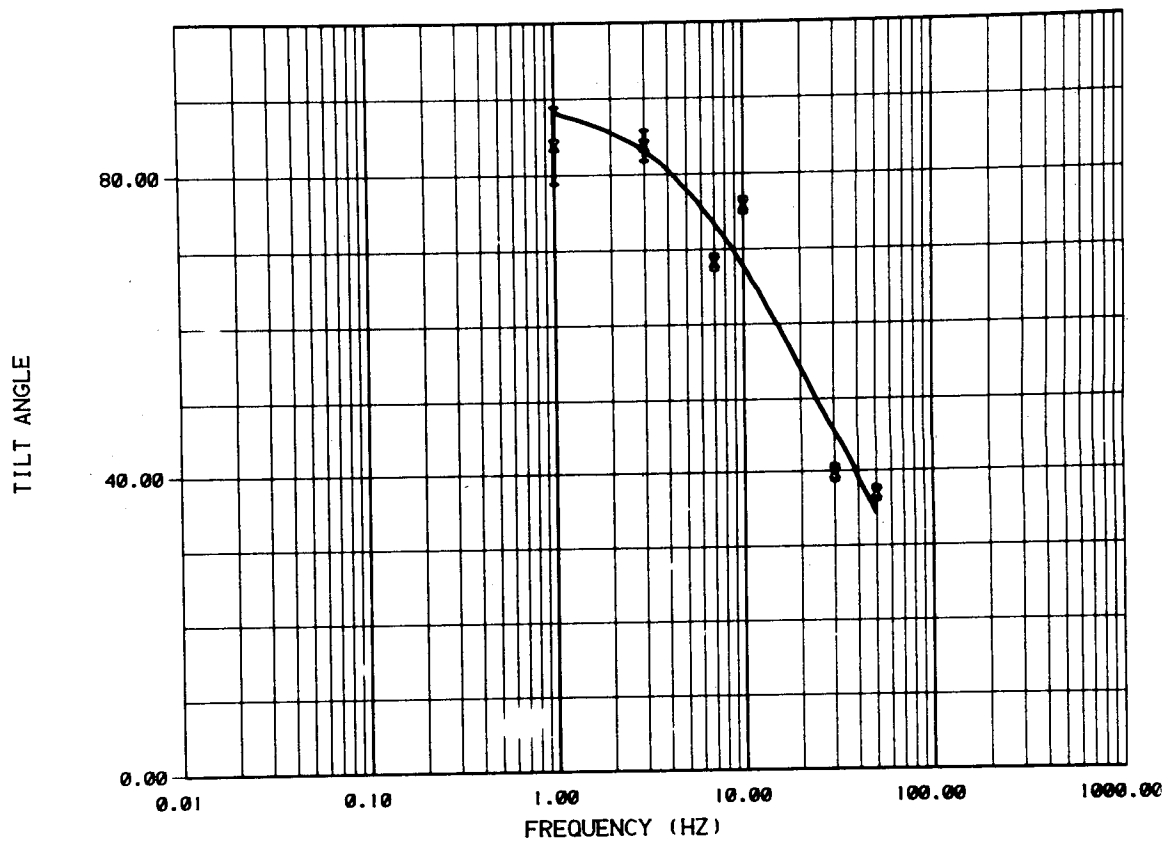
MCCOY T3R2 VARIABLE DIPOLE

CALCULATED DATA	MEASURED DATA	LAYER	RESISTIVITY(OHM-M)	THICKNESS(M)
TILT ANGLE ———	TILT ANGLE	X 1	200.0 ± 0.	100.0 ± 0.
		2	100.0 ± 0.	.1000E+12 ± 0.

DATA VARIENCE ESTIMATE 135.6

XBL 8012-12973

COMPARISON OF CALCULATED AND MEASURED DATA



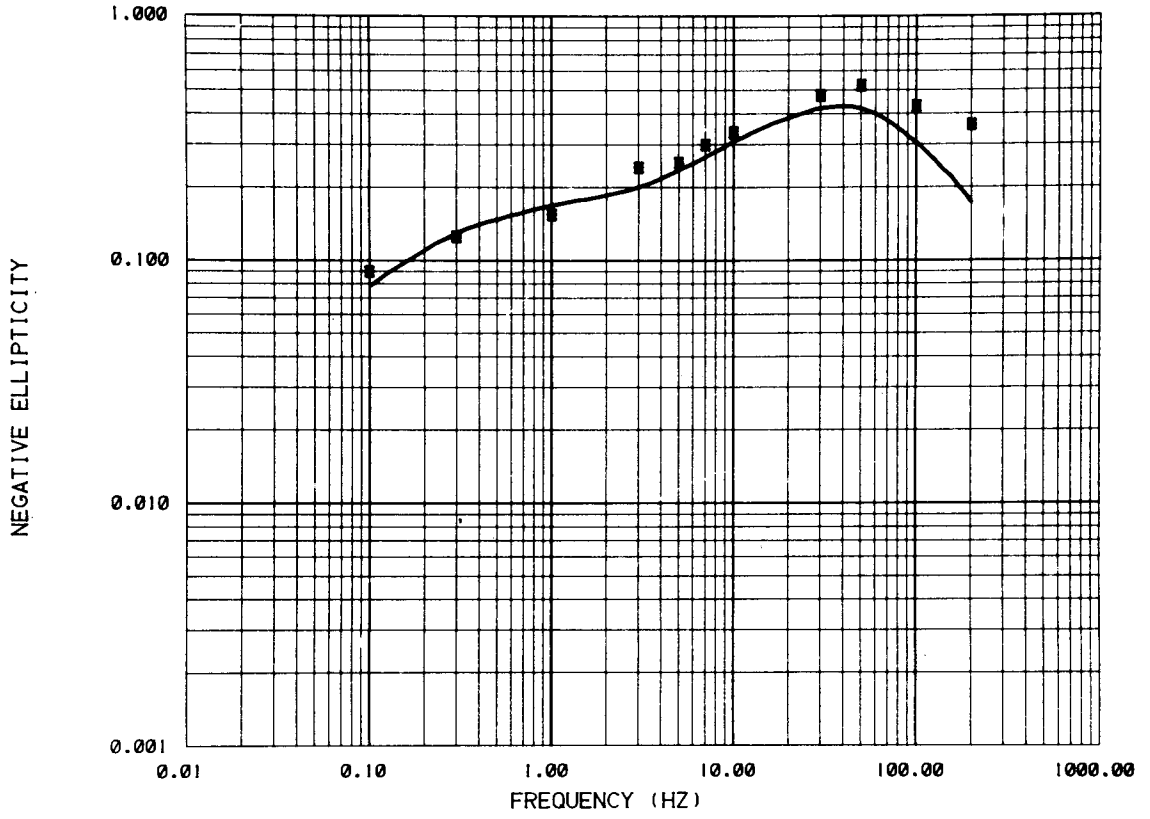
MCCOY T3R3

CALCULATED DATA	MEASURED DATA	LAYER	RESISTIVITY(OHM-M)	THICKNESS(M)
TILT ANGLE ———	TILT ANGLE X	1	22.81 ± .9410E-02	4.831 ± 27.
		2	81.03 ± 11.03	.1000E+11 ± 0.

DATA VARIANCE ESTIMATE 45.32

XBL 812-7995

COMPARISON OF CALCULATED AND MEASURED DATA



MCCOY T3R4

CALCULATED DATA
ELLIPTICITY ———

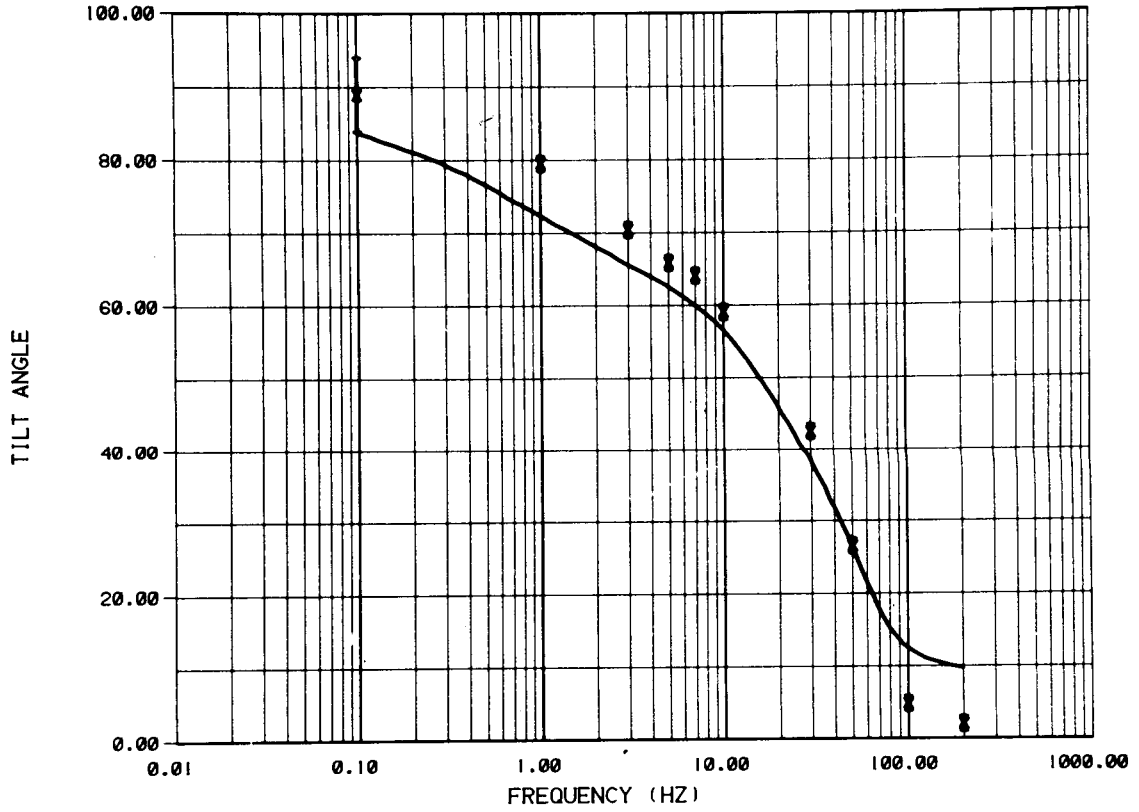
MEASURED DATA
ELLIPTICITY

LAYER	RESISTIVITY(OHM-M)	THICKNESS(M)
X 1	113.9 ± .5843E-02	1479. ± 7.
2	4.698 ± .6650E-01	.1000E+11 ± 0.

DATA VARIENCE ESTIMATE 483.2

XBL 812-7996

COMPARISON OF CALCULATED AND MEASURED DATA



MCCOY T3R4

CALCULATED DATA

TILT ANGLE

—————

MEASURED DATA

TILT ANGLE

X

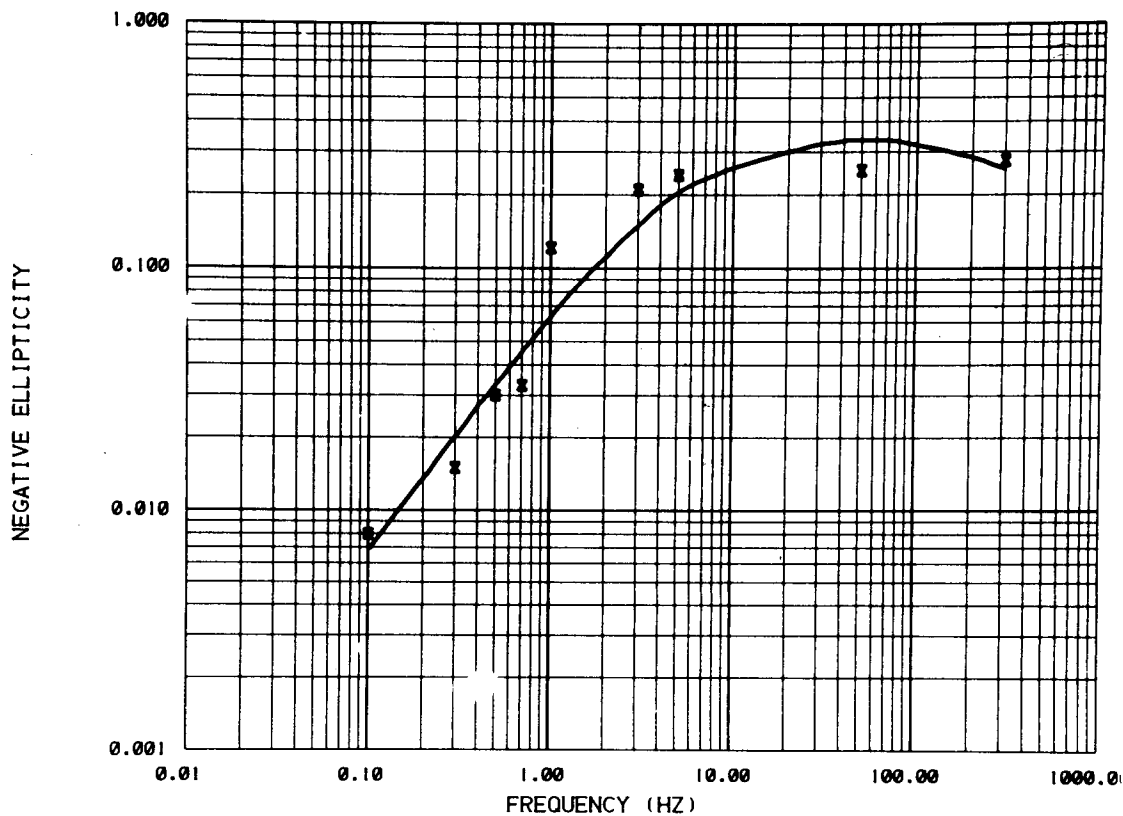
LAYER RESISTIVITY(OHM-M) THICKNESS(M)

1	113.9 ± .5843E-02	1479. ± 7.
2	4.698 ± .6650E-01	.1000E+11 ± 0.

DATA VARIANCE ESTIMATE 483.2

XBL 812-7997

COMPARISON OF CALCULATED AND MEASURED DATA



MCCOY T3R5

CALCULATED DATA
ELLIPTICITY ———

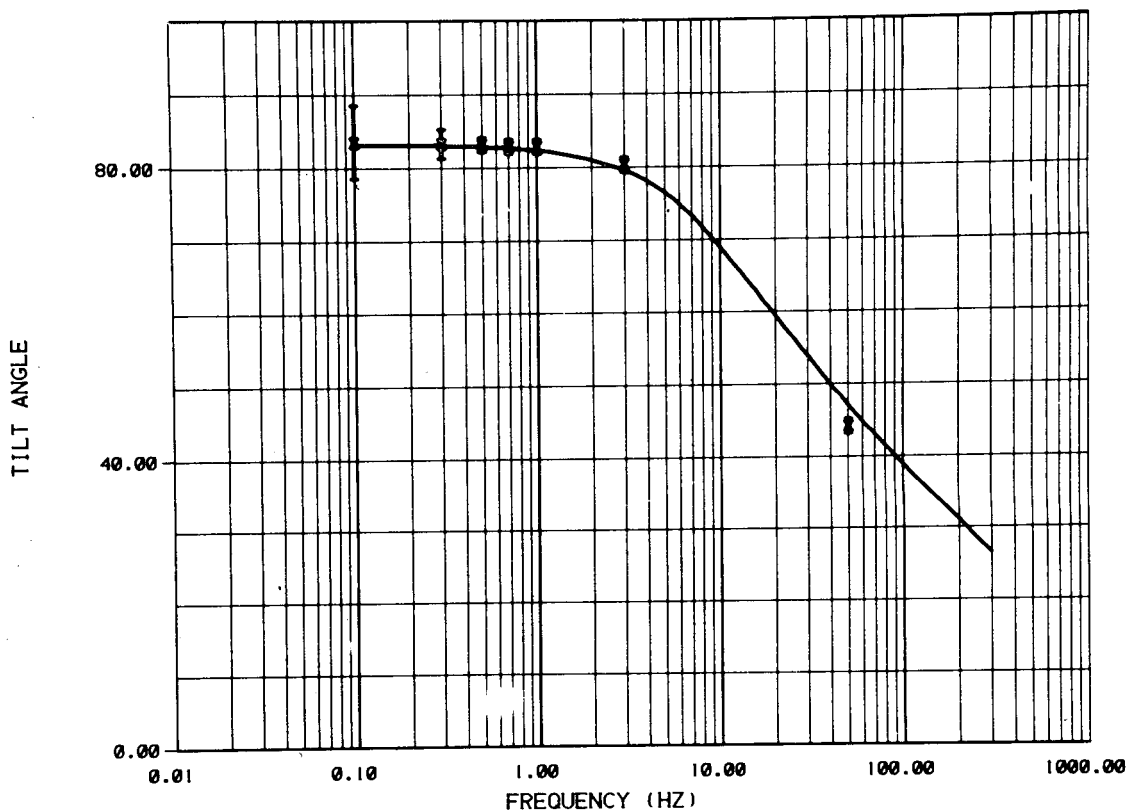
MEASURED DATA
ELLIPTICITY X

LAYER	RESISTIVITY(OHM-M)	THICKNESS(M)
1	526.9 ± .4841E-02	381.9 ± 25.
2	107.1 ± 3.051	.1000E+11 ± 0.

DATA VARIANCE ESTIMATE 75.70

XBL 812-7998

COMPARISON OF CALCULATED AND MEASURED DATA



MCCOY T3R5

CALCULATED DATA
TILT ANGLE ———

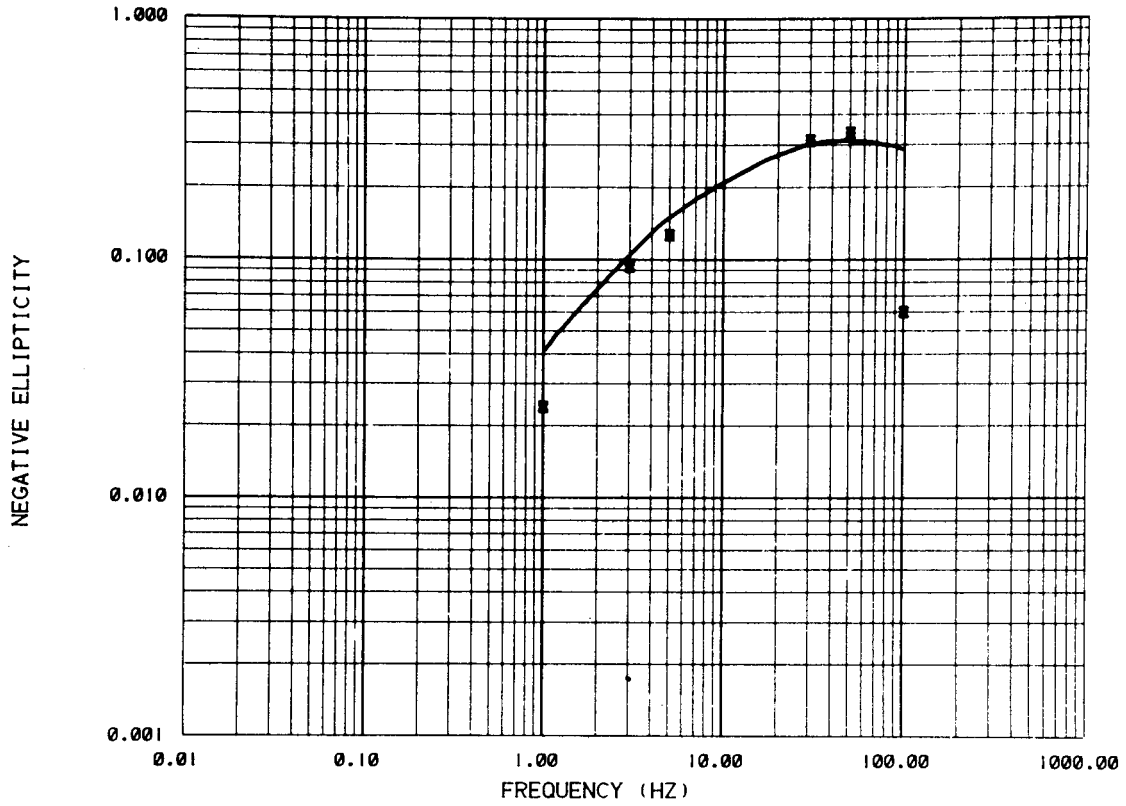
MEASURED DATA
TILT ANGLE X

LAYER	RESISTIVITY(OHM-M)	THICKNESS(M)
1	526.9 ± .4841E-02	381.9 ± 25.
2	107.1 ± 3.051	.1000E+11 ± 0.

DATA VARIENCE ESTIMATE 75.70

XBL 812-7999

COMPARISON OF CALCULATED AND MEASURED DATA



MCCOY T3R6

CALCULATED DATA	MEASURED DATA	LAYER	RESISTIVITY(OHM-M)	THICKNESS(M)
ELLIPTICITY ———	ELLIPTICITY	X 1	.3827E+09 ± 8.670	279.9 ± 8.
		2	87.08 ± 1.060	.1000E+11 ± 0.

DATA VARIANCE ESTIMATE 5079.

XBL 812-8000